COMPARISON OF WATER QUALITY AND QUANTITY IN EASTERN REDCEDAR-ENCROACHED WOODLAND AND NATIVE TALLGRASS PRAIRIE WATERSHEDS: A MONITORING AND MODELING STUDY

By

WHITNEY ALYSON LISENBEE

Bachelor of Science in Biosystems Engineering

Oklahoma State University

Stillwater, OK

2014

Submitted to the Faculty of the
Graduate College of the
Oklahoma State University
in partial fulfillment of
the requirements for
the Degree of
MASTER OF SCIENCE
July, 2016

COMPARISON OF WATER QUALITY AND

QUANTITY IN EASTERN REDCEDAR-

ENCROACHED WOODLAND AND NATIVE

TALLGRASS PRAIRIE WATERSHEDS: A

MONITORING AND MODELING STUDY

Thesis Approved:

Dr. Garey Fox

Thesis Adviser

Dr. Dan Storm

Dr. Chris Zou

ACKNOWLEDGEMENTS

This material is based upon work that is supported by the National Institute of Food and Agriculture, U.S. Department of Agriculture, under award number 2014-67010-21653.

A number of people have been instrumental to this research. First, I would like to thank my committee members, Dr. Fox, Dr. Storm and Dr. Zou, who have been extremely helpful throughout my project and my master's education. Specifically, I would like to thank my advisor, Dr. Fox, for his guidance of this project and review of my papers. He is always motivating me to strive higher and do my best. Beyond this project, I would like to thank him for his support and guidance the last six years. He has been an influential mentor in my academic career and I wouldn't be where I am today without his encouragement. I have gained so much valuable experience and knowledge from interacting with him in multiple ways over the years.

I also appreciate all the help I have received conducting field work on this project. I would like thank both Steven Leho and Chris Stansberry from the OSU Range Research Station for their assistance and cooperation on conducting JET tests. I would like to thank Elaine Stebler for managing data at CTER, ISCO programming and always being available to help in the field. A big thanks go to those that spent long days in the field with me including Ron Miller, Sahib Al-Madhhachi, Aaron Mittelstet, Brad Rogers and the Fox Research team (Kate Klavon, Holly Enlow, Rebecca Purvis, Yan "Joey" Zhou).

Friends and family have provided beneficial emotional support throughout this journey. My Fox Family which includes Erin Porter, Holly Enlow, Anish Khanal, Yan "Joey" Zhou adopted me as a new member right away. I will always remember the fun we had at our weekly family dinners and the traditions we built such as celebrating birthdays and defenses. Specifically, the triplets (Kate Klavon and Rebecca Purvis) that joined the Fox Family with me were great friends and support. Kate brought interesting new ideas to the group and was a great listener for lunch time walks. Rebecca has been with me since the beginning when we started at OSU as freshman. She has been a great friend throughout trials only engineering (and graduate) school can throw at you. There is no one else I would rather have spent the last two years with.

My family has also been a great support throughout my graduate career. I am so lucky to have siblings that I can count on that are always there for a phone call as needed. I couldn't have asked for better parents. I owe them so much but especially the fantastic education that got me here. Thank you for your unwavering support and guidance. Finally, thanks to all the other friends and family from OSU, BAE, and beyond that I have not mentioned. I appreciate your love and friendship throughout the years.

Name: WHITNEY LISENBEE

Date of Degree: JULY, 2016

Title of Study: COMPARISON OF WATER QUALITY AND QUANTITY IN EASTERN REDCEDAR-ENCROACHED WOODLAND AND NATIVE TALLGRASS PRAIRIE WATERSHEDS: A MONITORING AND MODELING STUDY

Major Field: BIOSYSTEMS AND AGRICULTURAL ENGINEERING

Abstract:

The encroachment of Eastern Redcedar (*Juniperus virginiana*) has become a major concern across the Great Plains region. This species has diminished ecological benefits provided by the grasslands they are replacing. It was suggested that Eastern Redcedar be used as a biofuel feedstock to serve a dual purpose of more biofuel production and restoration of native grasslands. This study compared two tallgrass prairie and two Eastern Redcedar encroached woodland watersheds identified in the Oklahoma State University Cross Timbers Experimental Range (CTER). Surface runoff samples were collected in each watershed to compare total runoff and sediment concentrations between encroached and tallgrass prairie watersheds prior to Eastern Redcedar removal. Measured data showed less runoff in the encroached sites compared to the tallgrass prairie. However, the sediment yield in all watersheds was similar. These data were also compared to uncalibrated Water Erosion Prediction Project (WEPP) simulations to evaluate the model. WEPP simulations were conducted using site-specific soil and slope inputs and a variety of climate inputs to represent wet, dry, long-term, and field site conditions. All site-specific WEPP simulations showed increased runoff and sediment yield in the encroached woodland compared to tallgrass prairie watersheds. Future work including calibration of WEPP using data from CTER will provide more guidance on if default values are sufficient or if field-measured parameters improve model predictions. The soil erodibility parameters were further investigated in WEPP. Currently, WEPP uses empirical equations to determine two major erodibility parameters within the soil input file: the critical shear stress (τ_c) and the erodibility coefficient (k_d). These erodibility parameters were determined mechanistically in the field using the Jet Erosion Test (JET). The JET-derived erodibility parameters were compared to WEPP-predicted values. The WEPP erodibility parameters were directly correlated with the soil texture. However, JET-derived erodibility parameters were significantly different between the two land covers with no relationship observed to soil texture. Uncalibrated WEPP simulations failed to indicate differences in predicted sediment transport between the erodibility parameters likely due to the small range in applied shear. This investigation highlights the need to use *in situ* testing to determine erodibility of a field site to better incorporate the effects of land cover when predicting hillslope sediment detachment in hydrologic modeling.

TABLE OF CONTENTS

Chapter Page

LIST OF TABLES

LIST OF FIGURES

Figure Page

CHAPTER I

COMPARING MEASURED WATER QUANTITY AND QUALITY OF EASTERN REDCEDAR-ENCROACHED AND TALLGRASS PRAIRIE WATERSHEDS TO AN UNCALIBRATED WEPP MODEL

1.1 Abstract

The encroachment of Eastern Redcedar (*Juniperus virginiana*) has become a major concern across the Great Plains region. This species has diminished the ecological benefits provided by the grasslands they are replacing. Removal of this species will allow the native grasslands to return to the region but is costly especially with large trees. It has been suggested that this species be used as a biofuel feedstock to serve a dual purpose of more biofuel production and restoration of native grasslands. This study compared two tallgrass prairie and two Eastern Redcedar-encroached woodland watersheds identified in the Cross Timbers Experimental Range (CTER) for this research. Water quality samples were collected in each watershed to compare total runoff and sediment concentrations between encroached and grassland sites prior to Eastern Redcedar removal. Measured data showed less runoff in the woodland compared to the tallgrass prairie. However, the sediment yield in all watersheds was similar. These data were also compared to uncalibrated Water Erosion Prediction Project (WEPP) simulations to evaluate the model. WEPP simulations were conducted using site-specific soil and slope inputs and a variety of climate inputs to represent wet, dry, long- term, and field site conditions. All site-specific WEPP simulations showed increased runoff and sediment yield in the encroached woodland compared to

tallgrass prairie watersheds. When comparing measured runoff to site-specific WEPP runoff using CTER weather data, WEPP underestimated runoff for all watersheds. Future work including calibration of WEPP using data from CTER will provide more guidance on if default values are sufficient or if field-measured parameters improve model predictions.

1.2 Introduction

1.2.1 Eastern Redcedar Encroachment

Many of the grasslands throughout the Great Plains have experienced encroachment of juniper species, specifically Eastern Redcedar (*Juniperus virginiana*). Juniper trees have encroached approximately five million hectares of grasslands in Oklahoma alone (Engle et al., 2008). In 2010, the United States Department of Agriculture (USDA) Natural Resources Conservation Service (NRCS) also found that among non-federal rangeland, native invasive juniper species made up five to 30% of land cover over about 20% of the state of Oklahoma, the majority of which is specifically Eastern Redcedar (Figure 1.1).

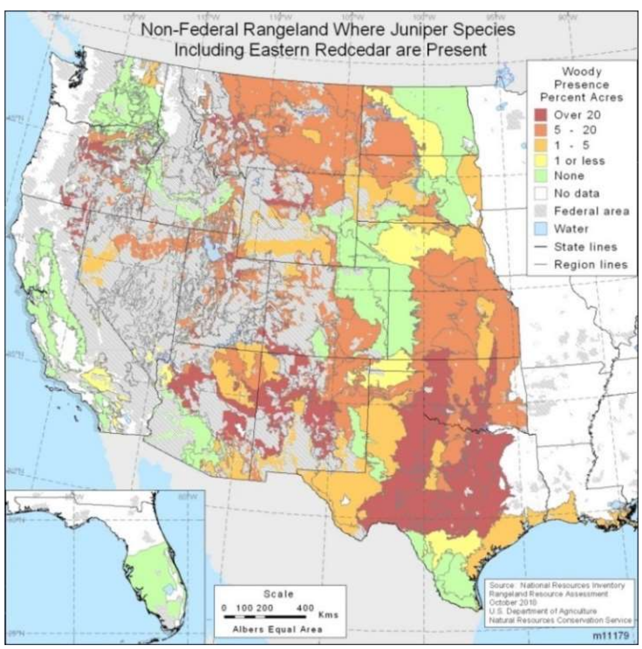

Figure 1.1. Encroachment of Juniper species including Eastern Redcedar in grasslands throughout the western United States (USDA-NRCS, 2010).

Eastern Redcedar has an undesirable impact on the grassland ecosystem, especially regarding water use and consumption. Eastern Redcedar encroachment has been shown to alter processes such as carbon and nitrogen cycling by increasing the amount of aboveground biomass as compared to grasslands (Norris et al., 2001). Eastern Redcedar is able to outcompete these grasses because it has deep root systems that can access water at depths that grasses cannot reach (Huxman et al., 2005; Tennesen, 2008). Additionally, Eastern Redcedar has drought-resistance strategies such that when water becomes available in the 0.05-0.5 m profile, it will draw from the upper roots instead where it competes with shallow grassland root systems (Eggemeyer et al., 2009). Previous studies have evaluated water use by Eastern Redcedar through both direct and indirect approaches but most were conducted in semi-arid regions that do not well-represent the climate in Central Oklahoma (Caterina et al., 2014). Therefore, Caterina et al. (2014) conducted experiments to better understand the water balance of a mesic prairie being encroached with Eastern Redcedar in north-central Oklahoma by measuring sap flow densities in individual trees using thermal dissipation probes (TDP) to quantify water use. A study from these same watersheds showed that encroached sites had reduced streamflow compared to grasslands and shorter streamflow duration than in grasslands (Zou et al., 2014). Pierce and Reich (2009) suggested that encroached areas that are restored to grasslands are able to recover from the transition and perform equally to non-encroached grasslands. Therefore, removing Eastern Redcedar in these encroached grasslands would reestablish many ecological benefits.

1.2.2 Eastern Redcedar and Biofuel Production

Currently, the cheapest method of Eastern Redcedar removal is prescribed burning but areas with trees greater than five feet or with closed canopies may not allow for enough grassy undergrowth to fuel a fire hot enough under allowed burn conditions to burn all the foliage and kill the cedars (Oklahoma Forestry Service, 2014). Clear cutting is a more expensive and timeconsuming option especially with larger trees (Ortmann et al., 1998), but could be a viable solution if used for biofuel production. Eastern Redcedar has been suggested as a sustainable fuel source due to the over-abundance and need to control this species in Oklahoma (Starks et al., 2011; Olukoya et al., 2014; Liu et al., 2015) and because it is predicted that the ethanol production potential of this species is about 2 billion liters from just 17 of the counties currently experiencing encroachment in northwestern Oklahoma (Ramachandriya et al., 2013). Increasing biofuel production has been a growing concern since 2007 when the United States implemented the Energy Independence Security Act, which included goals of creating more sustainable energy sources by increasing biofuel production by 2022 (Gopalakrishnan et al., 2009). One major concern of increasing biofuel production is a decrease in agricultural land that could be used for food production. A large area in the Great Plains has been identified as marginal lands that cannot be used for food production and instead can be used for biofuel production using feedstocks such as switchgrass (Wright and Turhollow, 2010). Harvesting encroaching juniper species as a biofuel feedstock can have a positive impact on the environment by increasing ecological services and providing a sustainable fuel source other than non-renewable oil and gas. After harvest, grassy biofuel feedstocks, such as switchgrass, can be planted to make use of marginal lands that can further increase cellulosic biofuel production in this region without inhibiting agricultural production.

Potential concerns of harvesting Eastern Redcedar are increased runoff and sediment yields. The harvesting procedure will likely disturb soil and result in more sediment transported by runoff that could be deposited in receiving water bodies. Sediment is one of the most common water quality pollutants and can carry nutrients harmful to an aquatic ecosystem and even human health when polluting a drinking water source. Access to clean abundant water is becoming more important as the growing population puts more demand on water sources and climate change affects the water budget. Therefore, it is important to investigate water quantity and quality changes under these changing land covers to understand how to best reduce the negative impacts on water resources.

1.2.3 The Water Erosion Prediction Project

The hydrologic model WEPP was used in this study to compare the water quality and quantity of Eastern Redcedar-encroached land cover to that of native un-encroached grassland. The WEPP model was developed at the USDA-ARS National Soil Erosion Research Laboratory (NSERL) in 1995 to estimate soil loss on a spatial and temporal scale along a hillslope. Hillslope applications of WEPP consider rill and interill erosion and deposition but do not consider gully erosion (Flanagan et al., 1995). WEPP has been used to model runoff, erosion, and management alternatives in agricultural settings (e.g. Das et al., 2004; Renschler and Lee, 2005; Williams et al., 2010, and Garbrecht and Zhang, 2015), in forested watersheds (e.g. Wade et al., 2012; Christie et al., 2013; Saghafian et al., 2015) and in grasslands (e.g. Zhang et al., 2008; Wang et al., 2014).

WEPP uses four main input parameters: climate, slope, soil and land management (Flanagan and Livingston, 1995). WEPP uses the Green-Ampt Mein-Larson infiltration equation so the effective hydraulic conductivity (K_e) is one of the most important infiltration parameters (Alberts et al., 1995). The baseline effective conductivity can be calculated by WEPP using the sand or clay content and the cation exchange capacity (CEC) of the soil and adjusted over time with changing soil management and plant characteristics. However, this method is only applicable to soils with CEC greater than 1 meq/100g (Alberts et al., 1995). Another method to estimate K_e as a constant time-invariant value that is based on hydrologic soil group and management practice (Flanagan and Livingston, 1995). The erodibility parameters such as the interrill erodibility (K_i), the rill erodibility (K_r), and the critical shear stress (τ_c) are determined by empirical equations described by Elliot et al. (1989). Sediment detachment and transport is modeled using the excess shear stress and Yalin equations (Foster et al., 1995; Stone et al., 1995).

Sensitivity analysis has shown K_e to be the most sensitive parameter among three separate management scenarios for runoff prediction (Ascough II et al., 2013). Additionally, a first-order error analysis showed that in runoff predictions K_e contributed the highest percentage of error variance, up to 74%. For soil loss predictions, K_r, τ_c, and clay content contributed the most error variance in cases dominated by rill detachment (Ascough II et al., 2013).

1.2.4 Objectives

This research focused on comparing runoff and sediment yield for two Eastern Redcedar-encroached woodland watersheds and two tallgrass prairie watersheds. The hydrology of each watershed was evaluated in the field using monitoring equipment to collect runoff samples that were analyzed for sediment concentrations. These data were also compared to model simulations by WEPP to evaluate runoff and sediment yield predictions in the two encroached woodland and two tallgrass prairie watersheds.

1.3 Materials and Methods

1.3.1 Field Research Sites-

Research was conducted in two tallgrass prairie watersheds and two Eastern Redcedar-encroached woodland watersheds at the Oklahoma State University (OSU) Cross Timbers Experimental Range (CTER) 11 km southwest of Stillwater, OK (36°04′N, 97°11′36″W) (Figure 1.2). This study area was located within the Cross Timbers ecoregion defined as a "complex mosaic of upland deciduous forest, savanna, and prairie" which spanned portions of Oklahoma, Texas, Kansas and Arkansas (Hoagland, 1999). The tallgrass prairie consisted of predominantly little bluestem (*Schizachyrium scoparium*), big bluestem (*Andropogon gerardii*), indiangrass

(*Sorghastrum nutans*), and switchgrass (*Panicum virgatum*) (Limb et al., 2010). Within CTER, Eastern Redcedar has invaded portions of the tallgrass prairie, and there are different stages of cedar encroachment with canopy coverage approaching 100% in some locations (Caterina et al., 2014). Observations from the field reported terracing throughout these watersheds remaining from historic agricultural practices in CTER. Gullies were also reported leading to H-flumes at the mouth of each watershed particularly in the encroached woodland watersheds. CTER has also had significant grazing; approximately 58 cows from March to November for the last six years.

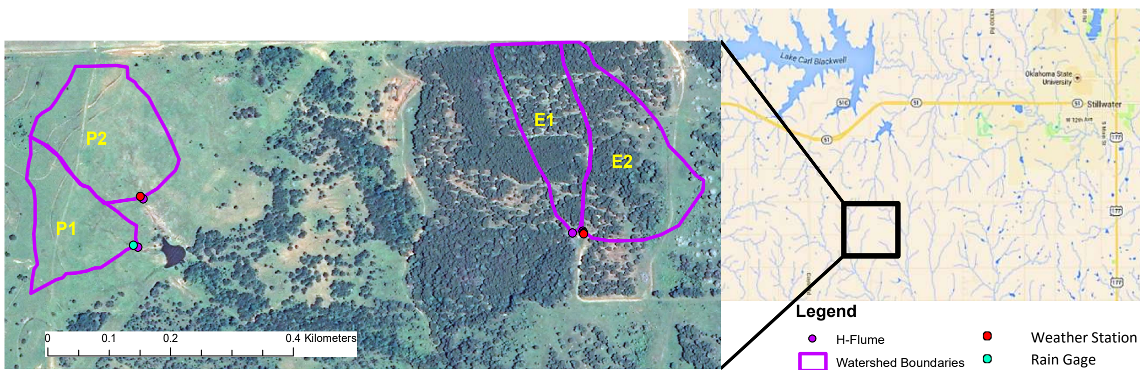

Figure 1.2. Cross Timbers Experimental Range field site including two tallgrass prairie (P1, P2) and two Eastern Redcedar-encroached woodland (E1, E2) watersheds located less than 15 km southwest of Stillwater, OK.

The climate was continental with an average growing season of 204 days and an average annual precipitation of 942 mm with 65% occurring from May to October (Brock et al., 1995; McPherson et al., 2007). The temperature ranged from an average daily minimum of 4.3°C in January to an average daily maximum of 34°C in August with an annual daily average of 15°C (Brock et al., 1995; McPherson et al., 2007). Data from two weather monitoring stations, one in a tallgrass prairie site (P2) and one in an encroached site (E2), were collected in these watersheds since 2011 and data from an Oklahoma Mesonet station located less than three kilometers northwest (36° 3' 51" N, 97° 12' 45" W) from the research site provided additional weather information.

Physical characteristics of each watershed were detailed in Table 1.1. The total drainage area and slope were estimated using in-field surveying to delineate watershed boundaries (Elaine Stebler, Personal Communication, December 9, 2015).

Table 1.1. Watershed characteristics for Eastern Redcedar-encroached woodland (E1, E2) and tallgrass prairie (P1, P2) land cover.

	E1	E2	P1	P2
Land Cover	Eastern Redcedar	Eastern Redcedar	Tallgrass Prairie	Tallgrass Prairie
Area (ha)	2.6	3.8	2.3	3.3
Average Slope (%)	5	4	4	4

1.3.2 Soil Sampling and Processing

Twenty to 30 site-specific soil samples were acquired throughout each watershed. Using ArcGIS 10.2 (ESRI, 2013), a grid sampling system was developed for each watershed with sampling points 25 to 35 m apart depending on the overall size of the watershed (Figure 1.3).

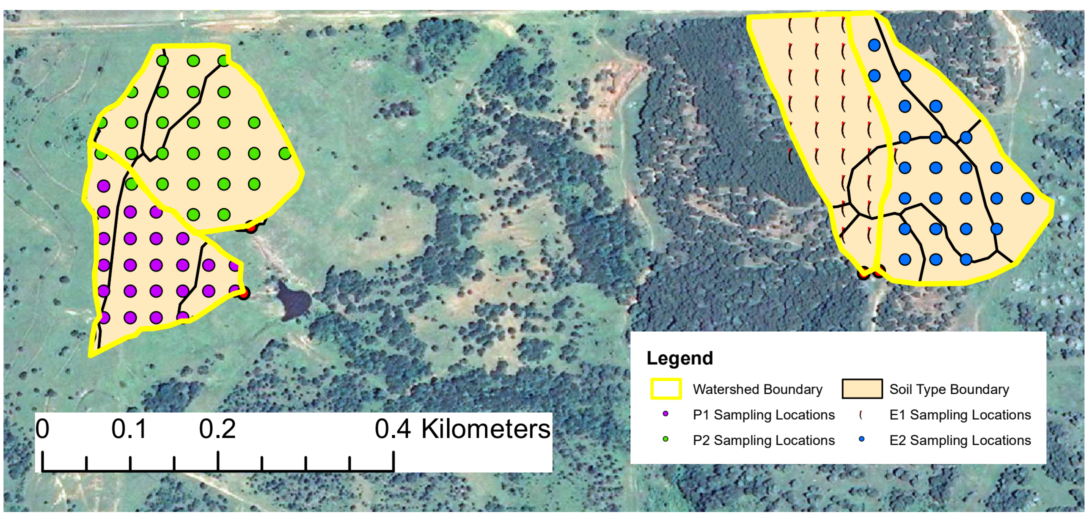

Figure 1.3. Cross Timbers Experimental Range watersheds displaying soil types and sampling locations.

Soil samples were taken at five depths which were chosen based on the layer depths of the Stephenville-Darnell complex which consists of loam and sandy loam, and covered the majority of the watershed study area. According to the Soil Survey Geographic Database (SSURGO), the Stephenville soil series consists of four soil horizons: A (0 to 13 cm), E (13 to 38 cm), B (38 to 84 cm), and C (84 to 130 cm-sandstone bedrock layer). The Darnell soil series consists of three layers: A (0 to 13 cm), B (13 to 38 cm), and the sandstone horizon C (38 to 76 cm). All of the soil types present in the watersheds can be seen in Figure 1.4 with the soil type descriptions and contributions to the watershed in Table 1.2.

Figure 1.4. Cross Timbers Experimental Range watersheds displaying soil types determined by SSURGO. The legend of soil type descriptions can be found in Table 1.2.

Table 1.2. Cross Timbers Experimental Range soil types determined by SSURGO including soil type descriptions and contribution to each watershed.

		% Contribution to Watershed			
Soil Type	**Soil Type Description**	**E1**	**E2**	**P1**	**P2**
StDD	Stephenville-Darnell complex, 3 to 8% slopes, rocky	77.8	29.3	63.7	67.4
3	Coyle loam, 3 to 5% slopes	0.0	0.0	0.0	18.2
49	Renfrow and Grainola soils, 3 to 8% slopes, severely eroded	11.0	29.0	0.0	0.0
51	Stephenville fine sandy loam, 3 to 5% slopes, severely eroded	8.4	8.6	0.0	0.0
CoyB	Coyle loam, 1 to 3% slopes	0.0	0.0	20.3	14.5
GrLE	Grainola-Lucien complex, 5 to 12% slopes, rocky	2.9	13.0	0.0	0.0
HaPE	Harrah-Pulaski complex, 0 to 12% slopes, very rocky	0.0	0.0	15.0	0.0
ZaHC	Zaneis-Huska complex, 1 to 5% slopes	0.0	0.0	1.0	0.0
CoLC	Coyle-Lucien complex, 1 to 5% slopes	0.0	20.1	0.0	0.0

This typical profile was assumed to be constant over the study area and soil samples were obtained from depths 127, 381, 635, 889, and 1143 mm. Individual samples from each watershed were composited into one sample per depth to act as an average soil sample from each depth per watershed. The composite samples were tested at the Oklahoma State University Soil, Water, and Forage Analytical Laboratory (SWFAL) for soil texture and organic matter.

1.3.3 Runoff Sampling and Processing

Three-foot or four-foot H-flumes at the mouth of each watershed have been used to measure runoff since 2010. ISCO 3700C autosamplers were installed in each of the four watersheds to collect runoff samples for sediment analysis (ISCO Product Data, 2000). ISCO autosamplers have not often been used in conjunction with flumes. To collect water quality samples without disrupting the stage-discharge relationship of the flume, a trough made of a half of a 160 mm polyvinyl chloride (PVC) pipe was placed at least 15 cm underneath the flume outlet (Figure 1.5). As water flowed into the trough, ISCO autosampler pumped water through flexible tubing to the individual bottles within the sampler. An intake strainer was made of wire screens and a 25 mm PVC pipe with 10 mm diameter holes drilled into it to prevent leaves, sticks or other material carried by the runoff from clogging the flexible tubing (Figure 1.5).

The sampling scheme on the ISCO autosamplers used a combined flow-weighted and time-weighted system. Every five minutes, the samplers measured the stage in the flume using a shaft encoder in the flume stilling well. A stage greater than 21 mm or 24 mm, depending on the size of the flume, activated the sampler to take the first sample. The ISCO also sampled if the absolute difference of the stage changed by more than 21 mm or 24 mm accordingly. After the initial sample, if there was no change in stage for 40 minutes then another sample was taken. This method ensured that samples characterized the whole event and captured the moments when the runoff changed.

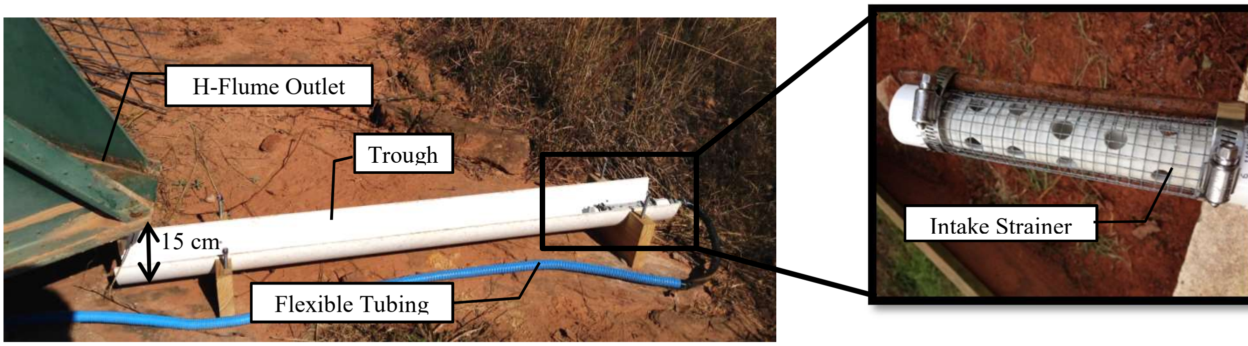

Figure 1.5. To prevent disturbing the stage-discharge relationship of the flume, runoff will free fall approximately 15 cm from the flume outlet into the trough made of half of a 160 mm PVC pipe. Then, the runoff will flow through the intake strainer to prevent leaves and debris from entering the flexible tubing that leads to the ISCO autosampler.

Water samples collected from ISCO autosamplers at each field site were processed to measure sediment concentration. Total water volume and sediment mass were measured to calculate the concentration for each sample. Next, the sample time was matched to the five-minute flow data. The volume in the flume was then multiplied by the concentration to estimate the total sediment load (kg) per five minute sampling period. Next, runoff hydrographs were created from the flume data and sampling times were noted along the duration of the runoff (Figure 1.6). These hydrographs showed runoff events that were poorly sampled such as those that only had samples on the falling tail of the runoff event or had a single sample at the event peak. Neither of these scenarios provided an accurate average of the sediment load over the duration of the runoff event.

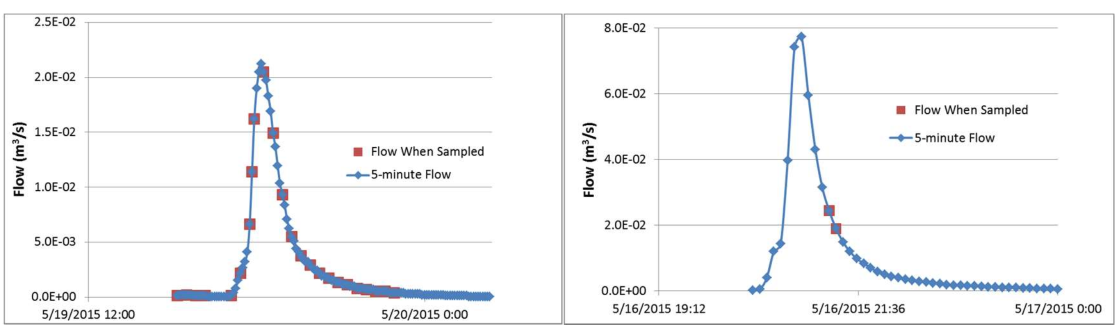

Figure 1.6. Runoff hydrographs were examined to determine if individual storms were a) well-sampled so that samples were taken throughout the runoff event or b) poorly-sampled such that only a few samples were taken on the falling limb of the hydrograph.

To overcome gaps in sample collection, a regression analysis was conducted for each watershed. Minitab 17 software (Minitab® 17.2.1) was used to perform a linear regression to compare the average sampled sediment load per storm (kg/hr) to the average storm runoff (m^3/s) for all properly sampled storms monitored in 2015. The sediment load was then multiplied by the duration of each storm to find the total sediment yield within the year of storms monitored. For watersheds that had very few well-sampled storms, a regression equation was not applicable so an average sediment load (kg/hr) was used instead and was multiplied by the storm duration to determine the total sediment yield.

1.3.4 WEPP Modeling

Simulations were conducted in WEPP to predict runoff and sediment yield from each watershed in CTER. Default and site-specific scenarios were compared to the observed runoff and sediment yield measured in the field to determine the importance of using detailed input data. A matrix of each simulation and inputs used are reported in Table 1.3.

Table 1.3. Water Erosion Prediction Project (WEPP) simulations and input files used for each simulation. Shaded boxes in each row indicate input files used for each of the four input categories: land management, slope, soil, and climate.

	Land Management		Slope		Soil		Climate				
WEPP Simulation	20 year forest	Tallgrass Prairie	Convex 5%	Individual Watershed Slope	Canisteo (Clay Loam)	Individual Watershed Texture	CLIGEN-Perry, OK	Mesonet Wet (2007)	Mesonet Dry (2011)	Mesonet (2005-2014)	Measured CTER (2015)
Default	■		■		■		■				
		■	■		■		■				
Site-Specific-Mesonet Wet (2007)	■			■		■		■			
		■		■		■		■			
Site-Specific-Mesonet Dry (2011)	■			■		■			■		
		■		■		■			■		
Site-Specific-Mesonet 2005-2014	■			■		■				■	
		■		■		■				■	
Site-Specific-CTER 2015	■			■		■					■
		■		■		■					■

Default inputs that best characterized the CTER watersheds were used to imitate a user that was utilizing WEPP as a quick assessment tool without further field work or testing. The land management default files offered many agricultural, forest, grassland, and rangeland options.

Each of these files included detailed ecological data including the bulk density, canopy cover, interill/rill cover, ridge height and roughness since last tillage and days of senescence. The land management chosen for these Eastern Redcedar-encroached woodlands was a 20-year old forest. This was based on aerial imagery that showed encroachment beginning at these sites in 1995. The land management selected to represent the grassland watersheds was the default file for a tallgrass prairie. The default climate file used the climate generator (CLIGEN) built into WEPP to estimate daily weather parameters using historic monthly averages from various CLIGEN stations throughout the United States. For all CTER watersheds, the Perry, OK CLIGEN station was used which is approximately 30 km north of CTER. The default slope chosen was a convex five percent slope over a length of 300 m. The default soil files had many preloaded hydrologic soil groups and include parameters such as the percent sand, clay, organic matter, rock, and CEC at each soil layer, albedo, and initial saturation level. The default soil series chosen was Canisteo which best matched the soil texture of these watersheds. Some other input data in the soil file included K_i (kg*s/m^4), K_r (s/m), τ_c (Pa), and K_e (mm/h) which were calculated within the model.

Using default values, the only input that differentiated between all four of these watersheds was the land management that divided them into encroached woodland and tallgrass prairie sites. Therefore, to further distinguish between individual watersheds, site-specific input files were created using data collected in the field. A breakpoint climate file containing mean daily precipitation, maximum and minimum daily temperatures, mean daily solar radiation, and mean daily wind direction and speed was created using weather data from each of the weather stations (one in a encroached woodland and one in tallgrass prairie). Additional breakpoint files using an hourly time-step were created using more long-term Mesonet data to include a 10-year period (2005-2014) as well as a single wet year (2007) with the highest annual total of rainfall (1370 mm) in the last 10 years and a single dry year (2011), which only reached an annual rainfall total of 585 mm (Brock et al., 1995; McPherson et al., 2007). The slope of each watershed was manually entered based on 2-m LiDAR elevation data analyzed with ArcGIS (ESRI, 2013). The soil file was specialized by entering the soil texture data for each layer based on composite soil texture determined from soil sampling throughout each watershed. Other important soil parameters include the soil albedo and initial saturation which were calculated with guidance from the WEPP User Summary. The erodibility parameters (K_i, K_r, τ_c) were calculated by WEPP but the K_e infiltration parameter was calculated and entered as a constant value (Flanagan and Livingston, 1995).

1.4 Results

1.4.1 Soil Texture

Soil texture was an important input to the soil file in WEPP. The composite soil texture at each layer depth was determined for each watershed in CTER. Then, WEPP computed a weighted average of the sand and clay content for the top 20 cm of soil (Table 1.4). This weighted average is used by WEPP when computing other erodibility parameters such as the K_r and τ_c.

Table 1.4. The composite topsoil texture in each watershed and the weighted average sand and clay content used by the Water Erosion Prediction Project.

Composite Topsoil Texture						
Watershed	Layer (cm)	Sand (%)	Average Sand (%)	Clay (%)	Average Clay (%)	Texture
E1	0-10	46.3		17.5		
	10-20	45.4	45.8	23.0	20.2	Loam
E2	0-10	58.8		17.5		
	10-20	53.3	56.1	24.8	21.2	Sandy Clay Loam
P1	0-10	55.0		15.0		
	10-20	53.2	54.1	20.5	17.7	Sandy Loam
P2	0-10	46.3		18.8		
	10-20	46.3	46.3	23.3	21.1	Loam

1.4.2 Sediment Loads

The concentration from each individual sample collected in 2015 was recorded and an average was calculated for each watershed (Table 1.5). A simple linear regression was developed to estimate the average sediment load per storm (kg/hr) based on the average storm runoff (m^3/s) for each of the encroached woodland watersheds. A total of ten sampled storms in E1 and nine in E2 were used to calculate the regression. A significant regression equation was found for the encroached woodlands using a $\log_{10}$ transformation on both variables. The regression equations and statistical measures are listed in Table 1.5. These equations were used to find the average sediment load per storm (kg/hr) for a total of 26 runoff events in E1 and 21 runoff events in E2.

The two tallgrass prairie watersheds had less than five storms each that were sampled enough to be used for the regression analysis. However, a regression with a good fit was not found for these two watersheds because so few storms were used. Therefore, a simple average of the sediment load measured for all storms was used in place of the regression equation. The average sediment load per storm in kg/hr was then multiplied by the duration to find different total sediment loads (kg) per storm. The estimated sediment yield using this method was reasonable compared to the estimations from the regressions in the encroached woodland watersheds.

Table 1.5. Regression analysis and estimated sediment yield for each watershed during the 2015 sampling period.

Watershed[a]	Regression Equation[b,c]	R^2	S (kg/hr)[d]	Sediment (kg/yr)	Sediment (kg/ha·yr)	Sediment (mg/L)
E1	$\log_{10}(ASL) = 4.64 + 1.463 \log_{10}(ASR)$	70.61%	0.34	1020	390	190
E2	$\log_{10}(ASL) = 3.541 + 1.181 \log_{10}(ASR)$	72.19%	0.37	860	230	210
P1	ASL=1.35	n/a	n/a	1130	500	160
P2	ASL=1.55	n/a	n/a	940	280	160

[a]E1 and E2 represent encroached woodland watersheds, P1 and P2 represent tallgrass prairie watersheds; [b]ASL=Average Sediment Load (kg/hr); [c]ASR=Average Storm Runoff (m^3/s); [d]S=Standard Error

1.4.3 Measured Runoff and Sediment Yield

Using sediment yields estimated from the regression analysis and averaging methods, the sediment yield per area was plotted for each watershed and compared to the runoff from each watershed. Measured runoff from the H-flumes at the mouth of each watershed showed runoff in the tallgrass prairie watersheds was more than double that of the encroached woodland watersheds (Figure 1.7). However, estimated sediment yield in each watershed was similar; varying by less than 300 kg/ha. Sediment yields were similar among all land covers because the concentration of sediment in runoff was less in tallgrass prairie but the increase in runoff made up for the difference in concentration, whereas encroached woodlands intercepted more rainfall leading to less runoff but the runoff was more concentrated with sediment. This was consistent with observations from the field which showed higher concentrations of sediment in the encroached woodland watersheds but fewer runoff samples during the study period.

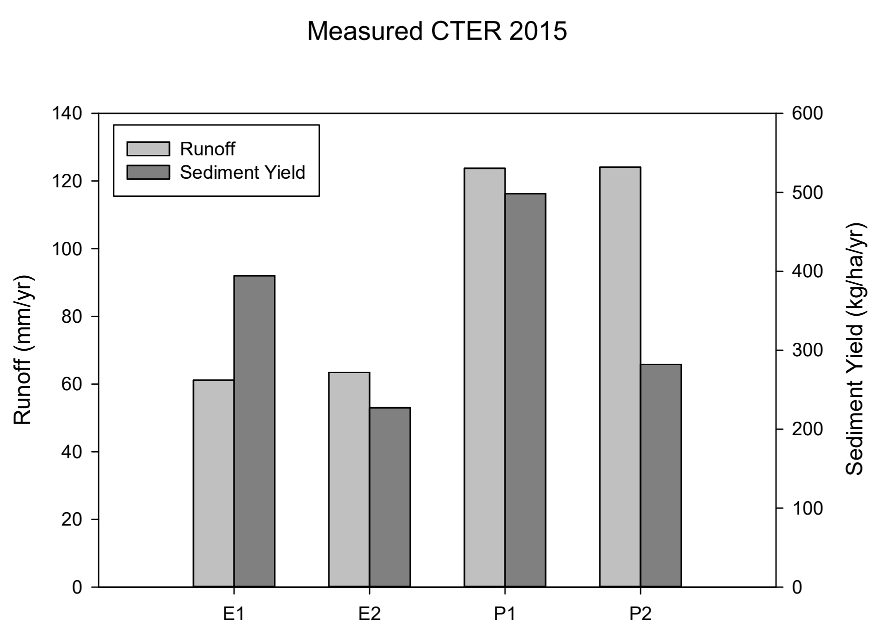

Figure 1.7. Measured runoff from H-flumes in each encroached woodland (E1, E2) and tallgrass prairie (P1, P2) watershed and estimated sediment yield from each watershed based on measured concentrations from ISCO runoff samples.

1.4.4 WEPP Modeling Comparisons

Measured runoff and sediment values were compared to the WEPP simulations that best represented the individual watersheds by using site-specific slope and soil inputs and the breakpoint climate file created from the weather stations at CTER (Figure 1.8). WEPP only predicted two or three runoff events in each watershed for the 2015 climate file from CTER. The number of measured runoff events in each watershed ranged from 14 to 26 meaning WEPP only predicted 10 to 17% of the runoff events in 2015. Therefore, WEPP simulations were compared on an average annual basis for runoff and sediment yield.

Predicted sediment covered a wide range (three orders of magnitude) with more predicted in encroached woodland watersheds and less in the tallgrass prairie watersheds. E2 showed the closest predicted sediment yield to measured values. WEPP predicted sediment yields did not consider the effects of gully erosion. Therefore, in CTER where gullies were present, especially in the encroached woodland watersheds, sediment yield may be higher than predicted. However, the site-specific WEPP simulations overpredicted sediment yield in some watersheds and underpredicted in others (Figure 1.7-1.8). The runoff predicted was similar in that it also spanned a wide range and predicted more sediment in the encroached woodland watersheds than the tallgrass prairie watersheds (Figure 1.8). This is surprising when comparing to the measured data because there was more observed runoff in the tallgrass prairie than the encroached woodland. The effective conductivity of the each watershed was similar despite the land cover so this discrepancy in runoff shows that WEPP's infiltration equations were not adequately depicting the change in interception between the two land covers. Also, measured runoff ranged from 63-124 mm but the site-specific CTER 2015 predicted runoff ranged from 1.5-19.5 mm across tallgrass prairie and encroached woodland watersheds (Figure 1.7-1.8). This difference can be partially explained by the number of runoff events not simulated by WEPP that were measured in 2015.

However, the runoff measured for only the events simulated by WEPP was still higher than predicted especially in the tallgrass prairie watersheds. Additionally, grazing is present in these watersheds but not considered by WEPP leading to underestimation of runoff by the model.

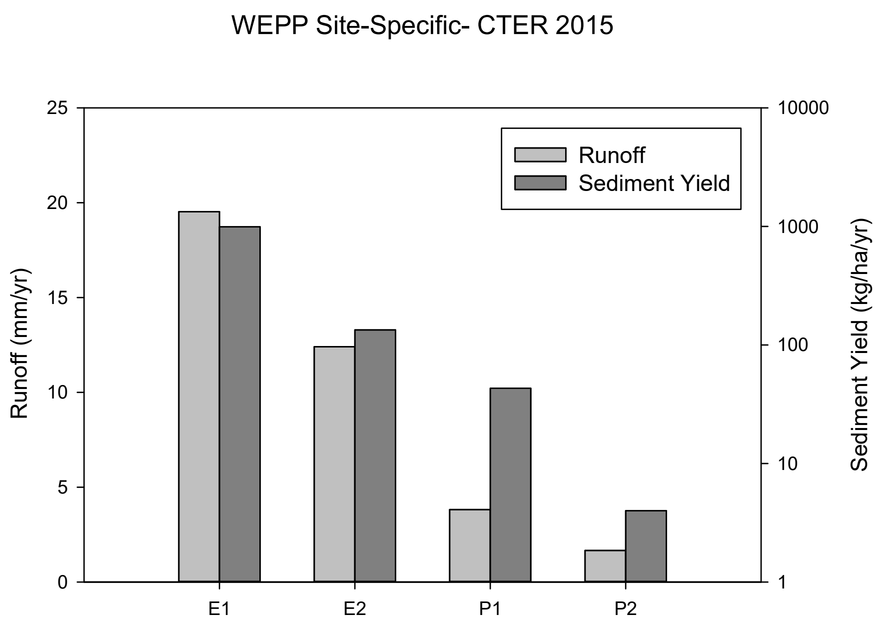

Figure 1.8. WEPP predicted runoff and sediment yield for all encroached woodland (E1, E2) and tallgrass prairie (P1, P2) watersheds using the site-specific inputs.

Next, all WEPP scenarios were compared to see how different inputs affected the predictions of runoff and sediment yield. For the encroached woodland watersheds, the runoff predicted by WEPP using default parameters was almost equal to the measured runoff even though more precipitation was measured than predicted (Figure 1.9). Predicted sediment yield did not correlate to predicted runoff as expected. In E1, even when the runoff predicted by WEPP was less than measured, the predicted sediment yield was higher. E2 predicted sediment yields within one order of magnitude for all scenarios (except the dry year) despite changes in runoff. Also in E1, WEPP predicted more sediment than was measured in all scenarios except the dry climate file that predicted zero sediment yield (Figure 1.9).

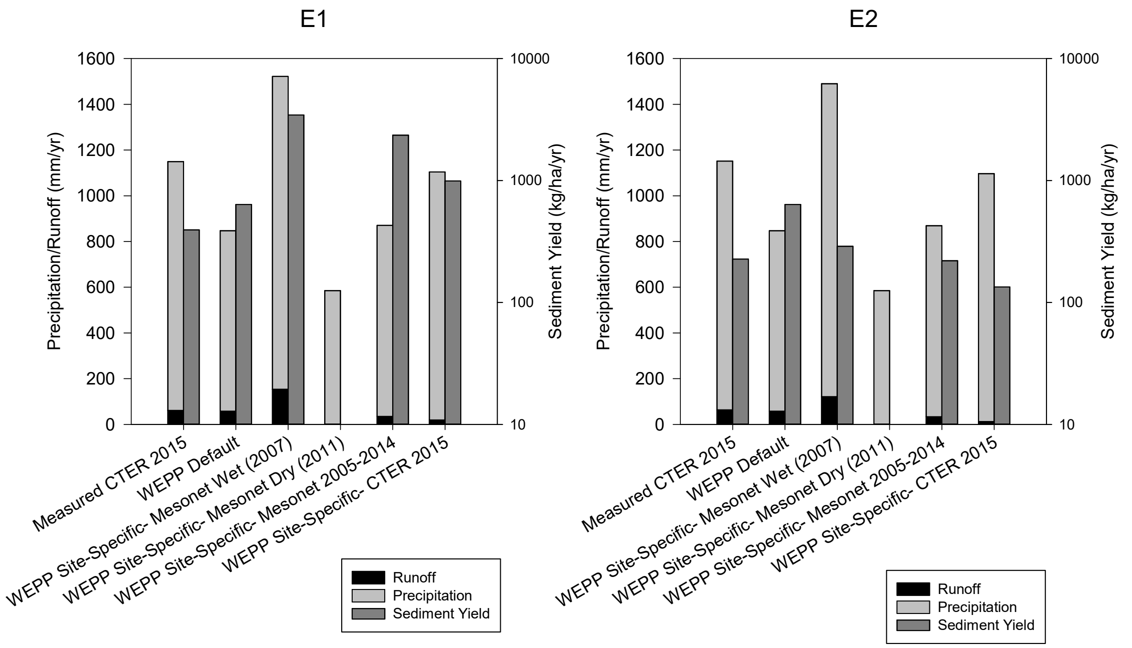

Figure 1.9. Measured precipitation, runoff and sediment yield from CTER was compared to that predicted by WEPP default scenarios and WEPP site-specific scenarios with various climate inputs for encroached woodland (E1 and E2) watersheds.

Another observation was that watershed E1 predicted the most runoff and sediment yield among the four watersheds in all scenarios. This was because the slope of this watershed differs from the other three. It varied between two to eight percent slopes with an average five percent slope compared to most other watersheds that had one to six percent slopes averaging four percent. It also had the longest hillslope length of almost 300 m whereas the other watersheds were all closer to 200 m. Therefore, WEPP placed a large influence on the slope input. This was corroborated with a study by Yu and Rosewell (2001) which found that the WEPP overpredicted soil loss for plots of large slope length. Additionally, a sensitivity analysis showed the soil loss predicted by WEPP to be highly sensitive to the average slope and the hillslope length (Ascough II, et al., 2013).

For the two tallgrass prairie watersheds, the runoff was underpredicted by WEPP for all scenarios including the wet year that had over 400 mm more precipitation than measured at

CTER in 2015 (Figure 1.10). Runoff in tallgrass prairie watersheds was always predicted to be less than encroached woodland watersheds but there was more observed runoff in the tallgrass prairies than the encroached woodlands. The predicted runoff and sediment yield that was closest to that measured was different in each tallgrass prairie watershed. In P1, the wet year had the closest predicted runoff and sediment to measured values. In P2, the sediment yield predicted in the default scenario was closest to measured sediment yield and was much higher than the wet year which had the highest precipitation and second highest runoff (Figure 1.10). Also, P1 and P2 showed the site-specific CTER 2015 prediction to be the lowest sediment yield (besides the dry year) and all others were within one order of magnitude. Overall, the tallgrass prairie watersheds were more variable in the predicted runoff and sediment yields compared to the encroached woodland watersheds.

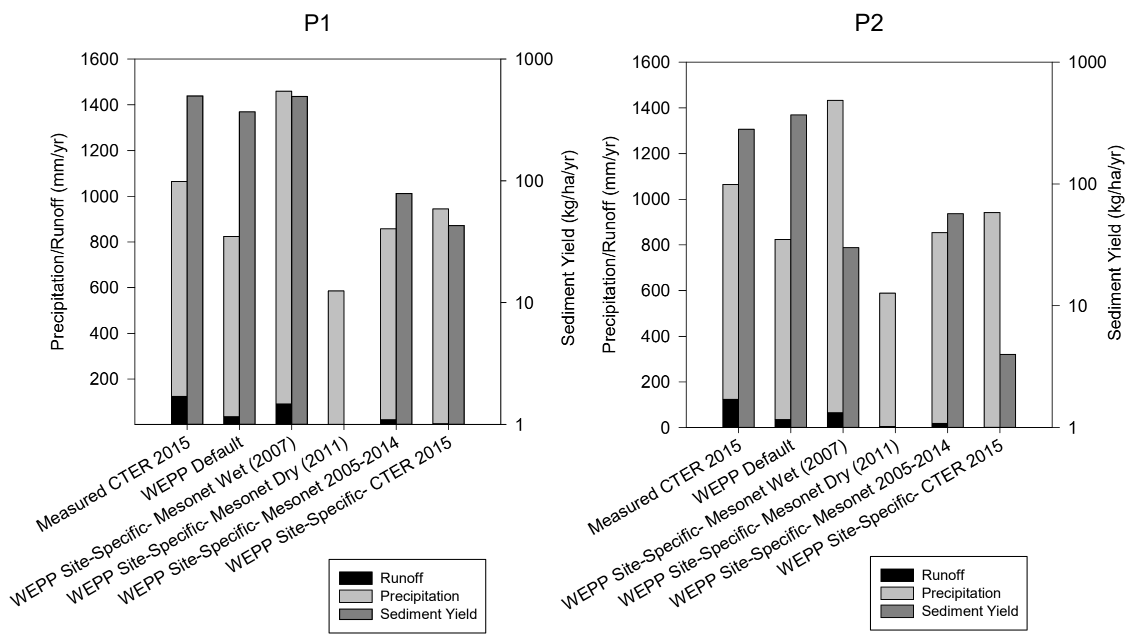

Figure 1.10. Measured precipitation, runoff and sediment yield from CTER was compared to that predicted by WEPP default scenarios and WEPP site-specific scenarios with various climate inputs for tallgrass prairie (P1 and P2) watersheds.

The measured runoff and sediment yield were also compared to the default values used by WEPP to determine how well the model predicted these parameters without any site-specific inputs. In all watersheds, the default values predicted a sediment yield that was close to the measured values. In the encroached woodland watersheds, the runoff predicted from the default values was almost identical to the measured runoff. The default runoff predicted in the tallgrass prairie was not as accurate. However, in P1 and P2, the default scenario predicted sediment yields close to measured even when predicted runoff was much smaller.

1.4.5 Future Research

Although this data suggested that default values could be used to predict runoff and sediment yield in an encroached woodland or tallgrass prairie watershed, it was counterintuitive that the more site-specific values did not provide a better prediction. Therefore, the fit of default parameters to measured values could be random and defaults may not be as accurate at other field locations. Calibration of WEPP using data from CTER would be a good next step.

For calibration of WEPP, it was suggested to begin with K_e to adjust the predicted runoff. Then adjust soil properties including K_i, K_r and τ_c to better simulate the sediment yield (Flanagan et al., 2012). A study in Australia calibrated WEPP to determine if it was suitable for modeling a sandy-soiled pineapple farm (Yu et al., 2000). They found WEPP overestimated runoff for events with high intensity and underestimated runoff for events with low rainfall intensity. Another study reported overprediction of runoff for events less than 5 mm and underprediction for larger storm events (Gronsten and Lundekvam, 2006). Risse et al. (1994) suggested that this occurs because low intensity events over a long duration will change the wetting profile which would affect predicted runoff for larger storms. When calibrating soil parameters, K_i was increased by two orders of magnitude which had more influence on the predicted sediment yield than K_r or τ_c (Yu et al., 2000). Ascough II et al. (2013) found that land cover that was dominated by interrill detachment was not sensitive to the same parameters as those dominated by rill detachment, such as K_r or τ_c. Another Australian study "resisted the temptation of adjusting parameter values to improve simulation results" and used an uncalibrated WEPP to determine the effects of various input parameters on model performance (Yu and Rosewell, 2001). K_e and erodibility parameters were estimated from empirical equations suggested by the WEPP User Summary with no further adjustments. Runoff was still overestimated and CLIGEN predicted larger peak intensities that resulted in higher runoff and sediment loss predicted.

WEPP calibration was suggested when the land management or climate inputs vary from those WEPP has previously tested. Calibration was especially needed in addition to this study because few land management files were available for forest or woodland applications in WEPP. Additionally, many users have been hesitant to use the forest default files available because there were not enough options to represent all forest types. For example, many of the forest land management files currently available used pine species instead of juniper species which have different biophysiological characteristics (Qiao et al, 2015). In the future, the creation of a land management file specifically for Eastern-Redcedar encroached woodlands should be considered.

1.5 Conclusions

Eastern Redcedar encroachment is an ecological problem plaguing the Great Plains. One beneficial method of removing these trees is to use them as a biofuel feedstock. Research on the hydrology of native tallgrass prairie and Easter Redcedar-encroached woodlands is necessary to prevent damaging effects to water quality and quantity in areas where Eastern Redcedar harvest would be considered. Measured runoff and sediment yield under encroached woodlands and tallgrass prairies was compared to WEPP simulations to determine how this model can be used to predict changes water quantity and quality in each land cover. WEPP simulations covered a variety of inputs from basic defaults to site-specific parameters and a variety of climate files. In all simulations, runoff and sediment yield was predicted higher in encroached woodlands than the tallgrass prairies. However, measured data showed double the runoff in tallgrass prairie compared to encroached woodland but similar sediment yields among all watersheds. Therefore, runoff in the encroached woodlands was more concentrated with sediment than in the tallgrass prairies but there was less overall runoff. Furthermore, the WEPP Site-Specific CTER 2015 simulation should have runoff and sediment yield predictions closest to the measured data because it had inputs closest to observed field conditions. However, the default simulation results seemed to best match measured runoff and sediment yield. Future work including calibration of WEPP using data from CTER will provide more guidance on if default values are sufficient or if field-measured parameters improve model predictions.

CHAPTER II

COMPARISON OF FIELD JET EROSION TESTS AND WEPP-PREDICTED ERODIBILITY PARAMETERS FOR VARYING LAND COVER

2.1 Abstract

Hydrologic models are often used to predict the erosion within a watershed and attempt to predict the influence of land cover changes on predicted sediment detachment. One such model is the Water Erosion Prediction Project (WEPP), which determines the runoff and sediment yield of a given hillslope using input data such as the slope, climate, soil and land management characteristics. Currently, WEPP uses empirical equations to determine two major erodibility parameters within the soil input file: the critical shear stress (τ_c) and the erodibility coefficient (k_d). WEPP also uses adjustment coefficients to account for vegetation, such as roots and incorporated residue, and seasonal effects, such as freeze/thaw cycles, on erodibility. This study evaluated soil erodibility parameters under two distinct land covers: native tallgrass prairie and encroaching Eastern Redcedar (*Juniperus virginiana*) woodland. The erodibility parameters from each watershed were first estimated using WEPP and then determined mechanistically in the field using the Jet Erosion Test (JET). The JET-derived erodibility parameters were compared to WEPP-predicted values. The adjusted k_d predicted by WEPP for all watersheds was less than JET-derived k_d by one to two orders of magnitude. The WEPP erodibility parameters were directly correlated with the soil texture and were independent of land cover. Alternatively, JET-derived erodibility parameters were significantly different between the two land covers with no

relationship observed to soil texture. Uncalibrated WEPP simulations failed to indicate differences in predicted sediment transport between the erodibility parameters likely due to the small range in applied shear stress predicted by the model; in cases with greater applied shear significant differences in predicted sediment detachment were expected. This study highlighted the need to use *in situ* testing to determine erodibility of a field site to better incorporate the effects of land cover when predicting hillslope sediment detachment in hydrologic modeling.

2.2 Introduction

Hydrologic models are important tools that can be used to weigh the impacts of land use changes on the detachment of soil from land surfaces. Soil erosion is an important process that impacts many aspects of land and water management, including soil conservation, agricultural productivity, and transport of sediment and other pollutants into receiving waters (Renschler and Harbor, 2002). Changes to agricultural practices and alterations of land cover, such as deforestation or forest encroachment, can have significant effects on soil erosion (Dale et al., 2005), with important environmental consequences. The hydrology of a watershed depends on a variety of factors such as slope, soil characteristics, climate conditions and vegetation cover. Process-based hydrologic models use these parameters to determine the runoff and sediment yields expected in a given watershed or hillslope.

Soil characteristics such as the soil texture can easily be tested to help understand the susceptibility of an area to erosion. However, the effect of land cover on soil erodibility is much harder to quantify. Increased vegetation has consistently been shown to reduce erosion through root reinforcement and aboveground biomass coverage (Simon and Collison, 2002; Simon et al., 2006; DeBaets and Poesen, 2010). There is little quantitative data on the soil erodibility differences in land cover types. Most work considers vegetation characteristics of agricultural crops (Mamo and Bubenzer, 2001) or cover crops (Zhou and Shangguan, 2008; De Baets et al., 2011). This study uniquely focuses on two native land covers common in the southern Great Plains: tallgrass prairie and Eastern Redcedar-encroached woodland.

The excess shear stress equation is used in many hydrologic models such as Bank Stability and Toe Erosion Model (BSTEM), Conservational Channel Evolution and Pollutant Transport Systems (CONCEPTS), Soil and Water Assessment Tool (SWAT), and the Water Erosion Prediction Project (WEPP) to predict sediment detachment (Clark and Wynn, 2007; Daly et al., 2015b):

$$\varepsilon_r = k_d(\tau - \tau_c)^a \quad (1)$$

where ε_r is the erosion rate (m s^{-1}), k_d is coefficient of erodibility (m^3 N^{-1} s^{-1}), τ is the applied shear stress (Pa), τ_c is the critical shear stress (Pa), and a is an exponent usually assumed to be unity (Partheniades, 1965).

Many hydrologic models use empirical equations to predict the erodibility parameters, τ_c and k_d, which commonly do not account for vegetation effects or do so with coefficients that are broad characterizations. Additionally, the overall effect of land cover on erosion parameters used in the excess shear stress equation, such as k_d and τ_c, needs to be further examined to determine how these parameters alter hydrologic modeling.

2.2.1 Jet Erosion Test Studies

The Jet Erosion Test (JET) provides an *in situ* measurement technique to determine the k_d and τ_c. The JET was originally designed at the USDA-Agricultural Research Service (ARS) Hydraulic Engineering Research Laboratory to determine the erodibility of earthen dams and embankments (Hanson and Temple, 2002; Hanson and Hunt, 2007) but has since been used for other applications. Wynn and Mostaghini (2006) and Wynn et al. (2008) applied the JET to streambank locations over time in Virginia and found that root area density and freeze/thaw cycle had significant effects on k_d and τ_c, variability that would not be evident in a soil texture analysis. Using an *in situ* test such as the JET provides a mechanistic way to determine the erodibility parameters that incorporates variability observed in the field.

More recently, the mini-JET was developed as a smaller, more user-friendly version of the original JET. Al-Madhhachi et al. (2013) reported that the mini-JET and original JET provided comparable results. Many studies have utilized the mini-JET in streambank stability and erosion research (e.g., Midgley et al., 2013; Al-Madhhachi et al., 2014; Miller et al., 2014; Daly et al., 2015a; Daly et al., 2015b). However, few studies have been conducted using JETs in a field such as cropland, rangeland, or native vegetation. One study by Potter et al. (2002) performed field JETs using the original JET device on six soils in central Mexico. They discovered that the JET results varied among many soil properties (soil texture, bulk density, organic carbon content, and Atterberg limits) similarly to other erodibility measurement methods such as flume tests. They also determined that changes in land management affected JET results but were not associated with soil properties. This suggests that the land cover can have an effect on the erodibility parameters and that determining these parameters based solely on soil properties can lead to inaccurate erodibility parameter predictions. It is important to note that in contrast to flume-based erosion methods the JET can be deployed *in situ* and thus can directly investigate the variability in soil erodibility that exists in the natural environment with little sample disturbance.

2.2.2 The Water Erosion Prediction Project

The hydrologic model WEPP was used in this study to compare the empirically-derived erodibility parameters to those measured in the field with the JET. WEPP is a process-based erosion model developed by the USDA-ARS National Soil Erosion Research Laboratory (NSERL) to estimate soil loss along a hillslope or within a small watershed based on

“…fundamentals of stochastic weather generation, infiltration theory, hydrology, soil physics, plant science, hydraulics, and erosion mechanics” (Ascough II et al., 1996). WEPP has been used to model runoff, erosion, and management alternatives in agricultural settings (e.g. Das et al., 2004; Renschler and Lee, 2005; Williams et al., 2010; Garbrecht and Zhang, 2015), in forested watersheds (e.g. Wade et al., 2012; Christie et al., 2013; Saghafian et al., 2015) and in grasslands (e.g. Zhang et al., 2008; Wang et al., 2014). Sediment detachment in WEPP is modeled with the excess shear stress equation, and subsequent transport with the Yalin equation (Foster et al., 1995; Stone et al., 1995). The rill erodibility coefficient (k_d) and critical shear stress (τ_c) are determined with empirical equations derived from field experiments by Elliot et al. (1989). The parameters for those equations are drawn from estimates of soil texture, specifically the percent very fine sand (Alberts et al., 1995). In WEPP, the baseline k_d is intended to model characteristics of a “freshly-tilled soil” (Alberts et al., 1995), to which adjustment factors are applied to account for the root biomass and incorporated residue of vegetation and soil consolidation.

However, as WEPP is applied to environments such as woodlands or prairies, the soil conditions to be modeled depart dramatically from tilled agricultural soil. Encroached woodland and prairie soils also include various forms of soil aggregates, root biomass consisting of roots of many ages and species, and seasonal texture changes induced by freeze/thaw, any or all of which may affect soil detachment and erosion (Sabatini et al., 2015; Yu et al., 2015). It is unlikely that soil texture alone will capture these characteristics, and therefore the accuracy of WEPP sediment yield predictions in these environments will rely primarily on application of the adjustment factors. When applying a process-based model like WEPP to developed soils in natural landscapes, it may be preferable to utilize *in situ* erodibility parameters that directly account for those characteristics and more closely estimate the actual soil erodibility.

2.2.3 Objectives

The objective of this research was to determine if JET-derived k_d and τ_c indicate changes in land cover better than WEPP's empirically-predicted k_d and τ_c. This study compared erodibility parameters (k_d and τ_c) for two land cover types: native tallgrass prairie or 20-yr stands of Eastern Redcedar-encroached woodland. The k_d and τ_c were measured at various locations in these watersheds using *in situ* JETs. Soil samples from those locations were analyzed, and the percent very fine sand, clay and organic matter were used to determine k_d and τ_c using empirical equations from WEPP.

2.3 Materials and Methods

2.3.1 Field Research Sites

The research was conducted at the Cross Timbers Experimental Range (CTER) near Stillwater, OK. The CTER was located within the Cross Timbers ecoregion defined as a "complex mosaic of upland deciduous forest, savanna, and prairie" which spanned portions of Oklahoma, Texas, Kansas and Arkansas (Hoagland et al., 1999). Eastern Redcedar encroachment of native grasslands has become an increasing problem in this region in the past decade (Engle et al., 2008). This species negatively impacts the ecosystem, especially regarding water use and consumption (Zou et al., 2014). Four individual watersheds were identified at CTER with contrasting vegetative land cover: two native tallgrass prairie watersheds and two Eastern Redcedar-encroached woodland watersheds (Figure 2.1).

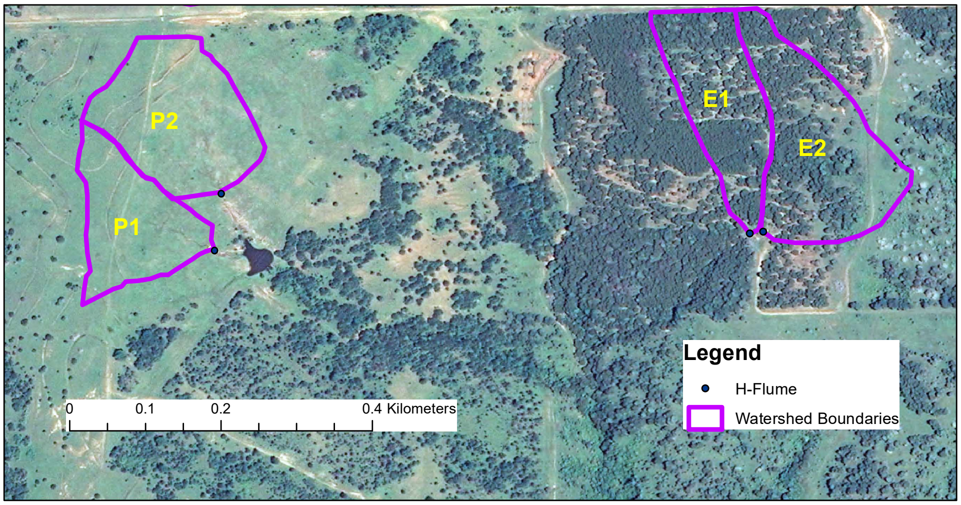

Figure 2.1. Cross Timbers Experimental Range (CTER) field site including two tallgrass prairie (P1, P2) and two Eastern Redcedar-encroached woodland (E1, E2) watersheds located less than 15 km southwest of Stillwater, OK.

The total area and slope were determined by in-field surveying to delineate watershed boundaries (Table 2.1). High-resolution GPS was used to map the watersheds in ArcGIS 10.2 (ESRI, 2013), and these were compared to watersheds delineated from LiDAR data to validate field results. Two weather monitoring stations, one in a tallgrass prairie watershed (P2) and one in an encroached woodland watershed (E2), have collected weather data since 2011. Additional weather data from an Oklahoma Mesonet station located less than three kilometers from the research site was also utilized. H-flumes at the mouth of each watershed have been in place since 2010 to measure water yield during runoff events, and ISCO autosamplers have been in place at each flume since 2014 to collect sediment samples. These background datasets provided local information for modeling water quality and quantity changes in each watershed.

Table 2.1. OSU Cross Timbers Experimental Range watershed characteristics for Eastern Redcedar-encroached woodland (E1, E2) and tallgrass prairie (P1, P2) land cover.

	Eastern Redcedar		Tallgrass Prairie	
	E1	E2	P1	P2
Area (ha)	2.6	3.8	2.3	3.3
Slope (%)	2.0-7.5	3.5-4.5	2.0-7.0	1.0-7.5

2.3.2 Soil Sampling and Processing

To determine more site-specific soil data, 20 to 30 soil samples were acquired throughout each watershed. Using ArcGIS 10.2 (ESRI, 2013), a grid sampling system was set up for each of the experimental watersheds so that each sampling point was 25 to 35 m apart. Soil samples were taken corresponding to five soil layers. The depths of these layers were chosen based on the layer depths of the Stephenville-Darnell complex which consists of loam and sandy loam, and covers the majority of the watershed study area (SSURGO). This Stephenville soil series typically consists of four soil horizons: A (0 to 13 cm), E (13 to 38 cm), B (38 to 84 cm), and C (84 to 130 cm-sandstone bedrock layer). The Darnell soil series consists of three layers: A (0 to 13 cm), B (13 to 38 cm), and the sandstone horizon C (38 to 76 cm). This typical profile was assumed to be constant over the study area, and soil samples were obtained from depths 0-13, 13-38, 38-64, 64-89, and 89-114 cm.

Individual samples from each watershed were composited into one sample per depth to act as an average soil sample from each depth per watershed. The composite samples were tested at the Oklahoma State University Soil, Water, and Forage Analytical Laboratory for soil texture and organic matter. The results for each depth per watershed was entered as a soil layer within the WEPP soil database editor and saved as a new soil for each watershed. More detailed particle size analyses to determine very fine sand content and clay content were performed using the hydrometer method as described by ASTM D-422-63 (ASTM, 2002) on samples obtained at individual locations where JETs were conducted (Figure 2.2).

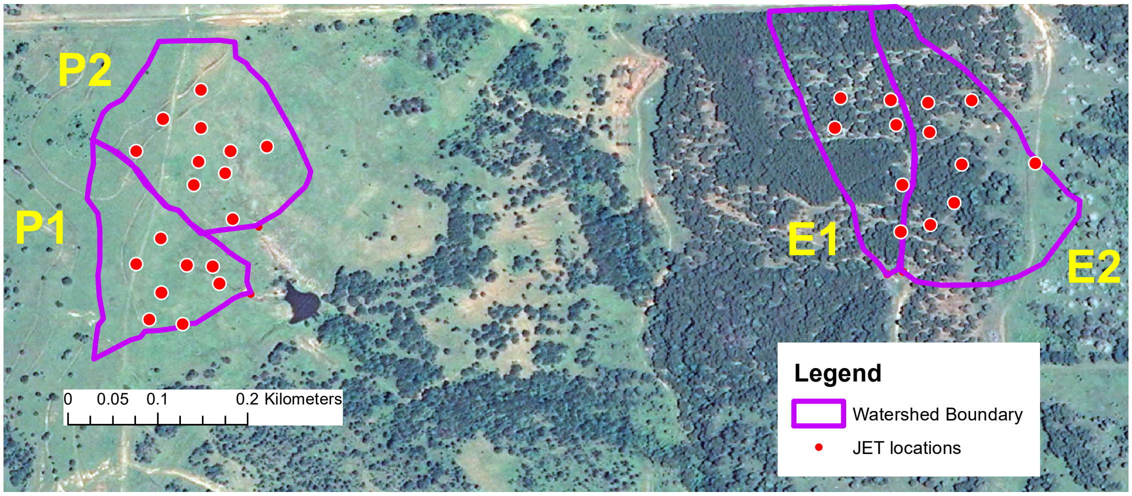

Figure 2.2. Aerial image of experimental watersheds at the Cross Timbers Experimental Range field site including two tallgrass prairie (P1, P2) and two Eastern Redcedar-encroached woodland (E1, E2) watersheds displaying JET testing locations.

2.3.3 WEPP Estimation of Erodibility

In WEPP, sediment detachment and transport is modeled using the excess shear stress and Yalin equations (Foster et al., 1995; Stone et al., 1995). The rill erodibility (k_d) and critical shear stress (τ_c) are determined by empirical equations derived from field experiments by Elliot et al. (1989). WEPP calculates the k_d and τ_c for each soil file unless user-input parameters are used. The empirical formula considers various factors such as sand, clay and organic matter fractions to determine baseline erodibility parameters. The baseline rill erodibility (k_{db}) was calculated as a function of the percent of very fine sand (*vfs*) and organic matter (*orgmat*) in the top 20 cm of the soil:

$$k_{db} = 0.00197 + 0.030vfs + 0.03863\mathrm{e}^{(-184orgma\ )} \quad (2)$$

Adjustment factors are multiplied by k_{db} to derive an adjusted rill erodibility (k_{dadj}) which accounts for aspects that change over time such as incorporated residue, roots, sealing and crusting, and freezing and thawing.

The baseline critical shear stress (τ_{cb}) was calculated as a function of the percent of clay and *vfs* in the top 20 cm of soil:

$$\tau_{cb} = 2.67 + (6.5\text{clay}) - (5.8vfs) \tag{3}$$

Similarly, the model had adjustments such as random roughness, sealing and crusting, and freezing and thawing which were multiplied by τ_{cb} calculated in equation (3).

2.3.4 JET Estimation of Erodibility

In a mini-JET (from here forward, referred to as simply the JET), a submerged jet of water impinges on and erodes the soil surface, and the scour depth over time is measured with a depth gauge. The scour depth over time and the head pressure for each JET is entered into a macro-enabled Excel spreadsheet which uses an iterative solver routine to determine k_d and τ_c. The Blaisdell and scour depth solution techniques described by Daly et al. (2013) are used in the spreadsheet to transform the raw test data into erodibility parameters. The Blaisdell solution is currently the standard solution for JETs but has been shown to underestimate τ_c. The scour depth solution was developed to fit the scour depth over time data using a simultaneous iterative solver technique (Daly et al., 2013).

JETs were conducted to provide site-specific quantification of erodibility parameters including effects of land cover and cohesive characteristics of below-ground root biomass. Five to ten JETs were conducted in each watershed with individual tests located so that all soil types in the watershed as indicated by the SSURGO database were represented. Test locations were concentrated in the lower half of the watershed closer to the H-flume so the results better represented the sediment detachment in runoff samples collected at the flume (Figure 2.2).

When JETs are conducted to measure streambank erosion in the field, access to water is rarely a test constraint. In the test watersheds, which were far from flowing streams, special arrangements were made to conduct JETs. A truck designed for managing controlled burns was moved close to the test site then water was pumped from its 3000 L tank through a hose to the head tank (Figure 2.3). Water under constant pressure from the head tank was then dispensed through another hose to the JET device. Return water from the constant head tank was pumped upslope to the storage on the truck for later reuse (Figure 2.3). For these tests, the head difference between the top of the tank and the jet aperture was typically set at 66 to 76 cm but some tests were higher due to constraints such as the slope or compacted soil. A waste hose was used to direct the water leaving the JET device away from the test area (Figure 2.3). Erodibility parameters derived from JETs with the Blaisdell and scour depth solutions were compared to erodibility parameter values estimated from the empirical equations used in WEPP. Also, relationships between JET-derived erodibility parameters with the percent *vfs* were investigated. Two sample t-tests were conducted on the erodibility parameters determined from both WEPP and JETs to determine statistical differences between the two land cover types and the two dominant soil textures.

Figure 2.3. Controlled-burn truck used to provide water to field site (left), head tank that delivers constant pressure to JET and recycle loop to send water back to tank (middle), and JET device in field (right).

2.3.5 WEPP Modeling

Uncalibrated WEPP simulations were completed using inputs that best represented each watershed. WEPP uses four main input parameters: climate, slope, soil and land management. The climate file used was a breakpoint file containing weather data from two weather stations at CTER;

one in the encroached woodland (E2) and one in a tallgrass prairie (P2). A few other climate files were tested as well including long-term Mesonet data over a 10-year period (2005-2015), a single wet year (2007) with the highest annual total rainfall (1370 mm) in the last 10 years, and a single dry year (2011) which only reached an annual rainfall total of 585 mm. The slope file was created using 2-m LiDAR elevation datasets in ArcGIS. The land management file corresponded to the two default vegetation types already present in the WEPP model: 20-year forest to represent the Eastern Redcedar encroached watersheds and tallgrass prairie to represent the native grasslands. Lastly, the soil file was composed using detailed soil texture data from each watershed as well as the effective conductivity, soil albedo, and initial saturation. The erodibility parameters were initially calculated by WEPP. Next, each of the WEPP soil input files were adjusted using JET-derived k_d and τ_c for the corresponding watershed. These uncalibrated simulations were compared to determine the effect of altering erodibility parameters on WEPP-predicted runoff and sediment yield in these watersheds.

2.4 Results and Discussion

2.4.1 Soil Texture Analysis

Soil texture classification is important for this study because WEPP emphasizes its influence on erodibility parameters. The composite topsoil texture was loam, sandy loam, or sandy clay loam but was generally split into two groups: greater than or less than 50 percent sand (Table 2.2). The averaged topsoil texture from the individual JET locations was primarily sandy loam with one sandy clay loam watershed (Table 2.3). Twenty-six of the thirty-one individual sample locations were either sandy loam or sandy clay loam; the remaining points were loam except one that was loamy fine sand. The erodibility experiments by Elliot et al. (1989) covered a wide range of soil textures to develop the empirical equations used in WEPP which corresponded to a wide range of k_d and τ_c.

Table 2.2. Composite soil texture in the top two layers for each watershed: tallgrass prairie (P1, P2) and encroached woodland (E1, E2).

Composite Topsoil Texture						
Watershed	Layer (cm)	Sand (%)	Average Sand (%)	Clay (%)	Average Clay (%)	Texture
E1	0-10	46.3		17.5		
	10-20	45.4	45.8	23.0	20.2	Loam
E2	0-10	58.8		17.5		
	10-20	53.3	56.1	24.8	21.2	Sandy Clay Loam
P1	0-10	55.0		15.0		
	10-20	53.2	54.1	20.5	17.7	Sandy Loam
P2	0-10	46.3		18.8		
	10-20	46.3	46.3	23.3	21.1	Loam

Table 2.3. Averaged soil texture in the top two layers from JET locations in each watershed: tallgrass prairie (P1, P2) and encroached woodland (E1, E2).

Averaged Topsoil Texture						
Watershed	Layer (cm)	Sand (%)	Average Sand (%)	Clay (%)	Average Clay (%)	Texture
E1	0-10	65.3		17.7		
	10-20	56.0	60.6	24.6	21.1	Sandy Clay Loam
E2	0-10	58.7		16.4		
	10-20	54.0	56.4	22.7	19.5	Sandy Loam
P1	0-10	55.6		16.6		
	10-20	55.8	55.7	20.7	18.6	Sandy Loam
P2	0-10	49.3		16.6		
	10-20	57.6	53.4	22.3	19.5	Sandy Loam

2.4.2 Relationship to Very Fine Sand Content

The empirical equations used in determining k_d and τ_c in WEPP are both dependent on the percent *vfs* which was calculated as 25% of the total sand content (J. Frankenburger, personal communication, July 21, 2015). The WEPP baseline k_d had an increasing linear relationship with *vfs* content and the τ_c had a linear decreasing relationship with *vfs* (Figure 2.4). The scatter around the regression line was due to the effect of organic matter and clay content on the k_d and τ_c, respectively, as these were the only other contributing factors in the empirical equations (Figure

2.4). In contrast, no linear relationship was apparent when analyzing the relationship between *vfs* and JET-derived k_d and τ_c (Figure 2.5). This may be due to the effects of secondary soil characteristics such as soil and root cohesion, and supports the hypothesis that *in situ* JET testing indicated more variation in soil erodibility than can be determined with an empirical equation based on *vfs*. This emphasized that there are numerous factors to consider when estimating erodibility parameters.

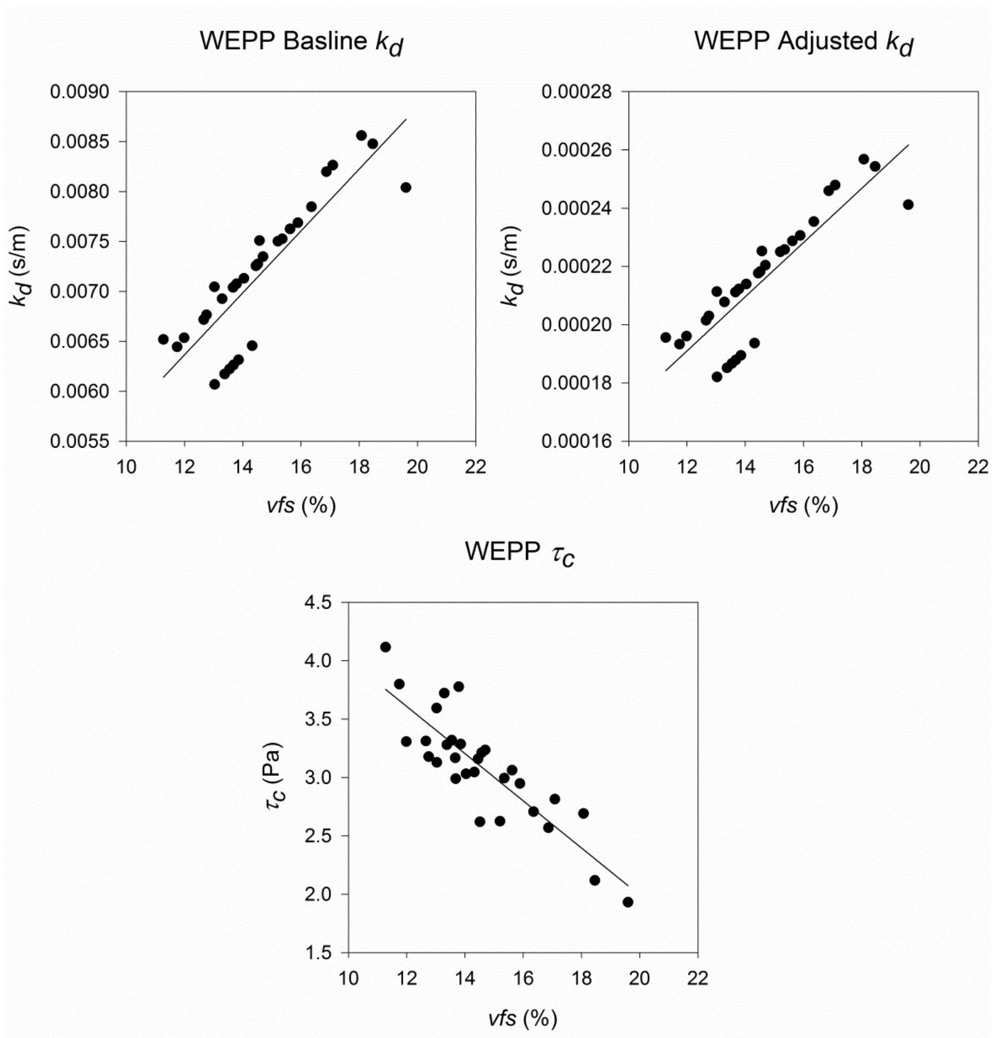

Figure 2.4. Very fine sand (*vfs*) percentage from each JET location compared to the WEPP baseline and adjusted k_d and the baseline τ_c calculated from equations (2) and (3). A line of best fit was used to demonstrate the linear relationship predicted.

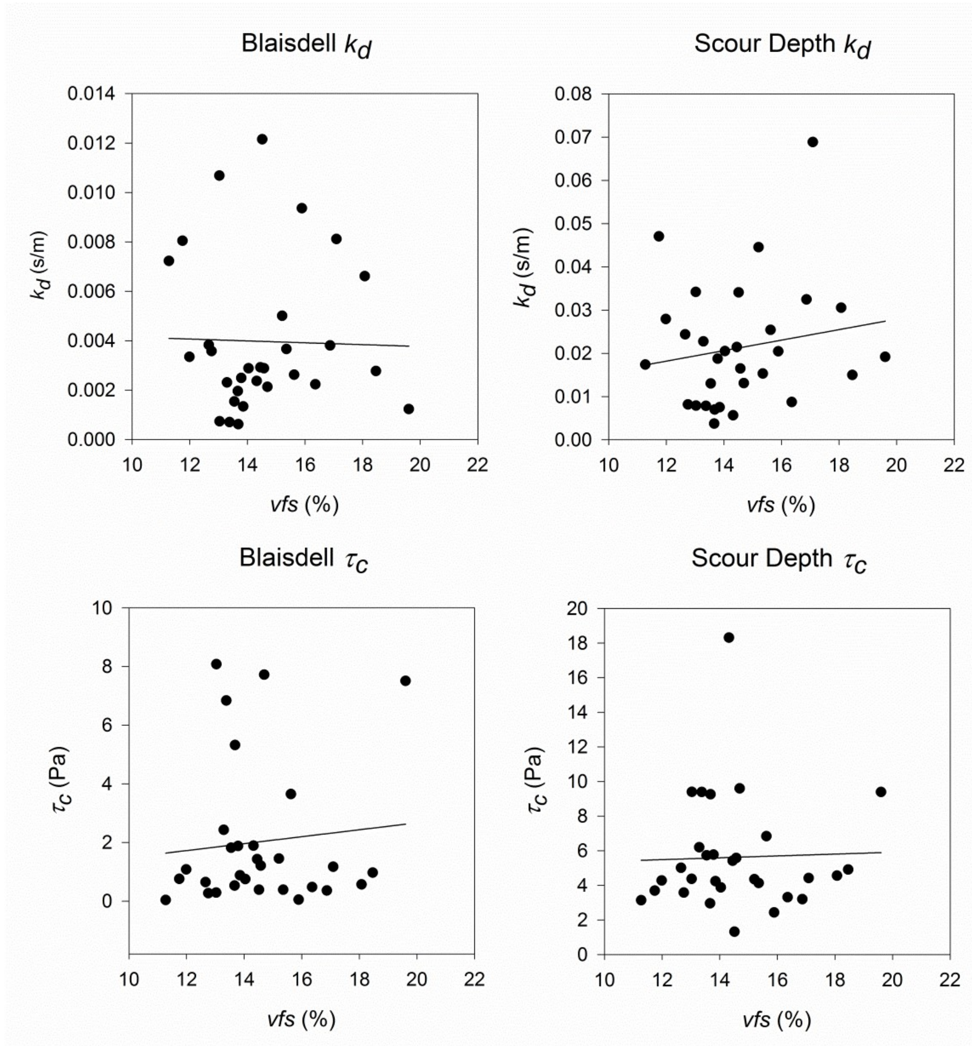

Figure 2.5. Very fine sand (*vfs*) percentage from each JET location compared to k_d and τ_c derived from JET solution techniques (Blaisdell and scour depth). A line of best fit was used to demonstrate the non-linear relationship.

2.4.3 Comparing WEPP and JET Estimations of Erodibility

In the encroached woodland watersheds, the average τ_c from the scour depth solution better matched the τ_c estimated from WEPP. However, the upper k_d values from the Blaisdell solution were more similar to the k_d from the WEPP composite baseline data (Figure 2.6). In the tallgrass prairie watersheds, the composite baseline k_d estimated from WEPP matched the individual scour depth k_d values better than the Blaisdell k_d values but was on the lower end of the scour depth k_d values. The τ_c predicted by WEPP and the τ_c from both the scour depth and

Blaisdell solutions in the tallgrass prairie watersheds were all within the same order of magnitude (Figure 2.6).

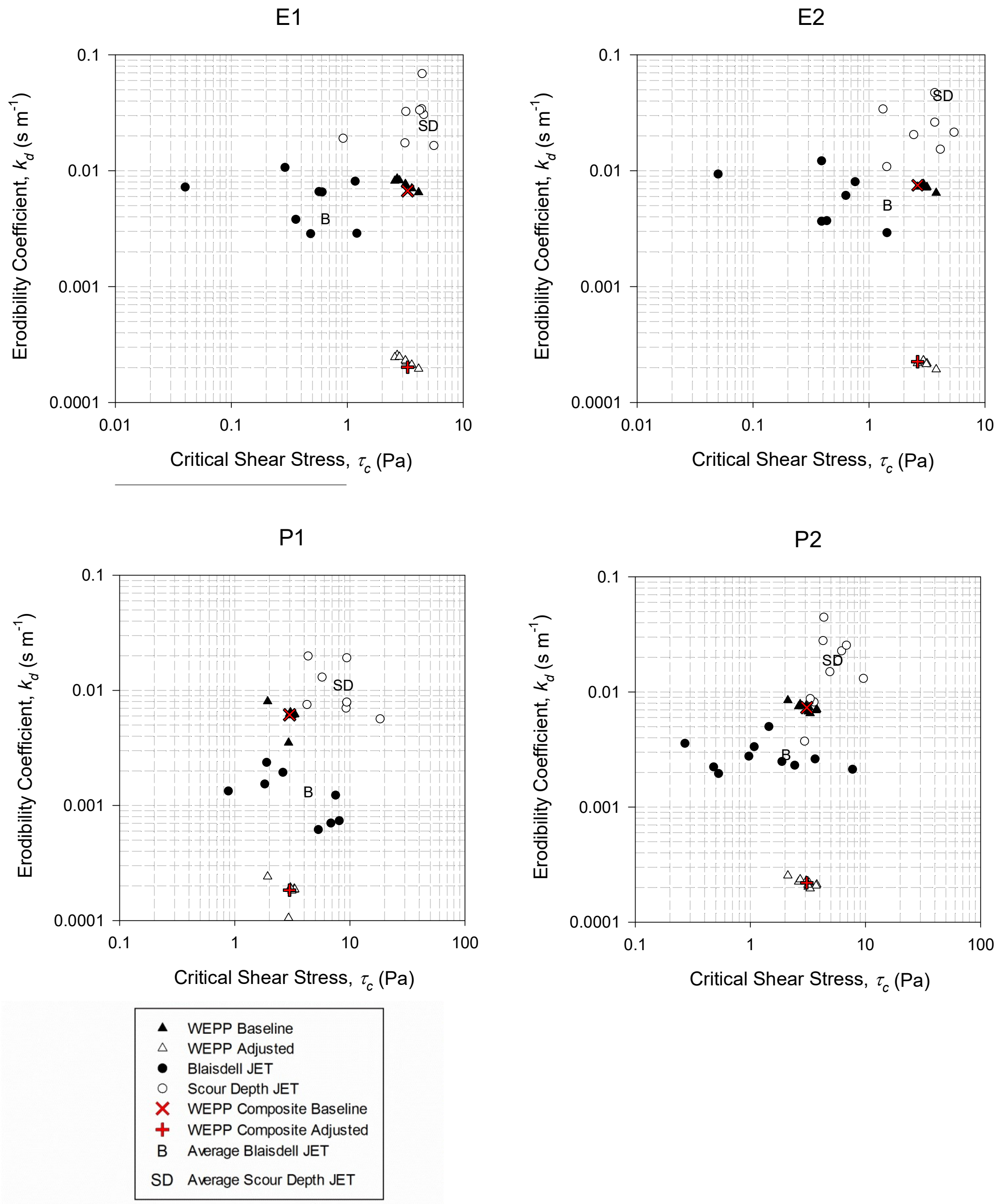

Figure 2.6. Distribution of erodibility coefficients for each watershed: tallgrass prairie (P1, P2) and encroached woodland (E1, E2). Shown are Blaisdell and scour depth JET solution values and WEPP baseline and adjusted values for composited and individual texture samples.

WEPP uses a single adjustment factor to account for effects of seasonal changes on erodibility such as incorporated crop residue, roots, sealing and crusting, and freezing and thawing. The adjustment factor is determined based on inputs such as the land management and climate, and there is no method for the user to alter any of these influences individually. This adjustment factor was multiplied by the baseline k_d. The adjustment factor was consistently 0.03 for both land covers used in WEPP (Table 2.4). The adjusted k_d and τ_c estimates from WEPP were smaller than the baseline values by an order of magnitude (Table 2.4) and the adjusted k_d predicted by WEPP for all watersheds was less than JET-derived k_d (Figure 2.6).

In the encroached woodland watersheds, the average Blaisdell k_d was similar to the WEPP baseline k_d. In contrast, the WEPP baseline k_d for the tallgrass prairie watersheds was two to three times larger than the Blaisdell average k_d. At the extremes of k_d estimates, the average of the scour depth k_d was highest in all watersheds, and the adjusted WEPP k_d values were one to two orders of magnitude smaller than the other k_d estimation methods (Table 2.4). The empirical equations utilized in WEPP to predict the k_d values are dependent solely on soil texture. Therefore, because E1 and P1 have similar soils, they had similar WEPP-estimated k_d, and the same held true for E2 and P2. In contrast, the mean of JET-derived k_d and τ_c appear to group according to vegetation cover rather than soil texture (Table 2.4). For example, the scour depth k_d values at the tallgrass prairie sites were up to two times smaller than the encroached woodland values, and the Blaisdell k_d four times smaller (Table 2.4). Such results question whether erodibility parameters for these land cover types can be determined solely from soil texture as the JET-derived erodibility parameters exhibited no pattern among soil texture but more so with vegetative cover. This is supported by Potter et al. (2002) which found that changes in land management affected JET results but were not associated with measured soil properties.

Table 2.4. WEPP and JET values for k_d and τ_c in each watershed (tallgrass prairie (P1, P2) and encroached woodland (E1, E2)) shows relationship of erodibility parameters compared to soil texture and vegetation type.

	E1	E2	P1	P2
Top Soil Texture (0-20cm)	Loam	Sandy Clay Loam	Loam	Sandy Loam
WEPP Adjusted k_d (s/m)	1.97E-04	2.14E-04	1.95E-04	2.42E-04
WEPP Erodibility Adjustment Factor	0.03	0.03	0.03	0.03
WEPP Baseline k_d (s/m)	6.57E-03	7.13E-03	6.50E-03	8.07E-03
Blaisdell JET k_d (s/m)	6.46E-03	4.91E-03	1.73E-03	2.90E-03
Scour Depth JET k_d (s/m)	3.27E-02	2.61E-02	1.41E-02	1.96E-02
WEPP Baseline τ_c (Pa)	3.32	3.23	3.37	3.04
Blaisdell JET τ_c (Pa)	0.60	0.78	4.37	2.65
Scour Depth JET τ_c (Pa)	4.26	4.31	8.76	5.69

The erodibility parameters from JETs showed a significant difference between tallgrass prairie and encroached woodland covers but the WEPP values were not significantly different among land cover at α=0.05 (Table 2.5 and 2.6). Conversely, there was no significant difference between soil textures (sandy loam and sandy clay loam) for any erodibility parameters measured with JETs at α=0.05. There was a significant difference (α=0.05) among soil textures when erodibility parameters were estimated with WEPP, as was expected since soil texture was the main consideration of its empirical equations. Therefore, soil texture did not have a strong enough influence on the JET to differentiate erodibility parameters from alternate soil textures, but WEPP's empirical erodibility parameter equations placed so much influence on soil texture it was unable to distinguish erodibility differences between the two land covers.

Table 2.5. Two-sample t-tests results on erodibility parameters from WEPP baseline and JETs to determine if there was a significant difference between tallgrass prairie and encroached woodland watersheds. Bolded values indicate statistically significant at α=0.05. DF refers to degrees of freedom.

Land Cover t-test	p-value	DF
WEPP Baseline k_d (s/m)	0.116	27
Blaisdell JET k_d (s/m)	**0.001**	14
Scour Depth JET k_d (s/m)	**0.008**	20
WEPP Baseline τ_c (Pa)	0.605	26
Blaisdell JET τ_c (Pa)	**0.003**	16
Scour Depth JET τ_c (Pa)	**0.006**	20

Table 2.6. Two-sample t-tests results on erodibility parameters from WEPP baseline and JETs for each soil texture to determine if they were significantly different. Bolded values indicate statistically significant at α=0.05. DF refers to degrees of freedom.

Soil Texture t-test	p-value	DF
WEPP Baseline k_d (s/m)	**0.014**	23
Blaisdell JET k_d (s/m)	0.714	21
Scour Depth JET k_d (s/m)	0.640	23
WEPP Baseline τ_c (Pa)	**<0.001**	20
Blaisdell JET τ_c (Pa)	0.568	19
Scour Depth JET τ_c (Pa)	0.882	21

2.4.4 Erodibility Parameter Effects on WEPP Predictions

The next step in evaluating different erodibility parameters was to determine how changes in erodibility parameters affected sediment yield predictions in WEPP. No changes in sediment yield were evident in the preliminary uncalibrated WEPP simulations based on changes in erodibility parameters in the two encroached woodland watersheds (Table 2.7). P1 showed a small change in sediment yield in the climate scenario with the most precipitation.

Table 2.7. WEPP scenarios using site-specific inputs for each watershed and soil input files with JET-measured and WEPP-calculated erodibility parameters under various climates. SD stands for the scour depth method. Bolded values are those where a difference was found.

		E1			E2			P1			P2		
Climate	Simulation	P[b] (mm)	Q[c] (mm)	Sediment Yield (t/ha)	P (mm)	Q (mm)	Sediment Yield (t/ha)	P (mm)	Q (mm)	Sediment Yield (t/ha)	P (mm)	Q (mm)	Sediment Yield (t/ha)
Wet (2007)	WEPP	1370	153	3.45	1370	121	0.29	1370	91	0.49	1370	64.61	0.03
	JET Blaisdell	1370	153	3.45	1370	121	0.29	1370	91	**0.44**	1370	**64.64**	0.03
	JET SD[a]	1370	153	3.45	1370	121	0.29	1370	91	**0.44**	1370	**64.64**	0.03
Dry (2011)	WEPP	585	0	0	585	0	0	585	0	0	585	4.25	0
	JET Blaisdell	585	0	0	585	0	0	585	0	0	585	**0.2**	0
	JET SD	585	0	0	585	0	0	585	0	0	585	**0.2**	0
10 year (2005-2014)	WEPP	836	35	2.36	836	34	0.22	836	21	0.08	836	17.98	0.06
	JET Blaisdell	836	35	2.36	836	34	0.22	836	21	0.08	836	**17.99**	0.06
	JET SD	836	35	2.36	836	34	0.22	836	21	0.08	836	**17.99**	0.06
CTER 2015	WEPP	1085	20	0.99	1085	12	0.13	940	4	0.04	940	1.66	0.004
	JET Blaisdell	1085	20	0.99	1085	12	0.13	940	4	0.04	940	**0.33**	0.004
	JET SD	1085	20	0.99	1085	12	0.13	940	4	0.04	940	**0.33**	0.004

[a]SD=scour depth method; [b]P=Precipitation; [c]Q=Runoff

Note that the shear stress (τ) was calculated from the runoff depth, the rill width, and the slope produced by WEPP. The maximum τ was approximately 16 Pa determined from a maximum runoff depth per storm of 59 mm and five percent average slope which corresponded to the watershed with the highest slope (E1). The other three watersheds had an average slope of four percent and the maximum τ of those watersheds was approximately 13 Pa from a runoff event of 57 mm. WEPP adjusted the calculated τ based on friction factors related to surface roughness and interception due to aboveground biomass, which further reduced the overall τ acting on the soil. Therefore, WEPP calculated smaller τ impacting the soil than anticipated by calculating the shear stress from the runoff depth alone.

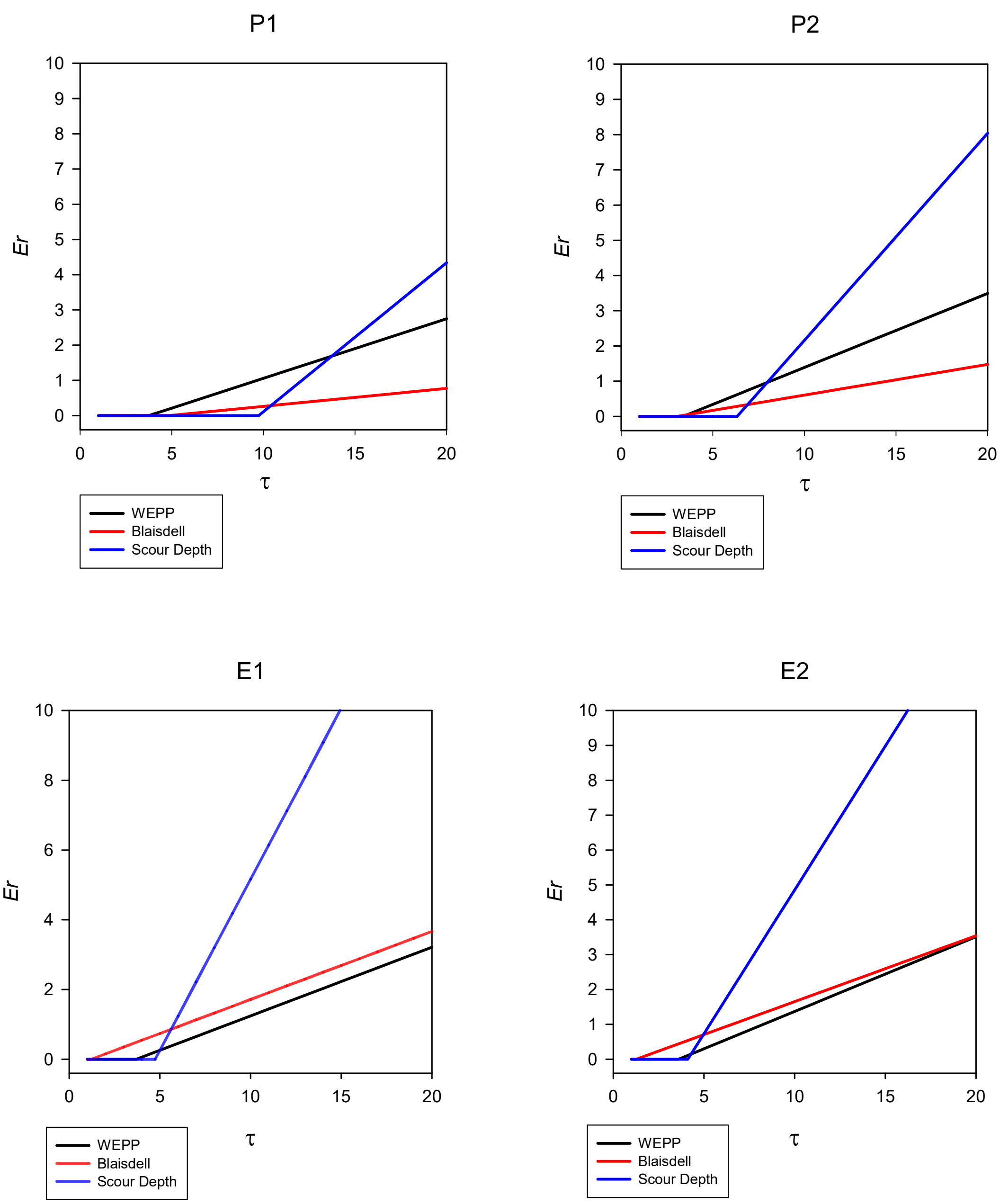

Figure 2.7. The excess shear stress was plotted for encroached woodland (E1 and E2) and tallgrass prairie (P1 and P2) watersheds to find the erosion rate (*Er*) in relation to the shear stress (τ) where τ_c is the point when *Er* increases above zero and k_d is the slope of the line. An equation was plotted for each of the sets of erodibility parameters (WEPP, Blaisdell and Scour Depth).

When using JET-derived and WEPP-predicted k_d and τ_c in the excess shear stress equation, predicted erosion rates were approximately equivalent when τ was close to τ_c because the slope (k_d) had a larger influence on the erosion rate as τ increased (Figure 2.7). So, smaller τ values led to similar erosion rates calculated using the JET-derived and WEPP-predicted erodibility parameters. The small changes in sediment yield seen in P1 may be attributed to slightly higher τ than in P2 which would accentuate the influence of the erodibility parameters. Also, the JETs did not account for the change in shear stress attributed to resistance from aboveground biomass but instead incorporated effects of site-specific soil characteristics such as root cohesion. By adjusting the τ with vegetative friction factors, WEPP emphasized the effect of aboveground biomass on reducing erosion.

2.5 Conclusions

Studies have suggested a relationship between changes in erosion and different vegetation or land cover. The k_d and τ_c are two parameters that are often used in hydrologic models to estimate sediment detachment using the excess shear stress equation. Therefore, the effects that land cover has on these erodibility parameters are research questions that could lead to improvement of the approximation of sediment detachment in hydrologic models. Many of these models empirically derive erodibility parameters based primarily on soil texture but some have adjustments for vegetation and seasonal effects. However, this method does not fully incorporate the variability seen in the field especially across a limited range in soil texture. Using *in situ* JETs provided estimated k_d and τ_c values that physically represented the erodibility at a location. In this research, k_d and τ_c were dependent on more than just soil texture alone; land cover had a significant impact on these parameters. Furthermore, the distinct differences in erodibility parameters did not appear to change predicted sediment yield using an uncalibrated WEPP for the range of shear stress simulated in these watersheds, but in cases with greater applied shear, significant differences in predicted sediment detachment are expected.

REFERENCES

Alberts, E.E., Nearing, M.A., Weltz, M.A., Risse, L.M., Pierson, F.B., Zhang, X.C., Laflen, J.M., & Simanton, J.R. (1995). USDA-Water Erosion Prediction Project (WEPP). Chapter 7: Soil Component. NSERL Report No. 10, USDA-ARS National Soil Erosion Research Lab., West Lafayette, IN.

Al-Madhhachi, A. T., Fox, G. A., & Hanson, G. J. (2014). Quantifying the Erodibility of Streambanks and Hillslopes Due to Surface and Subsurface Forces. *Transactions of the ASABE, 57*(4), 1057-1069.

Al-Madhhachi, A. T., Hanson, G. J., Fox, G. A., Tyagi, A. K., & Bulut, R. (2013). Measuring Soil Erodibility Using a Laboratory "Mini" Jet. *Transactions of the ASABE, 56*(3), 901-910.

Ascough II, J.C., Baffaut, C., Nearing, M.A., & Liu, B.Y. (1996). The WEPP Watershed Model: Chapter 1: Hydrology and Erosion. *Transactions of the ASAE* 40(4): 921-933.

Ascough, J.C., Flanagan, D.C., Nearing, M.A., & Engel, B.A. (2013). Sensitivity and First-Order/Monte Carlo Uncertainty Analysis of the Wepp Hillslope Erosion Model. *Transactions of the ASABE*, 56(2), 437-452.

ASTM Standard D422-63, 1998 (2002), “Standard Test Method for Particle-Size Analysis of Soils,” ASTM International, West Conshohocken, PA, 2002.

Brock, F.V., Crawford, K.C., Elliott, R.L., Cuperus, G.W., Stadler, S.J., Johnson, H.L., & Eilts, M.D. (1995): The Oklahoma Mesonet: A technical overview. *J. Atmos. Oceanic Technol.,* 12, 5-19.

Caterina, G.L., Will, R.E., Turton, D.J., Wilson, D.S., & C.B. Zou, (2014). Water use of *Juniperus virginiana* trees encroached into mesic prairies in Oklahoma, USA. *Ecohydrology* 7(4): 1124-1134. DOI:10.1002/eco.1444

Christie, A.M., Aust, W.M., Zedaker, S.M., & Strahm, B.D. (2013). Potential Erosion from Bladed Fire lines in the Appalachian Region Estimated with USLE-Forest and WEPP Models. *Southern Journal of Applied Forestry, 37*(3), 140-147. doi:10.5849/sjaf.12-021

Clark, L.A., & Wynn, T. M. (2007). Methods for determining streambank critical shear stress and soil erodibility: Implications for erosion rate predictions. *Transactions of the ASABE, 50*(1), 95-106.

Dale, V., Archer, S., Chang, M., & Ojima, D. (2005). Ecological impacts and mitigation strategies for rural land management. *Ecological Applications, 15*(6), 1879-1892. doi:10.1890/03-5330

Daly, E.R., Fox, G.A., Al-Madhhachi, A.T., & Miller, R.B. (2013). A Scour Depth Approach for Deriving Erodibility Parameters from Jet Erosion Tests. *Transactions of the ASABE, 56*(6), 1343-1351.

Daly, E.R., Fox, G.A., Enlow, H.K., Storm, D.E., & Hunt, S.L. (2015a). Site-scale variability of streambank fluvial erodibility parameters as measured with a jet erosion test. *Hydrological Processes, 29*(26), 5451-5464. doi:10.1002/hyp.10547

Daly, E.R., Miller, R.B., & Fox, G.A. (2015b). Modeling streambank erosion and failure along protected and unprotected composite streambanks. *Advances in Water Resources, 81*, 114-127. doi:10.1016/j.advwatres.2015.01.004

Das, C., Capehart, W.J., Mott, H.V., Zimmerman, P.R., & Schumacher, T.E. (2004). Assessing regional impacts of Conservation Reserve Program-type grass buffer strips on sediment load reduction from cultivated lands. *Journal of Soil and Water Conservation, 59*(4), 134-142.

De Baets, S., & Poesen, J. (2010). Empirical models for predicting the erosion-reducing effects of plant roots during concentrated flow erosion. *Geomorphology, 118*(3-4), 425-432. doi:10.1016/j.geomorph.2010.02.011

De Baets, S., Poesen, J., Meersmans, J., & Serlet, L. (2011). Cover crops and their erosion-reducing effects during concentrated flow erosion. *Catena, 85*(3), 237-244. doi:10.1016/j.catena.2011.01.009

Eggemeyer, K.D., Awada, T., Harvey, F.E., Wedin, D.A., Zhou, X., & Zanner, C.W. (2009). Seasonal changes in depth of water uptake for encroaching trees *Juniperus virginiana* and *Pinus ponderosa* and two dominant C4 grasses in a semiarid grassland. *Tree Physiology*, 29(2), 157-169. doi:10.1093/treephys/tpn019

Elliott, W.J., Liebenow, A.M., Laflen, J.M. & Kohl, K.D. (1989). A Compendium of Soil Erodibility Data From WEPP Cropland Soil Field Erodibility Experiments 1987 & 1988. NSERL Report No. 3, USDA-ARS National Soil Erosion Research Lab., West Lafayette, IN.

Engle, D., Coppedge, B.R. & Fuhlendorf, S.D. (2008). Western North American Juniperus Communities. In O.W. VanAuken, ed. From the Dust Bowl to the Green Glacier: Human Activity and Environmental Change in Great Plains Grasslands, (pp. 253-271). New York: Springer.

ESRI (Environmental Systems Resource Institute). (2013). ArcMap 10.2. ESRI, Redlands, California.

Flanagan, D.C., Ascough II, J.C., Nicks, A.D., Nearing, M.A., & Laflen, J.M. (1995). USDA-Water Erosion Prediction Project (WEPP). Chapter 1: Overview of the WEPP Erosion Prediction Model. NSERL Report No. 10, USDA-ARS National Soil Erosion Research Lab., West Lafayette, IN.

Flanagan, D.C., Frankenberger, J.R., & Ascough II, J.C. (2012). Wepp: Model Use, Calibration, and Validation. *Transactions of the ASABE, 55*(4), 1463-1477.

Flanagan, D.C., & Livingston, S.J. eds. (1995). Water Erosion Prediction Project (WEPP) Version 95.7: User Summary. NSERL Report No. 11. West Lafayette, Ind.: USDA-ARS

Foster, G.R., Flanagan, D.C., Nearing, M.A., Lane, L.J., Risse, L.M. & Finkner, S.C. (1995). USDA-Water Erosion Prediction Project (WEPP). Chapter 11: Hillslope Erosion Component. NSERL Report No. 10, USDA-ARS National Soil Erosion Research Lab., West Lafayette, IN.

Garbrecht, J.D., & Zhang, X.C. (2015). Soil Erosion from Winter Wheat Cropland under Climate Change in Central Oklahoma. *Applied Engineering in Agriculture, 31*(3), 439-454.

Gopalakrishnan, G., Negri, M.C., Wang, M., Wu, M., Snyder, S.W., & Lafreniere, L. (2009). Biofuels, Land, and Water: A Systems Approach to Sustainability. *Environmental Science & Technology* 43(15): 6094-6100.

Grønsten, H.A. & Lundekvam, H. (2006). Prediction of surface runoff and soil loss in southeastern Norway using the WEPP Hillslope model. *Soil and Tillage Research*. 85: 186-199.

Hanson, G.J., & Hunt, S.L. (2007). Lessons learned using laboratory jet method to measure soil erodibility of compacted soils. *Applied Engineering in Agriculture, 23*(3), 305-312.

Hanson, G.J., & Temple, D.M. (2002). Performance of bare-earth and vegetated steep channels under long-duration flows. *Transactions of the Asae, 45*(3), 695-701.

Hoagland, B.W., Butler, I.H., Johnson, F.L., & Glenn, S., (1999). The Cross Timbers. In: Anderson, R.C., Fralish, J.S., Baskin, J.M. (Eds.), Savannas, Barrens, and Rock Outcrop Plant Communities of North America. Cambridge University Press, Cambridge, U.K., pp. 231–245.

Huxman, T.E., Wilcox, B.P., Breshears, D.D., Scott, R.L., Snyder, K.A., Small, E.E., Hultine, K., Pockman, W.T., & Jackson, R.B. (2005). Ecohydrological implications of woody plant encroachment. *Ecology*, 86(2), 308-319. Doi 10.1890/03-0583

ISCO Product Data. (2000). *ISCO 3700C Compact Portable Sampler*. Teledyne Isco, Lincoln, NE. www.isco.com

Limb, R.F., Engle, D.M., Alford, A.L., & E.C. Hellgren, (2010). Tallgrass Prairie Plant Community Dynamics Along a Canopy Cover Gradient of Eastern Redcedar (*Juniperus virginiana L.*). *Rangeland Ecology & Management*, 63(6), 638-644. doi:10.2111/Rem-D-09-00056.1

Liu, K., Atiyeh, H.K., Pardo-Planas, O., Ramachandriya, K.D., Wilkins, M.R., Ezeji, T.C., Ujor, V. & R.S. Tanner. (2015). Process development for biological production of butanol from Eastern redcedar. *Bioresource Technology* 176: 88-97. DOI:10.1016/j.biortech.2014.10.148

Mamo, M., & Bubenzer, G. D. (2001). Detachment rate, soil erodibility, and soil strength as influenced by living plant roots part I: Laboratory study. *Transactions of the Asae, 44*(5), 1167-1174.

McPherson, R.A., Fiebrich, C., Crawford, K.C., Elliott, R.L., Kilby, J.R., Grimsley, D.L., Martinez, J.E., Basara, J.B., Illston, B.G., Morris, D.A., Kloesel, K.A., Stadler, S.J., Melvin, A.D., Sutherland, A.J. & Shrivastava, H. (2007): Statewide monitoring of the mesoscale environment: A technical update on the Oklahoma Mesonet. *J. Atmos. Oceanic Technol.*, 24, 301–321.

Midgley, T.L., Fox, G.A., Wilson, G.V., Felice, R.M., & Heeren, D.M. (2013). *In Situ* Soil Pipeflow Experiments on Contrasting Streambank Soils. *Transactions of the ASABE, 56*(2), 479-488.

Miller, R.B., Fox, G.A., Penn, C.J., Wilson, S., Parnell, A., Purvis, R.A., & Criswell, K. (2014). Estimating sediment and phosphorus loads from streambanks with and without riparian protection. *Agriculture Ecosystems & Environment, 189*, 70-81. doi:10.1016/j.agee.2014.03.016

Minitab 17 Statistical Software. (2016). Minitab, Inc., State College, PA. https://www.minitab.com/en-us/products/minitab/

Norris, M.D., Blair, J.M., Johnson, L.C. & Mckane, R.B. (2001). Assessing Changes in Biomass, Productivity, and C and N Stores following *Juniperus Virginiana* Forest Expansion into Tallgrass Prairie. *Canadian Journal of Forest Research*, 31(11): 1940-946.

Oklahoma Forestry Services, Department of Agriculture, Food and Forestry. (2014). *FAQs about Eastern Redcedar.* Oklahoma City, OK

Olukoya, I.A., Ramachandriya, K.D., Wilkins, M.R., & Aichele, C.P. (2014). Life cycle assessment of the production of ethanol from eastern redcedar. *Bioresource Technology* 173: 239-244. DOI:10.1016/j.biortech.2014.09.100

Ortmann, J., Stubbendieck, J., Masters, R.A., Pfeiffer, G.H., & Bragg, T.B. (1998). Efficacy and costs of controlling eastern redcedar. *Journal of Rangeland Management* 51(2): 158-163. DOI:Doi 10.2307/4003201

Pierce, A.M., & Reich, P.B. (2009). The effects of eastern red cedar (*Juniperus virginiana*) invasion and removal on a dry bluff prairie ecosystem. *Biological Invasions*, 12: 241-252.

Potter, K.N., Velazquez-Garcia, J.D., & Torbert, H.A. (2002). Use of a submerged jet device to determine channel erodibility coefficients of selected soils of Mexico. *Journal of Soil and Water Conservation, 57*(5), 272-277.

Qiao, L., Zou, C.B., Will, R.E., & Stebler, E. (2015). Calibration of SWAT model for woody plant encroachment using paired experimental watershed data. *Journal of Hydrology*, 523, 231-239. doi:10.1016/j.jhydrol.2015.01.056

Ramachandriya, K.D., Wilkins, M.R., Hiziroglu, S., Dunford, N.T., & Atiyeh, H.K. (2013). Development of an efficient pretreatment process for enzymatic saccharification of Eastern redcedar. *Bioresource Technology* 136: 131-139.

Renschler, C.S., & Harbor, J. (2002). Soil erosion assessment tools from point to regional scales-the role of geomorphologists in land management research and implementation. *Geomorphology, 47*(2-4), 189-209. doi:Pii S0169-555x(02)00082-X

Renschler, C.S., & Lee, T. (2005). Spatially distributed assessment of short- and long-term impacts of multiple best management practices in agricultural watersheds. *Journal of Soil and Water Conservation, 60*(6), 446-456.

Risse, L.M., Nearing, M.A., & Savabi, M.R. (1994). Determining the Green-Ampt Effective Hydraulic Conductivity from Rainfall-runoff Data for the WEPP Model. *Transactions of the ASAE*, 37(2): 411-418.

Sabatini, F.M., Zanini, M., Dowgiallo, G., & Burrascano, S. (2015). Multiscale heterogeneity of topsoil properties in southern European old-growth forests. *European Journal of Forest Research, 134*(5), 911-925. doi:10.1007/s10342-015-08996

Saghafian, B., Meghdadi, A.R., & Sima, S. (2015). Application of the WEPP model to determine sources of run-off and sediment in a forested watershed. *Hydrological Processes, 29*(4), 481-497. doi:10.1002/hyp.10168

Simon, A., & Collison, A.J.C. (2002). Quantifying the mechanical and hydrologic effects of riparian vegetation on streambank stability. *Earth Surface Processes and Landforms, 27*(5), 527-546. doi:10.1002/esp.325

Simon, A., Pollen, N., & Langendoen, E. (2006). Influence of two woody riparian species on critical conditions for streambank stability: Upper Truckee River, California. *Journal of the American Water Resources Association, 42*(1), 99-113. doi:10.1111/j.1752-1688.2006.tb03826.x

Soil Survey Staff, Natural Resources Conservation Service, United States Department of Agriculture. Soil Survey Geographic (SSURGO) Database. Available online at http://sdmdataaccess.nrcs.usda.gov/.

Starks, P.J., Venuto, B.C., Eckroat, J.A., & Lucas, T. (2011). Measuring Eastern Redcedar (*Juniperus virginiana*) Mass With the Use of Satellite Imagery. *Rangeland Ecology & Management* 64(2): 178-186. DOI:10.2111/rem-d-10-00057.1

Stone, J.J., Lane, L.J., Shirley, E.D., & Hernandez, M. (1995). USDA-Water Erosion Prediction Project (WEPP). Chapter 4: Hillslope Surface Hydrology Component. NSERL Report No. 10, USDA-ARS National Soil Erosion Research Lab., West Lafayette, IN.

Tennesen, M. (2008). ECOLOGY: When Juniper and Woody Plants Invade, Water May Retreat. *Science*, 322(5908), 1630-1631.

U.S. Department of Agriculture Natural Resources Conservation Service (NRCS), (2010). National Resources Inventory Rangeland Resource Assessment-Native Invasive Woody Species.Retrieved from: http://www.nrcs.usda.gov/wps/portal/nrcs/detail/national/landuse

Wade, C.R., Bolding, M.C., Aust, W.M., Lakel, W.A., & Schilling, E.B. (2012). Comparing Sediment Trap Data with the Usle-Forest, Rusle2, and Wepp-Road Erosion Models for Evaluation of Bladed Skid Trail Bmps. *Transactions of the ASABE, 55*(2), 403-414.

Wang, B., Zhang, G.H., Zhang, X.C., Li, Z.W., Su, Z.L., Yi, T., & Shi, Y.Y. (2014). Effects of Near Soil Surface Characteristics on Soil Detachment by Overland Flow in a Natural Succession Grassland. *Soil Science Society of America Journal, 78*(2), 589-597. doi:10.2136/sssaj2013.09.0392

Williams, J.D., Dun, S., Robertson, D.S., Wu, J.Q., Brooks, E.S., Flanagan, D.C., & McCool, D.K. (2010). WEPP simulations of dryland cropping systems in small drainages of northeastern Oregon. *Journal of Soil and Water Conservation, 65*(1), 22-33. doi:10.2489/jswc.65.1.22

Wright, L. & Turhollow, A. (2010). Switchgrass selection as a “model” bioenergy crop: A history of the process. *Biomass and Bioenergy* 34(6): 851-868.

Wynn, T.M., Henderson, M.B., & Vaughan, D.H. (2008). Changes in streambank erodibility and critical shear stress due to subaerial processes along a headwater stream, southwestern Virginia, USA. *Geomorphology, 97*(3-4), 260-273. doi:10.1016/j.geomorph.2007.08.010

Wynn, T., & Mostaghimi, S. (2006). The effects of vegetation and soil type on streambank erosion, southwestern Virginia, USA. *Journal of the American Water Resources Association, 42*(1), 69-82. doi:10.1111/j.1752-1688.2006.tb03824.x

Yu B., & Rosewell, C.J. (2001). Evaluation of WEPP for runoff and soil loss prediction at Gunnedah, NSW, Australia. *Australian Journal of Soil Research*, 39: 1131-1145.

Yu B., Ciesiolka, C.A.A., Rose, C.W., & Coughlan, K.J., (2000). A validation test of WEPP to predict runoff and soil loss from a pineapple farm on a sandy soil in subtropical Queensland, Australia. *Australian Journal of Soil Research*, 38: 537–554.

Yu, M.Z., Zhang, L.L., Xu, X.X., Feger, K.H., Wang, Y.H., Liu, W.Z., & Schwarzel, K. (2015). Impact of land-use changes on soil hydraulic properties of Calcaric Regosols on the Loess Plateau, NW China. *Journal of Plant Nutrition and Soil Science, 178*(3), 486-498. doi:10.1002/jpln.201400090

Zhang, G.H., Liu, G.B., Tang, K.M., & Zhang, X.C. (2008). Flow detachment of soils under different land uses in the Loess Plateau of China. *Transactions of the ASABE, 51*(3), 883-890.

Zhou, Z.C., & Shangguan, Z.P. (2008). Effect of ryegrasses on soil runoff and sediment control. *Pedosphere, 18*(1), 131-136. doi:10.1016/S1002-0160(07)60111-8

Zou, C.B., Turton, D.J., Will, R.E., Engle, D.M., & Fuhlendorf, S.D. (2014). Alteration of hydrological processes and streamflow with juniper (*Juniperus virginiana*) encroachment in a mesic grassland catchment. *Hydrological Processes, 28*(26), 6173-6182. doi:10.1002/hyp.10102

APPENDICES

RUNOFF HYDROGRAPHS

Watershed E1:

Storm #1&2- 5/5/15-5/6/15

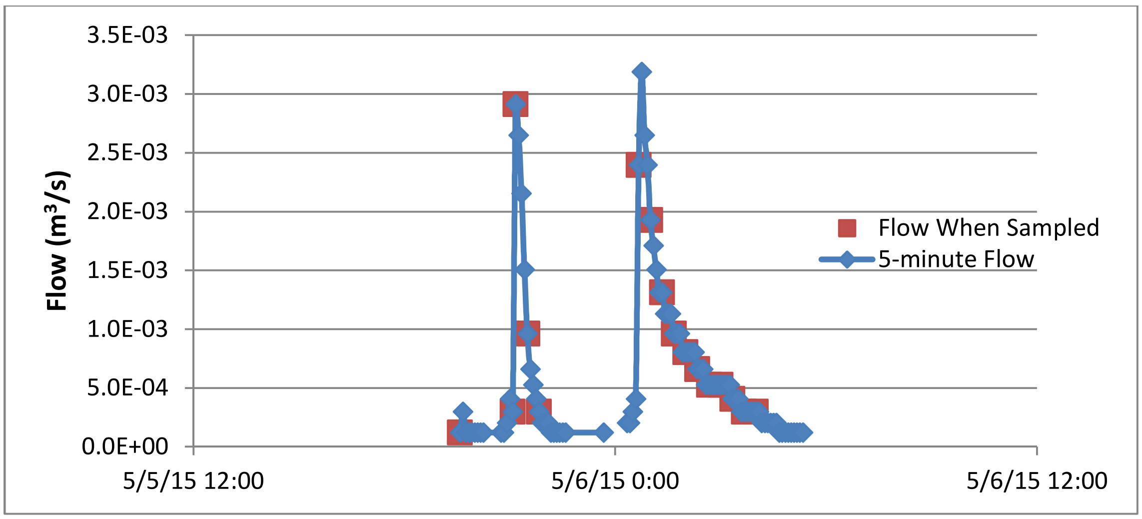

Storm #3- 5/8/15

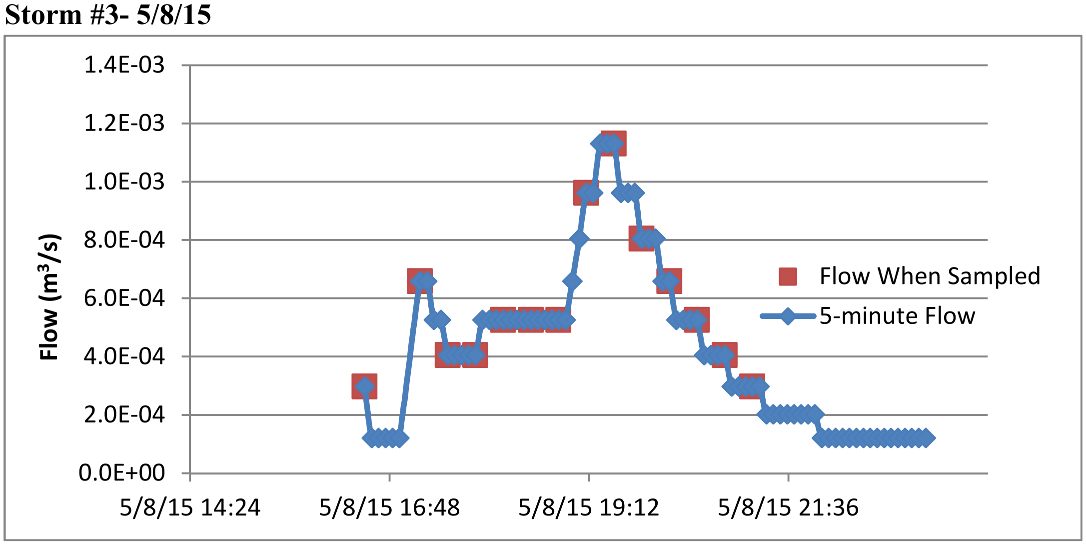

Storm #4- 5/19/15

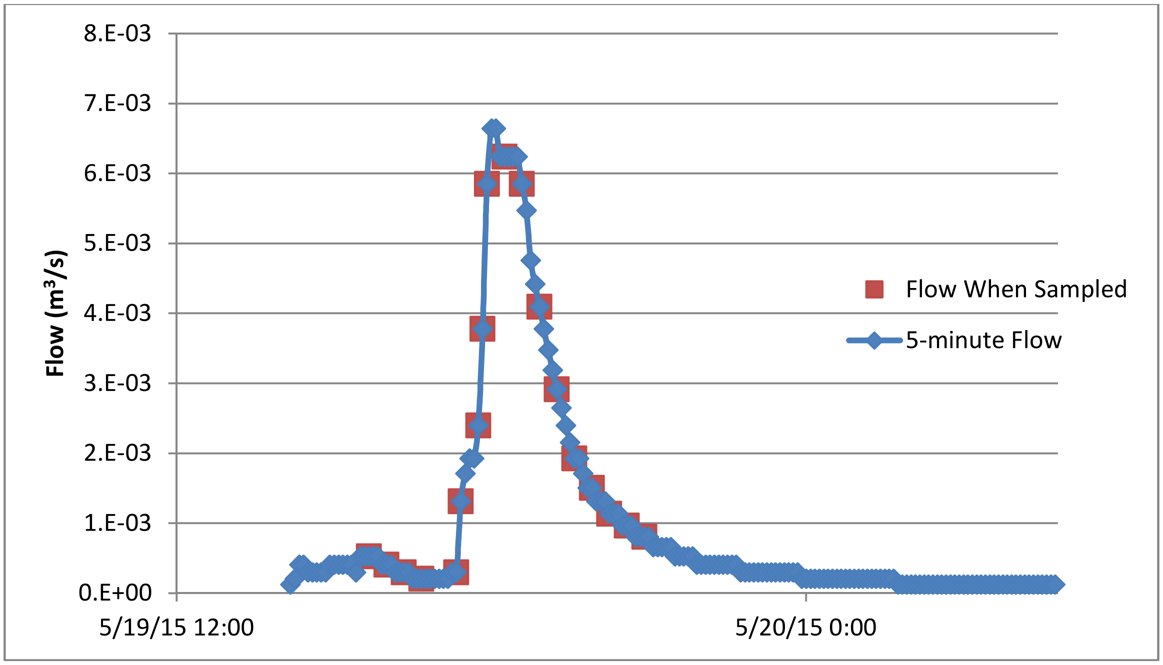

Storm #5-5/23/15

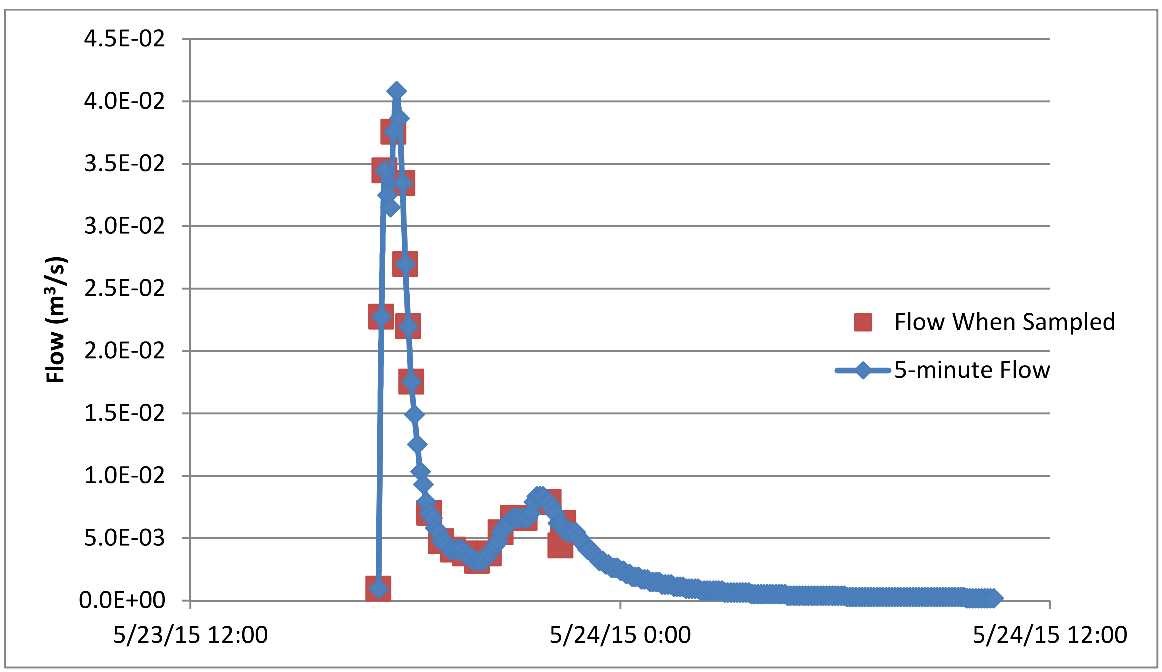

Storm #6-5/26/15

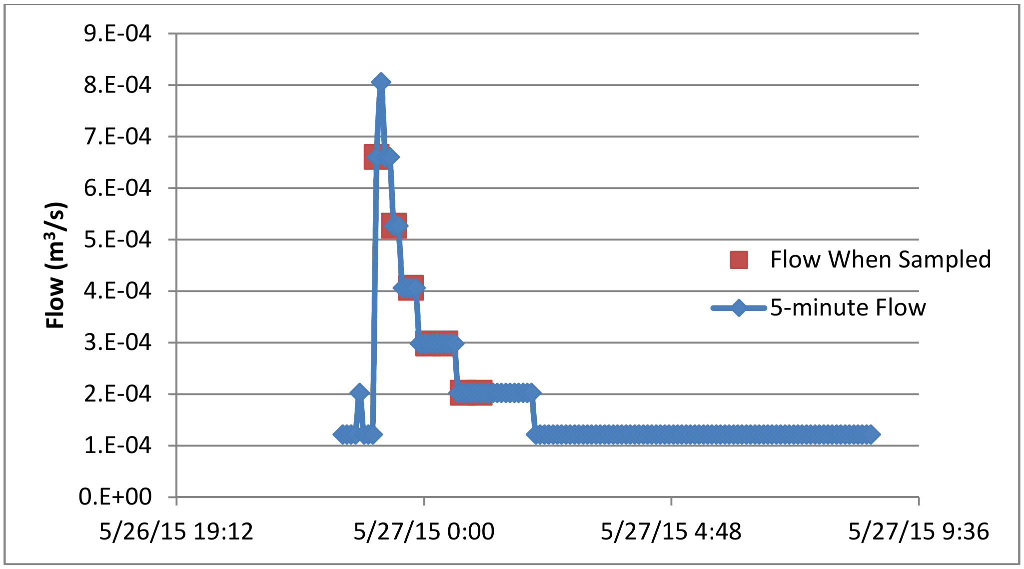

Storm #7-6/13/15

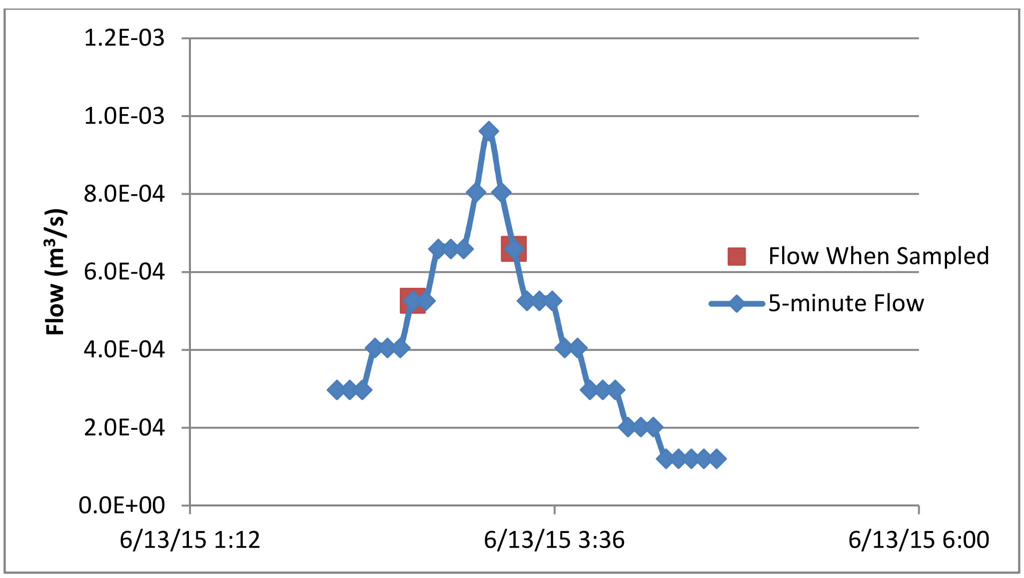

Storm #8-7/9/15

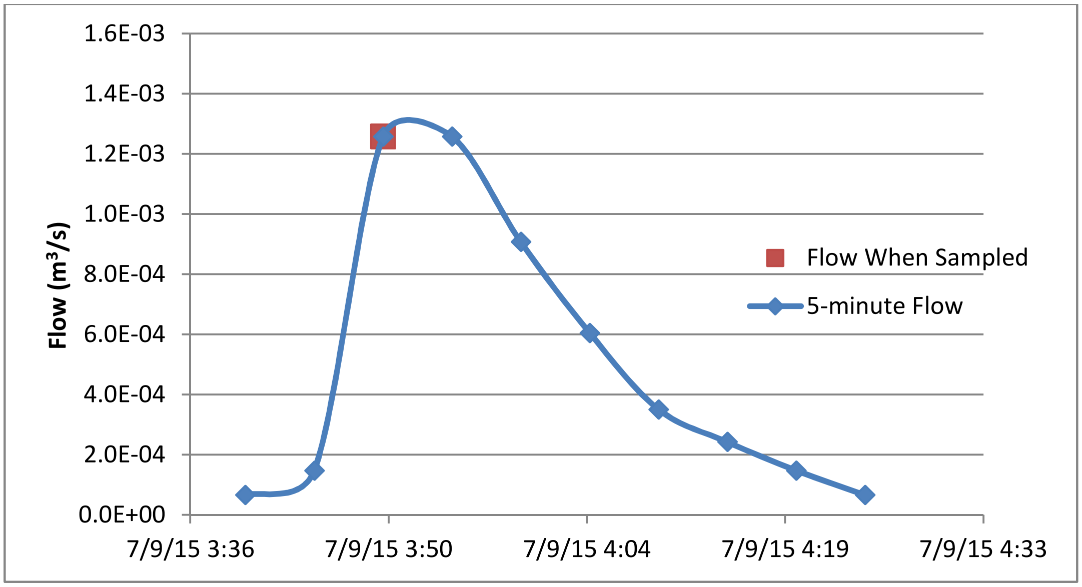

Storm #9-8/22/15

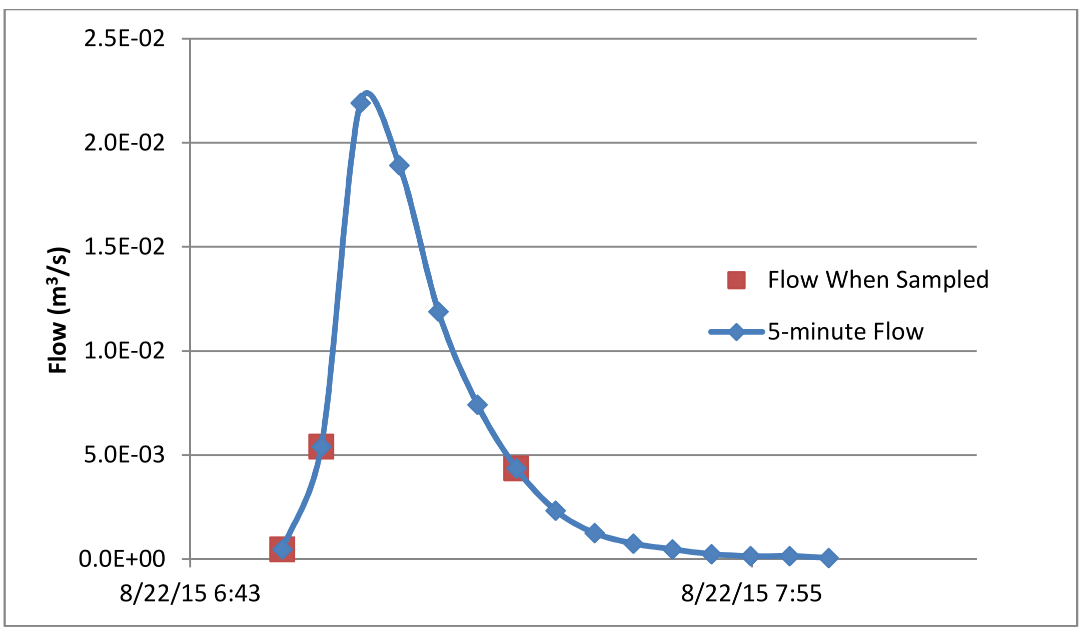

Storm #10-9/11/15

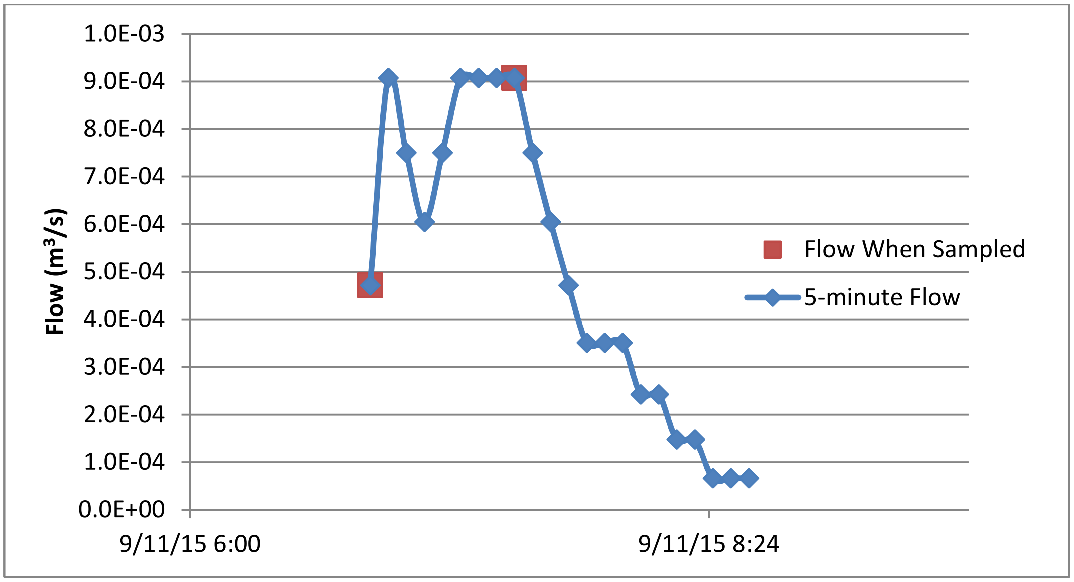

Storm #11- 10/30/15

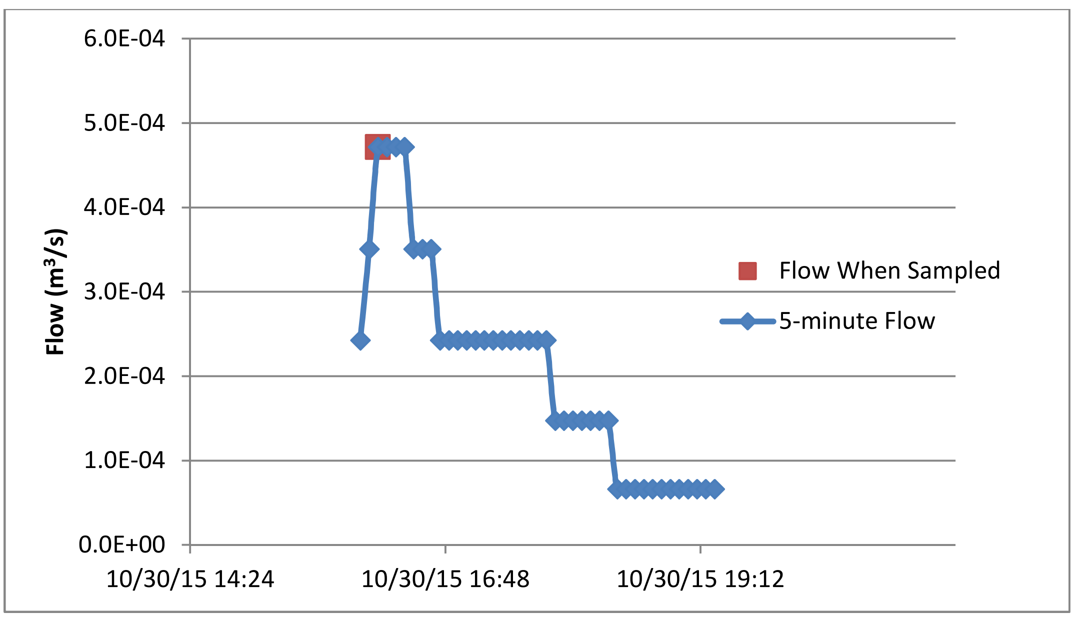

Storm #12-11/5/15

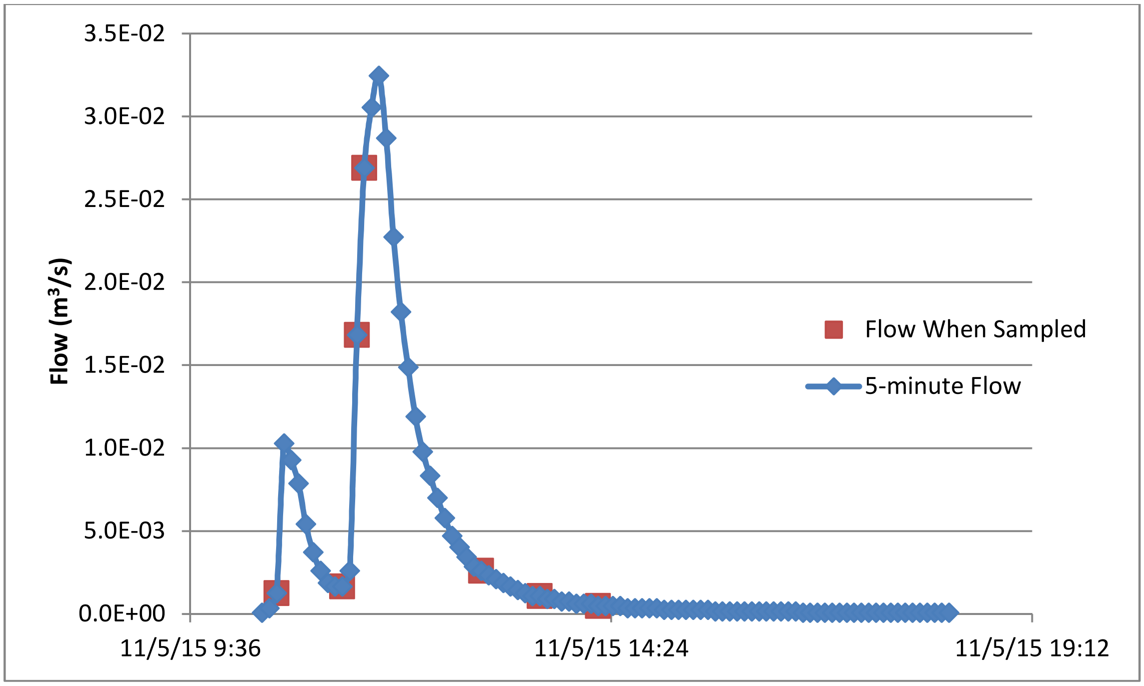

Storm #13-11/17/15

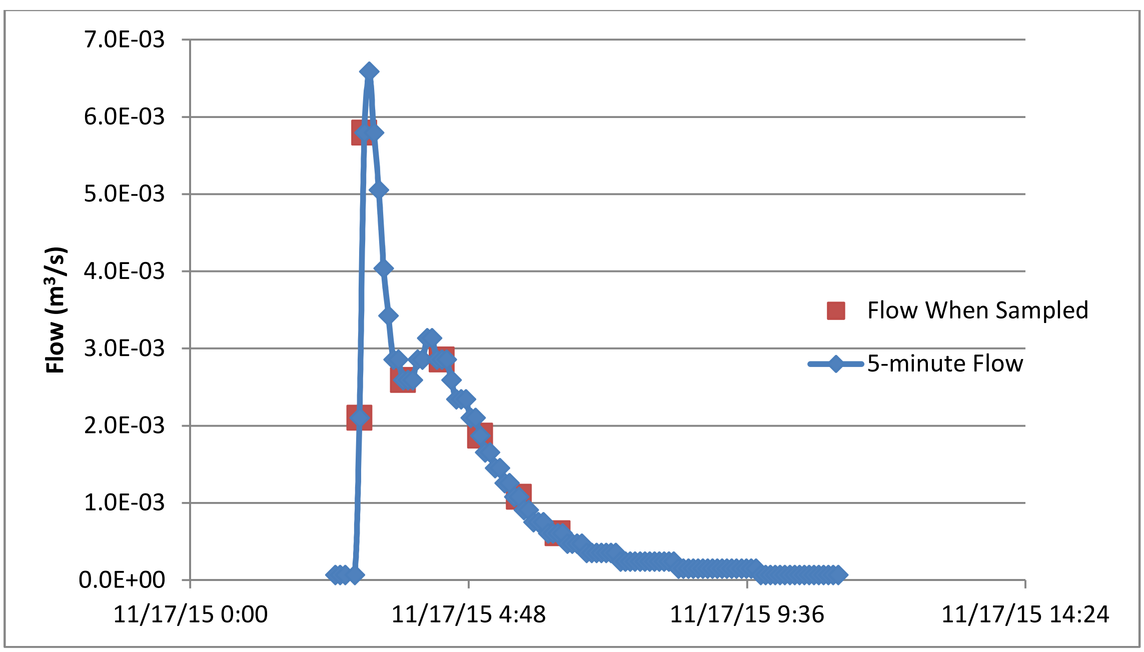

Storm #14- 11/26/15

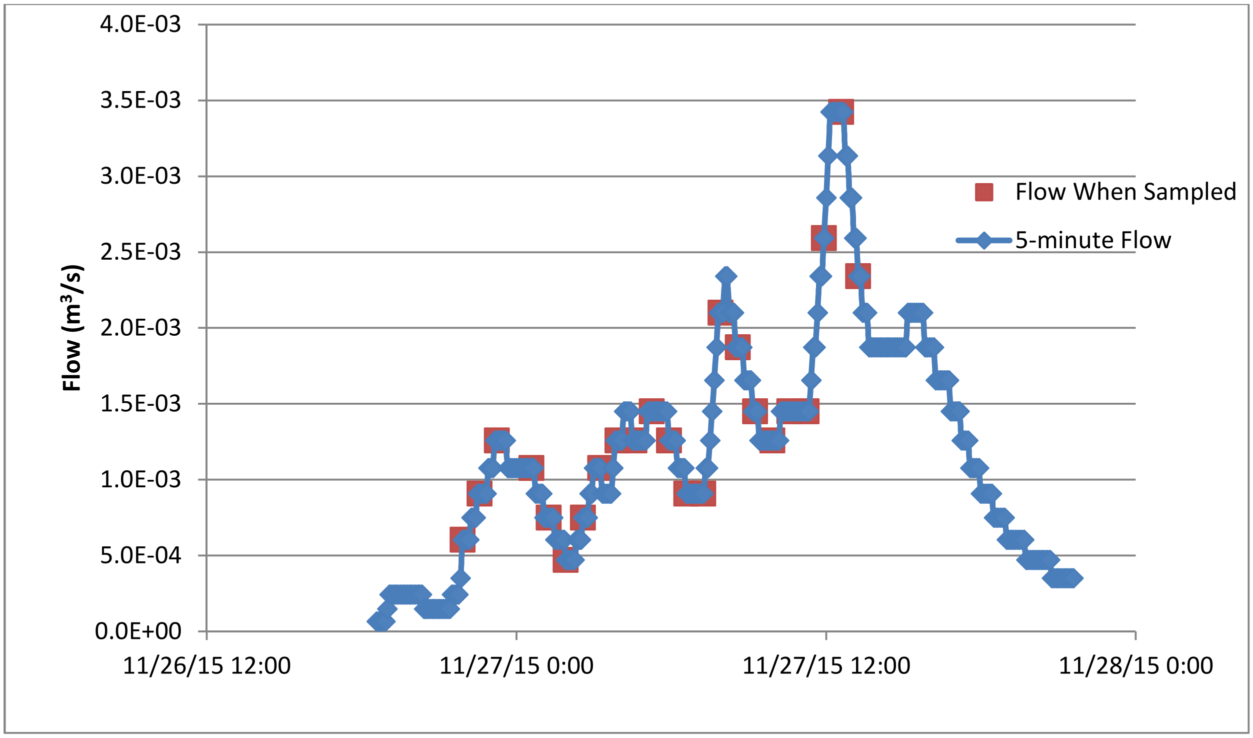

Storm #15-12/13/15

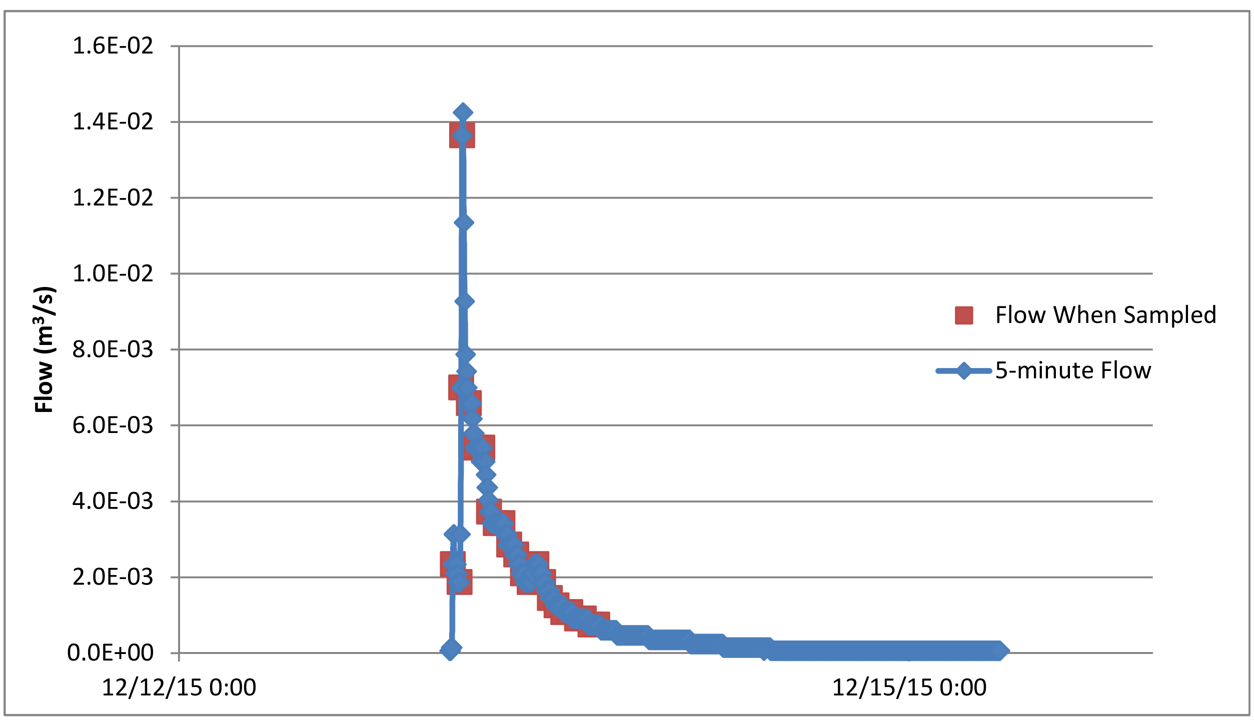

Watershed E2:

Storm #1-5/6/15

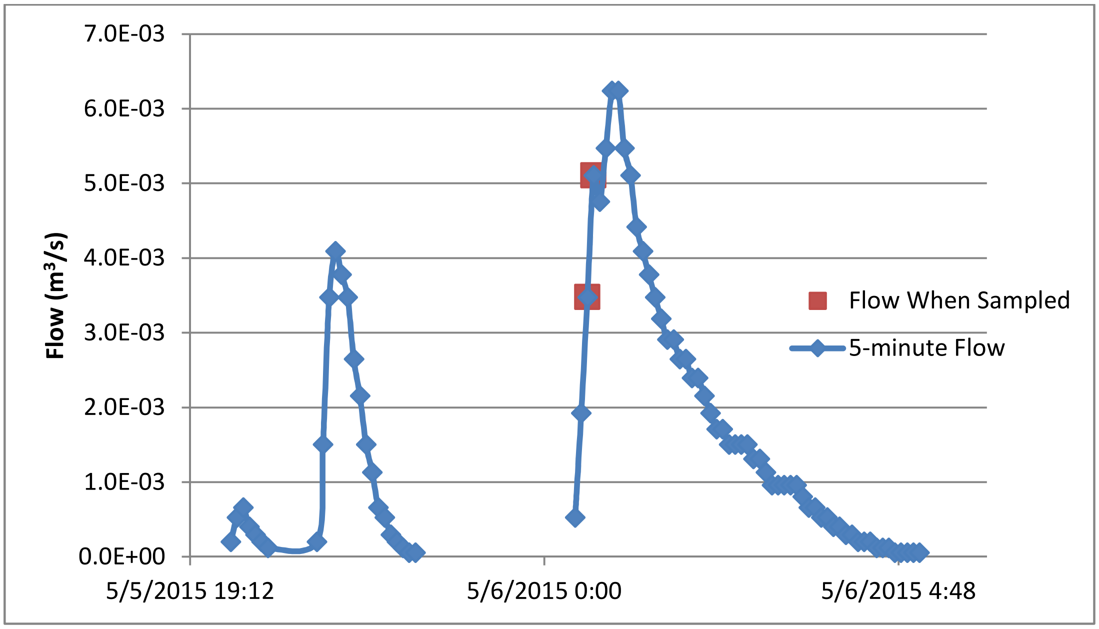

Storm #2-5/8/15

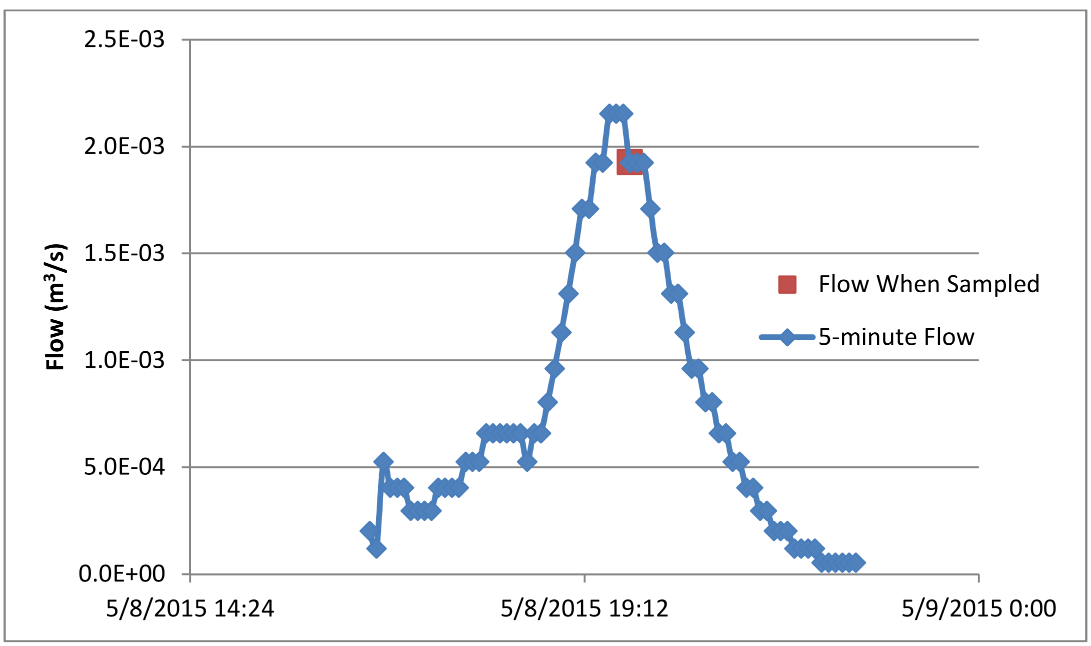

Storm #3-5/16/15

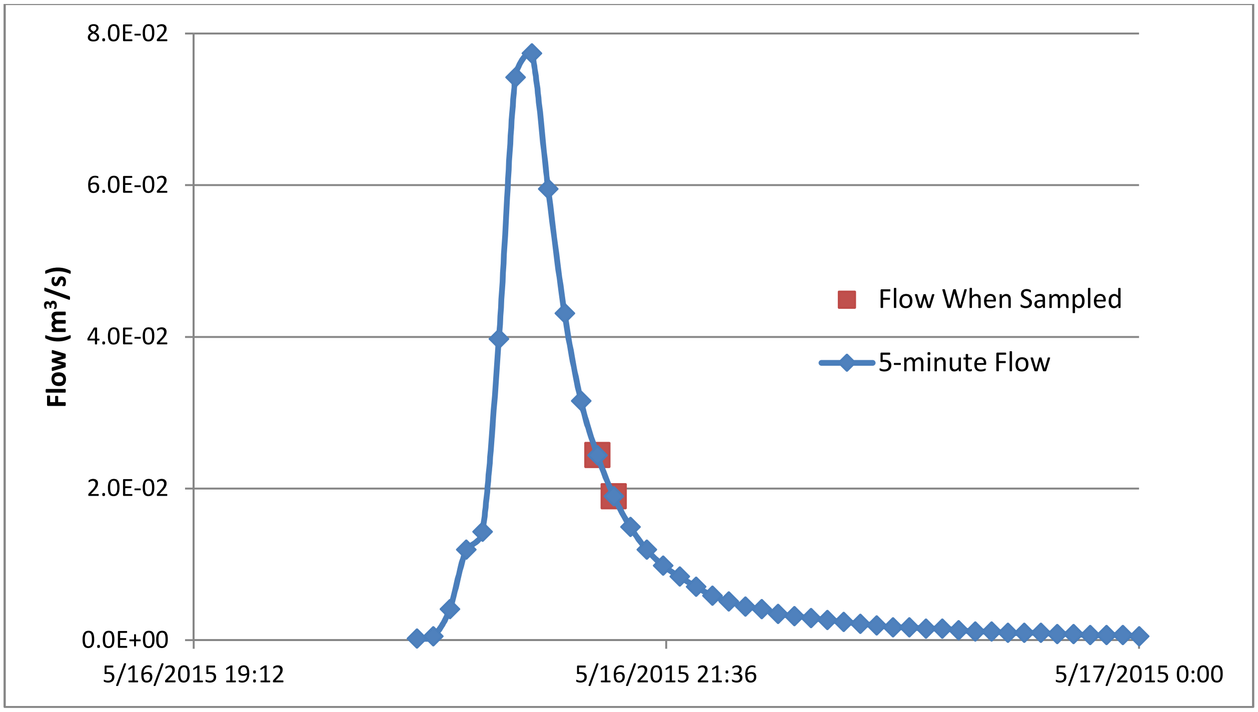

Storm #4- 5/19/15

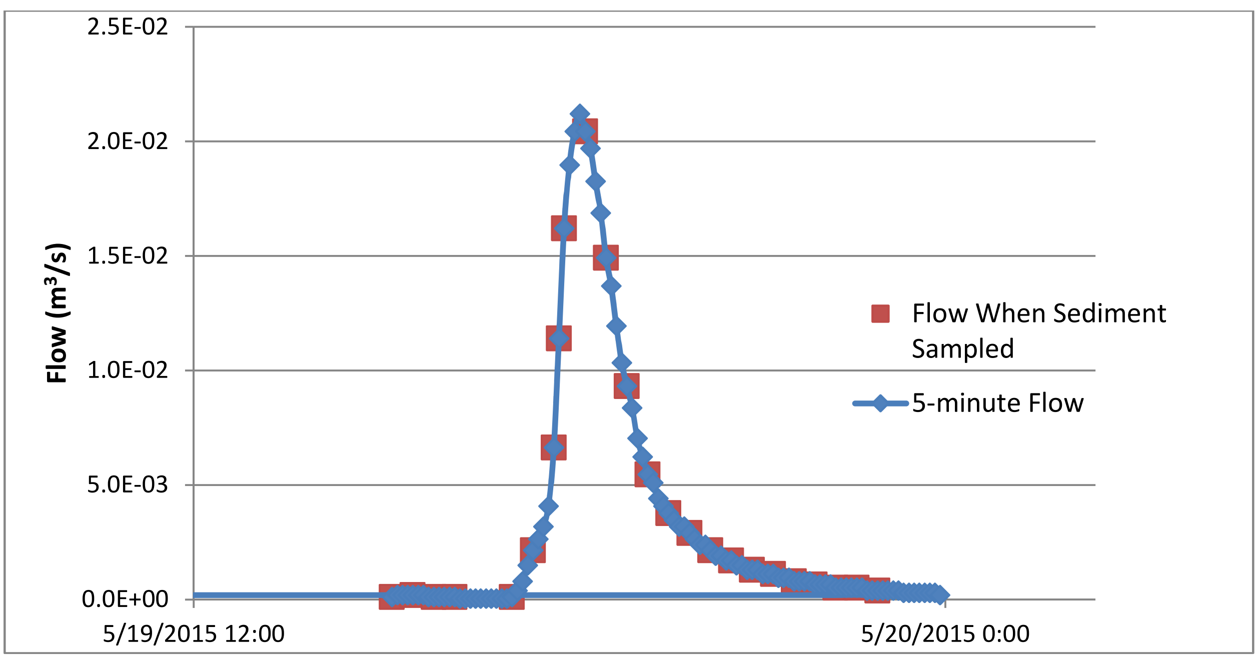

Storm #5-5/23/15

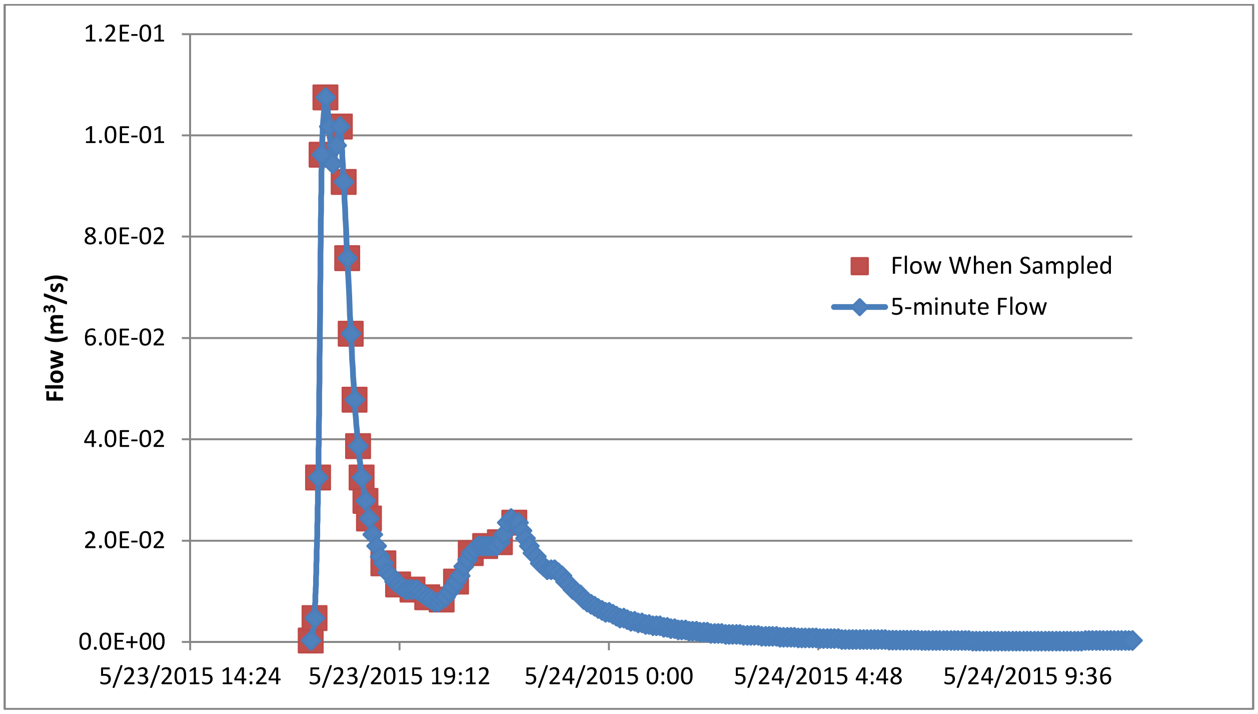

Storm #6-5/26/15

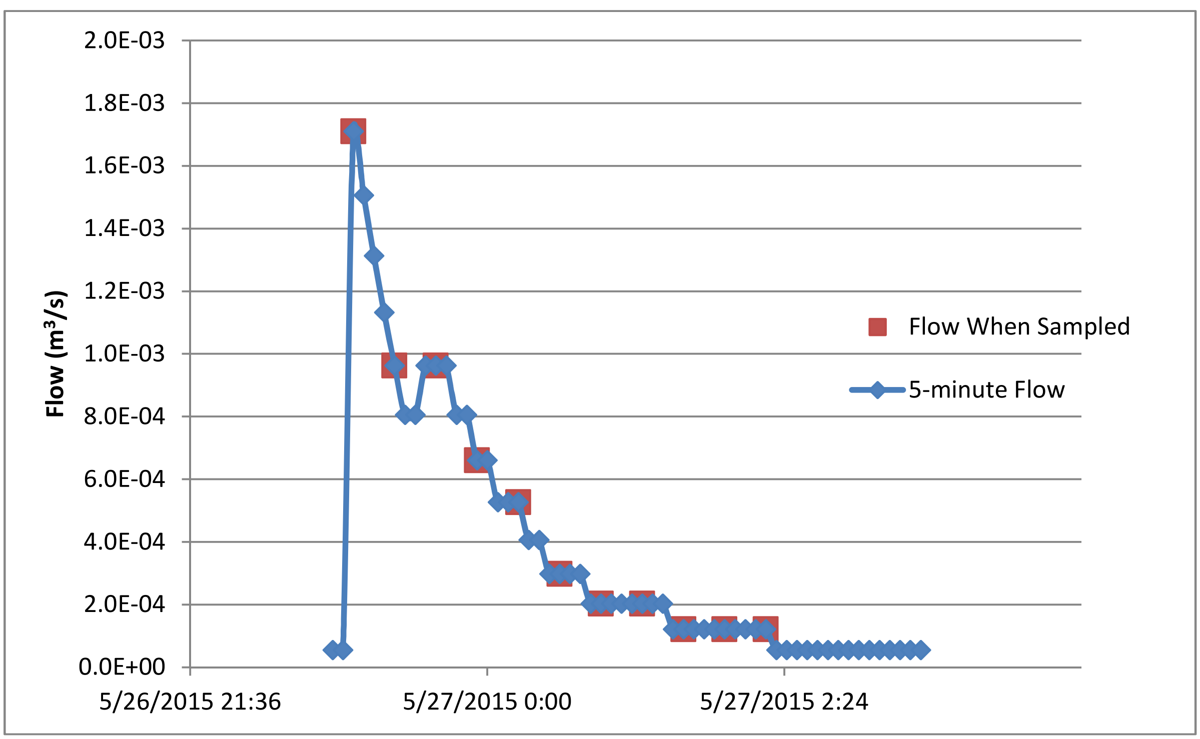

Storm #7-6/13/15

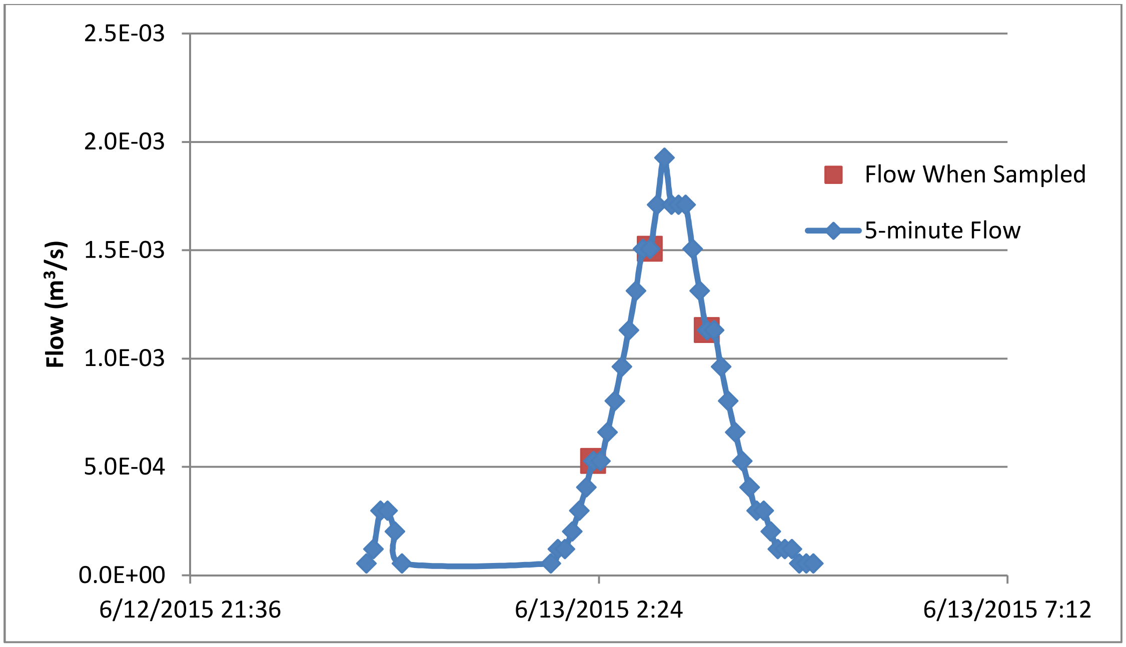

Storm #8-6/18/15

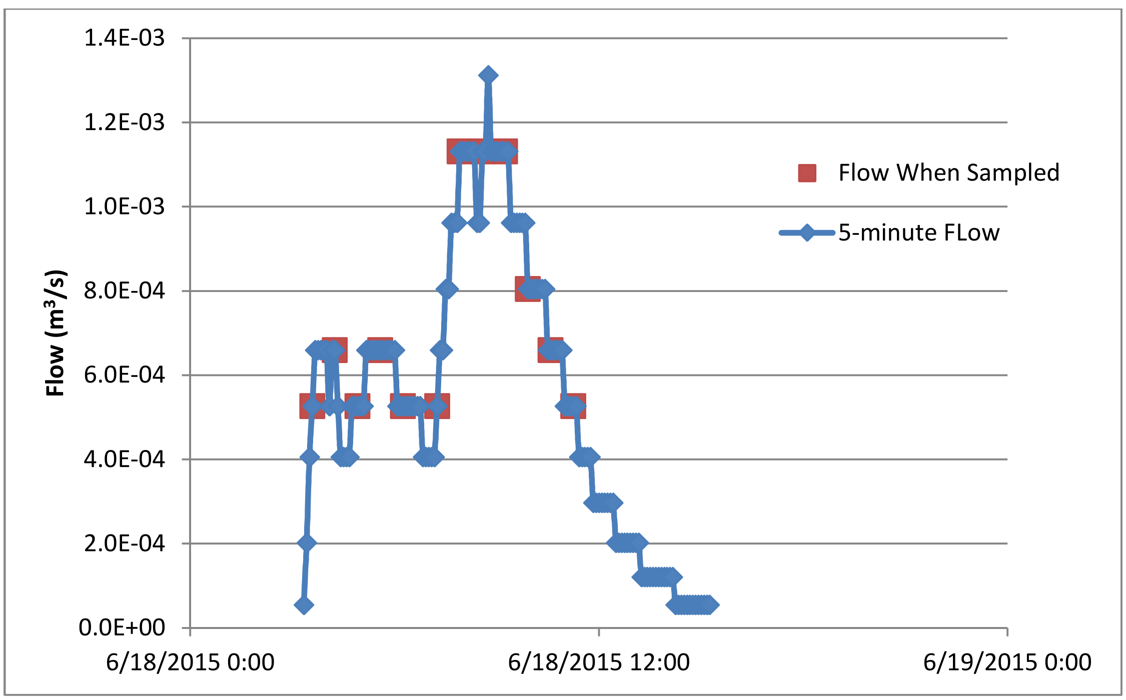

Storm #9-7/9/15

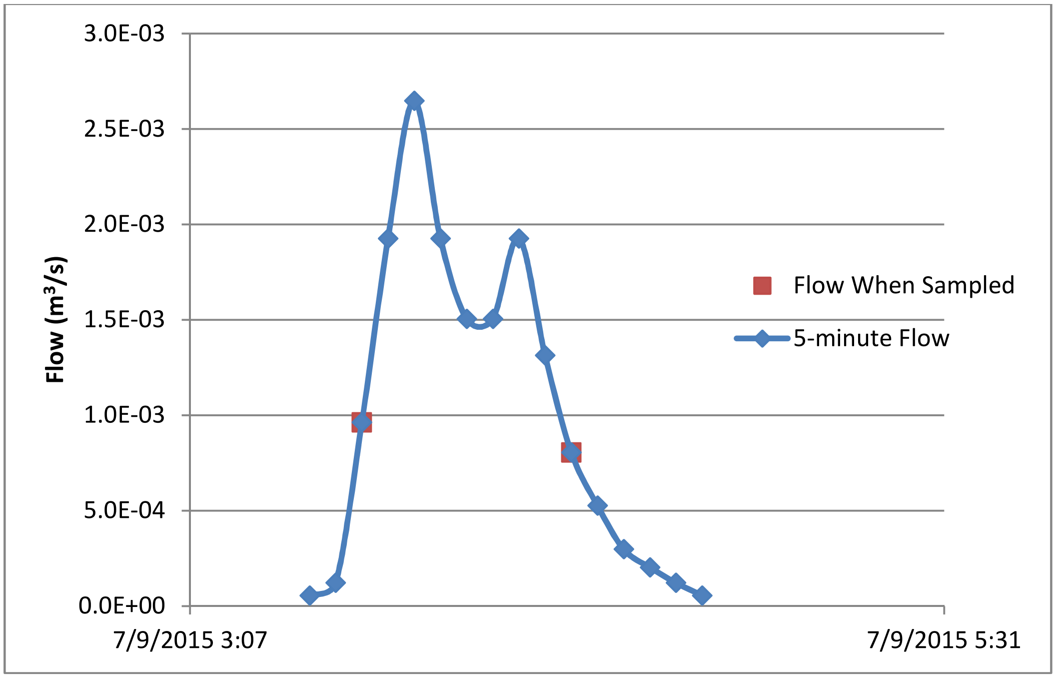

Storm #10- 8/22/15

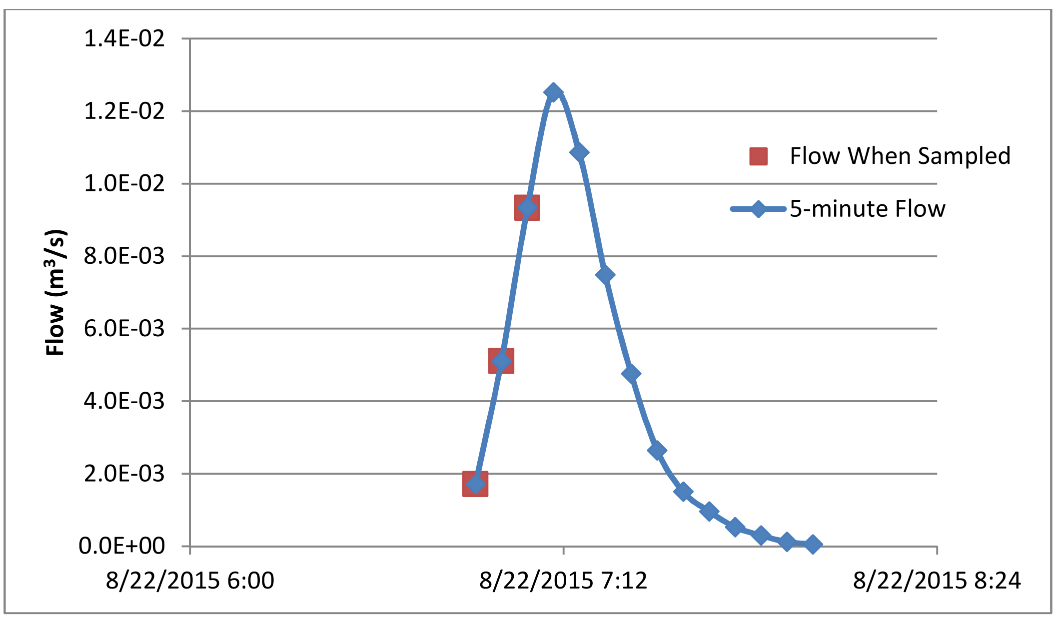

Storm #11-9/11/15

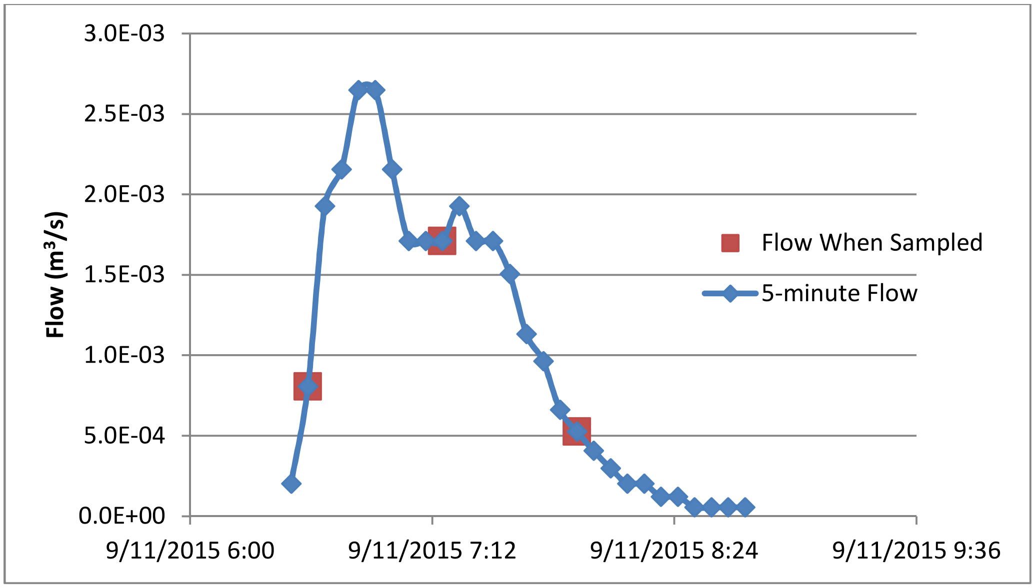

Storm #12-10/30/15

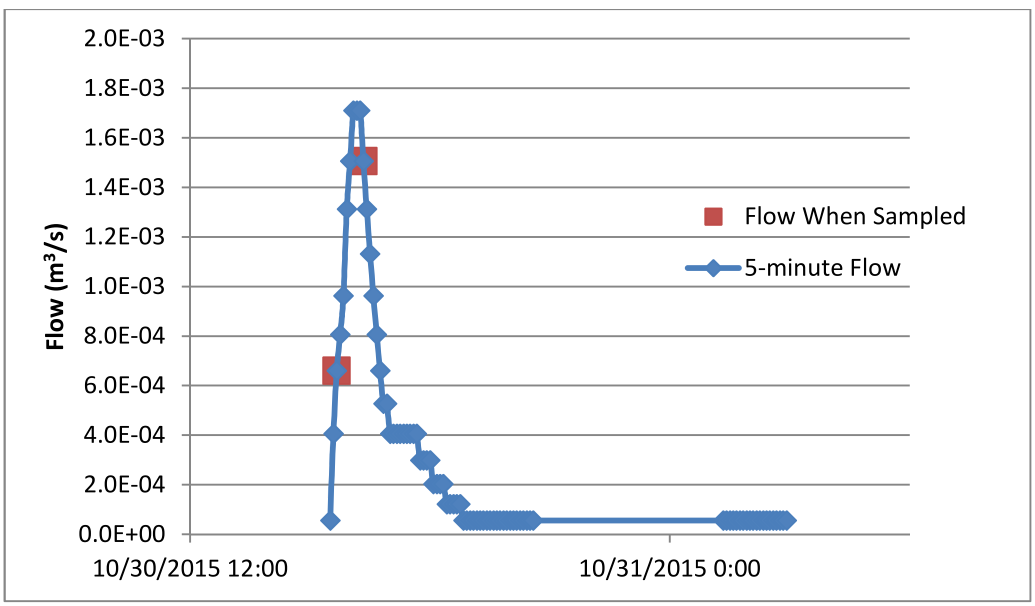

Storm #13- 11/5/15

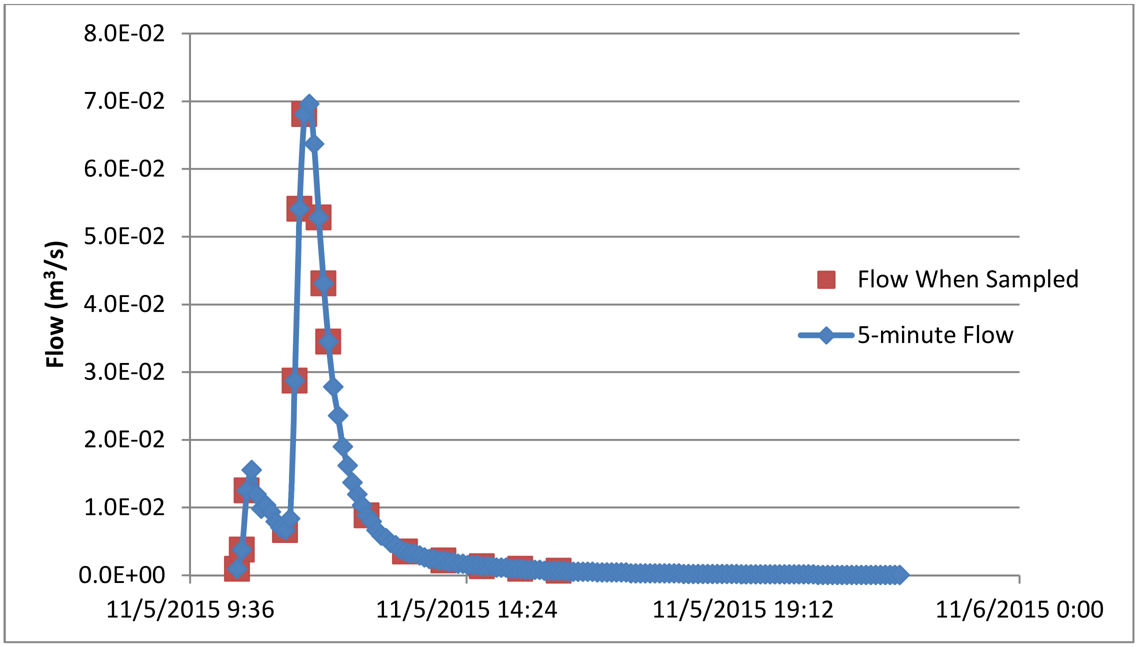

Storm #14-11/26/15

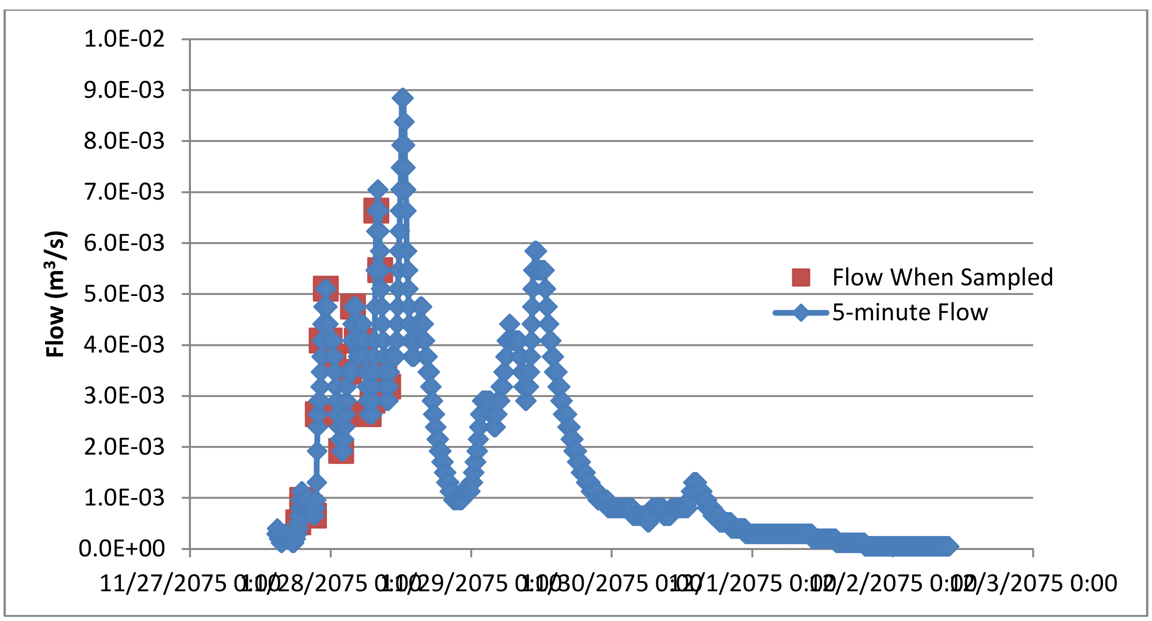

Storm #15-12/13/15

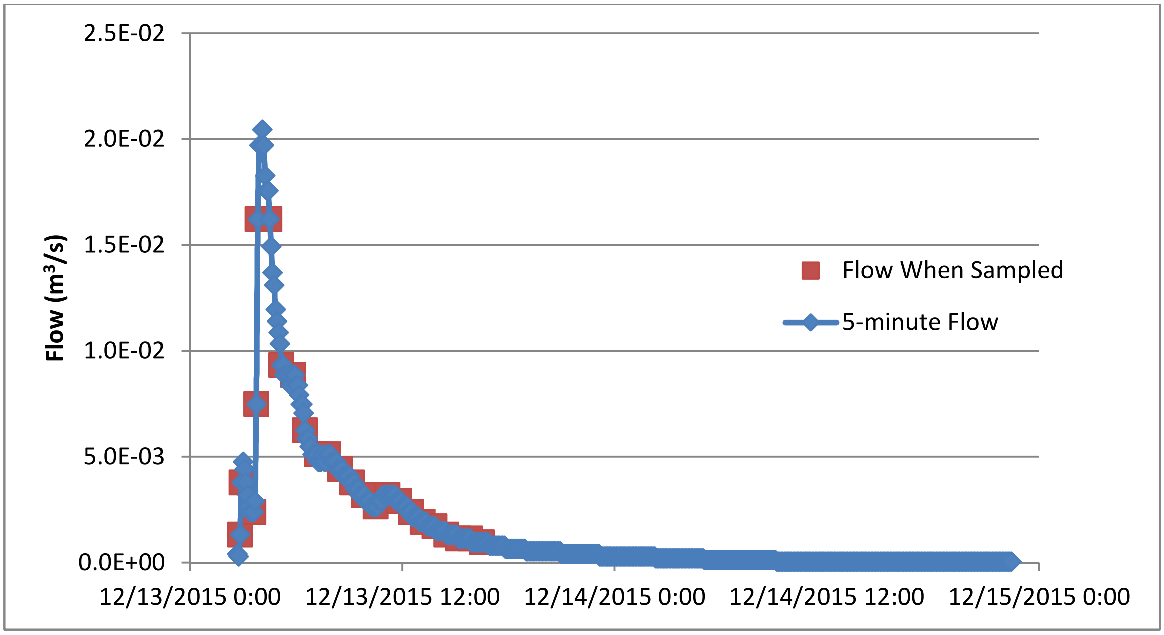

Storm #16-12/26/15

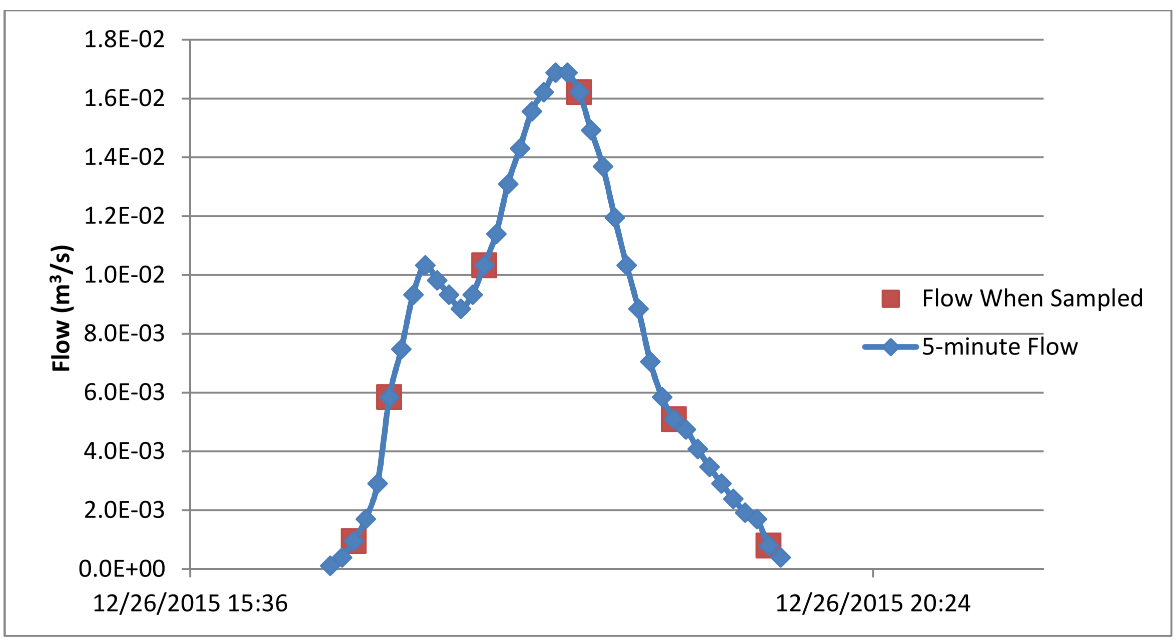

Storm #17- 12/27/15

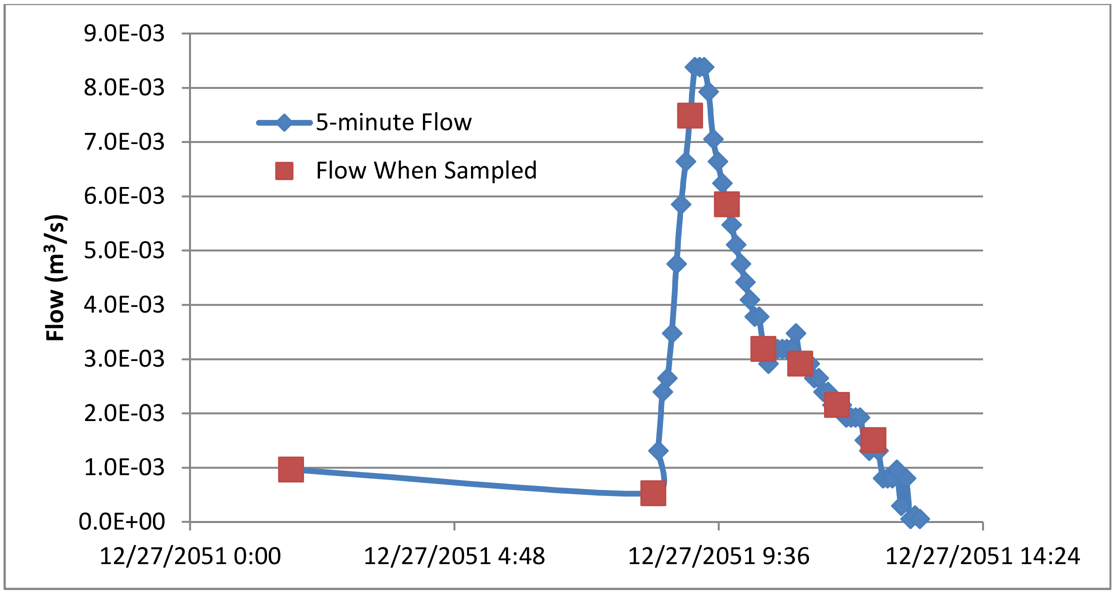

<u>Watershed P1:</u>

Storm 1 – 4/27/2015

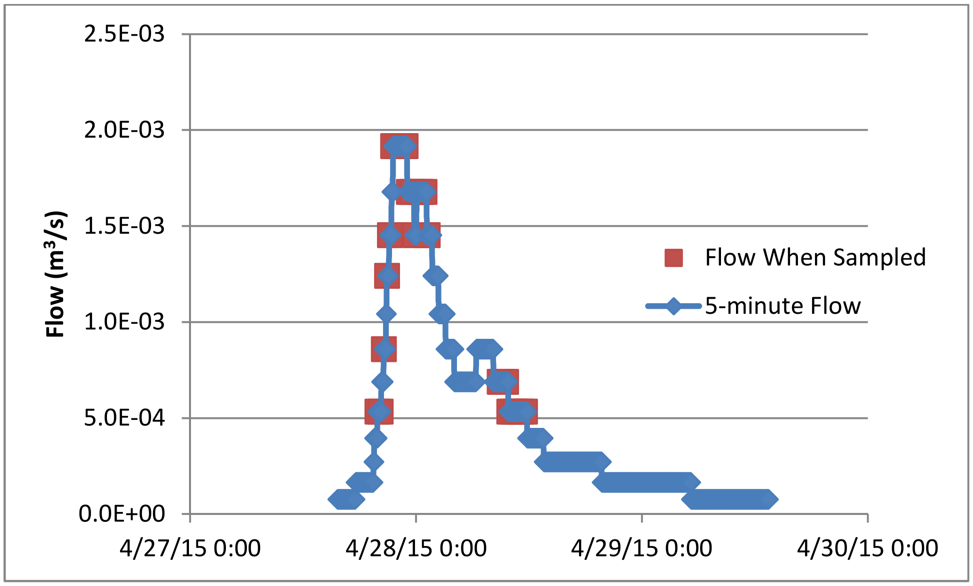

Storm 2 – 5/05/2015

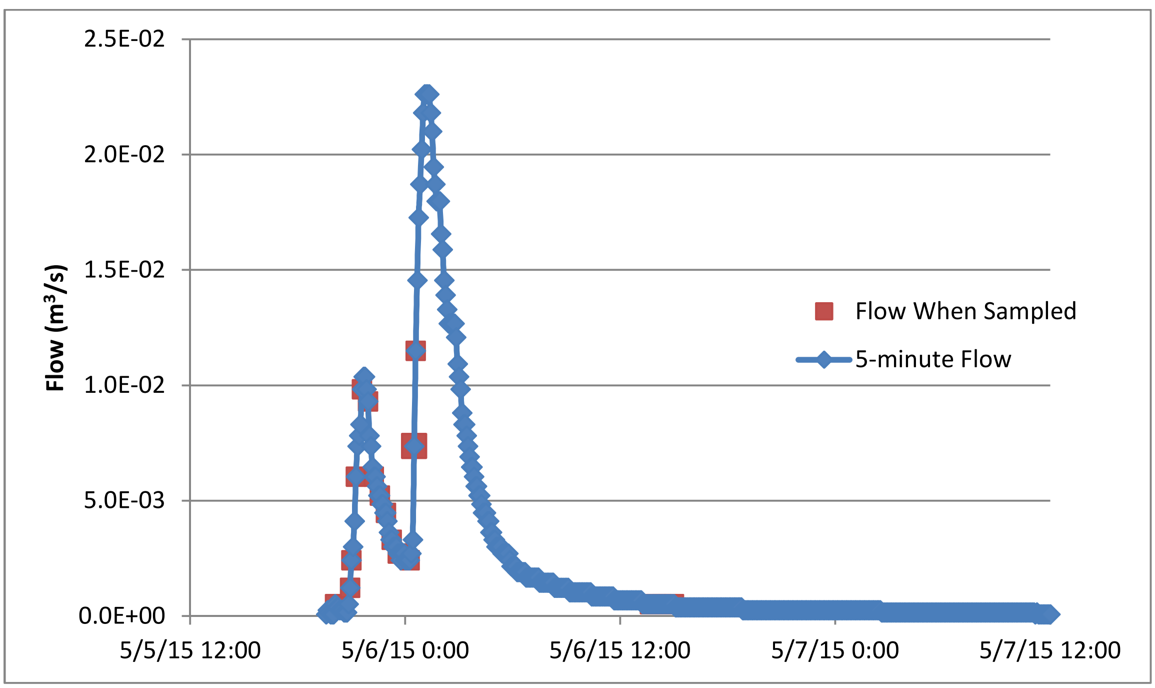

Storm 3 – 5/19/2015

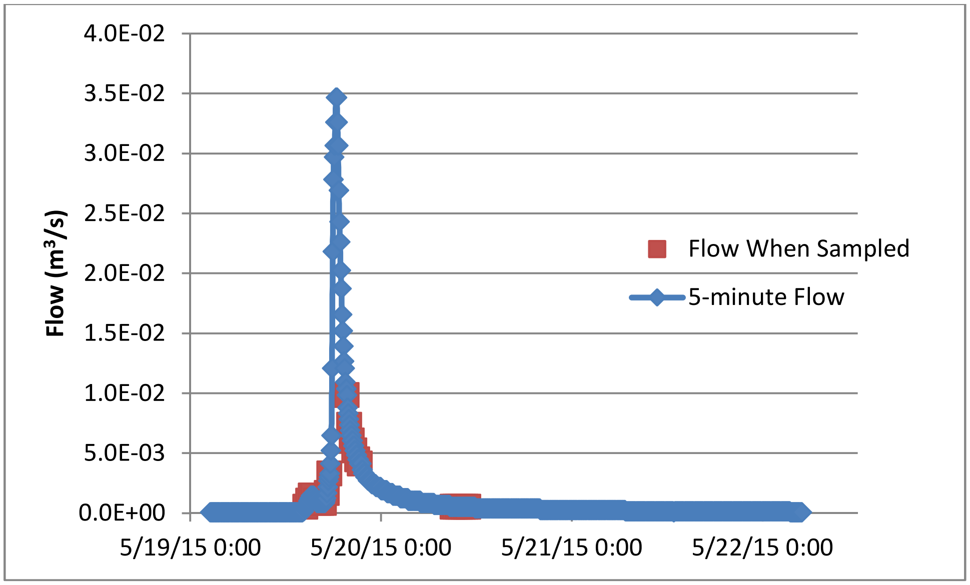

Storm 4 – 5/26/2015

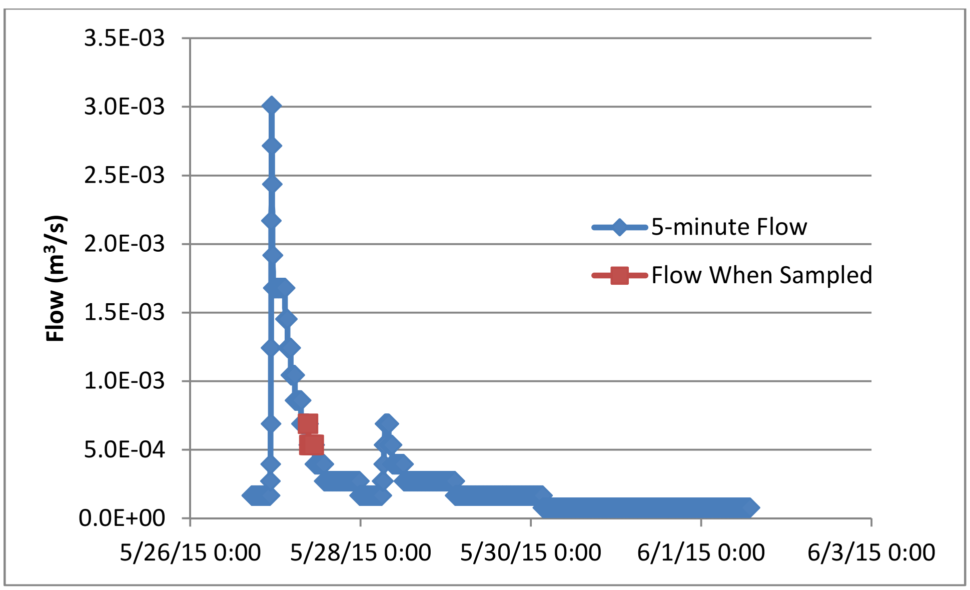

Storm 5 – 7/9/2015

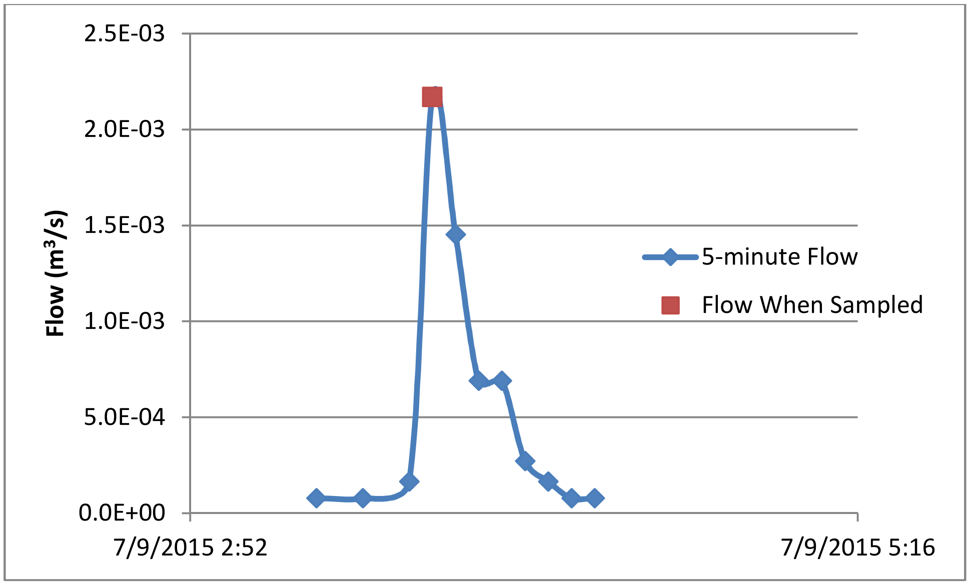

Storm 6 – 12/13/2015

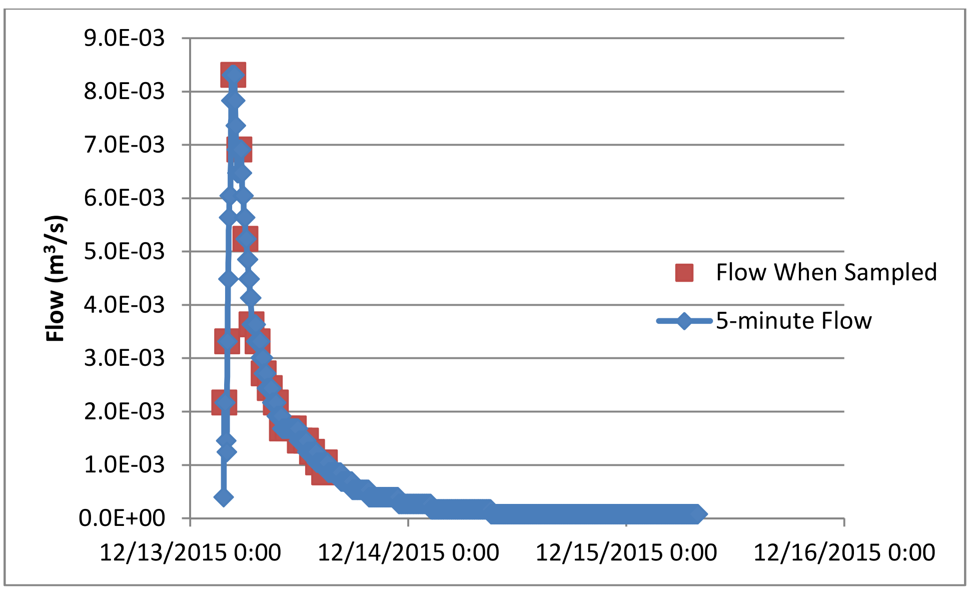

Storm 7 – 12/26/2015

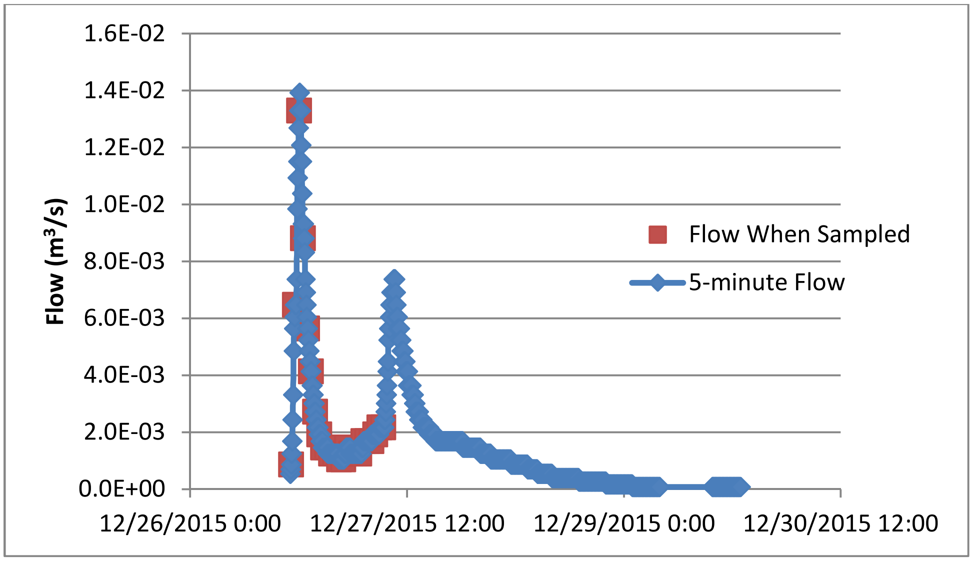

Watershed P2:

Storm 1 – 4/27/2015

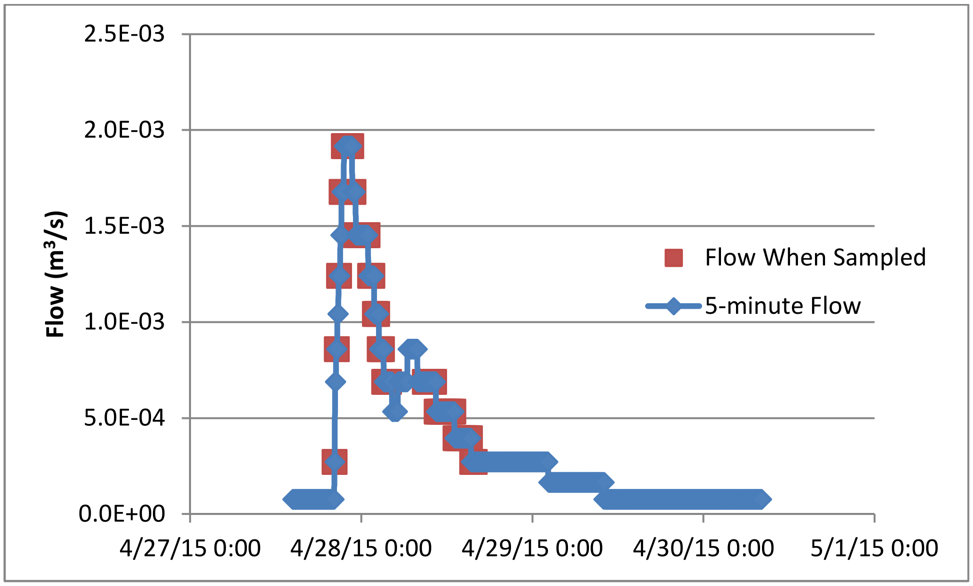

Storm 2 – 5/05/2015

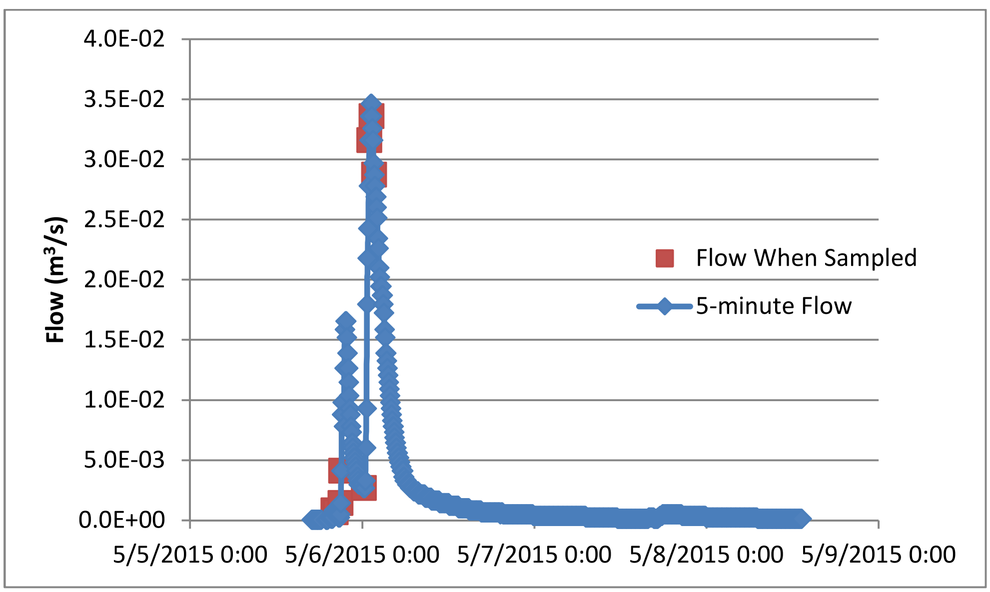

Storm 3 – 5/08/2015

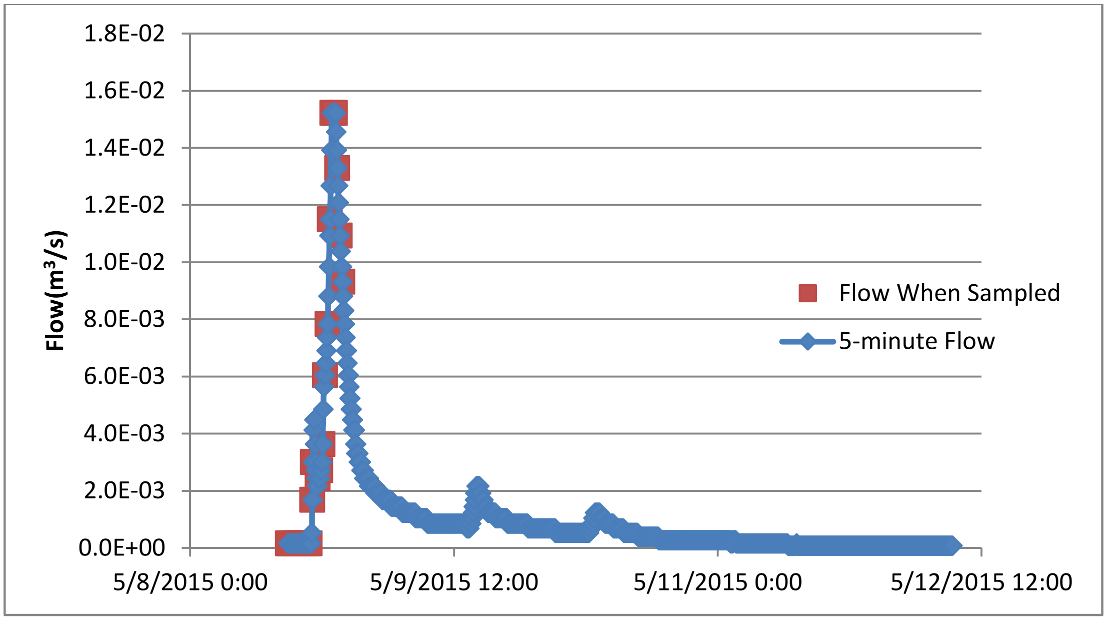

Storm 4 – 5/13/2015

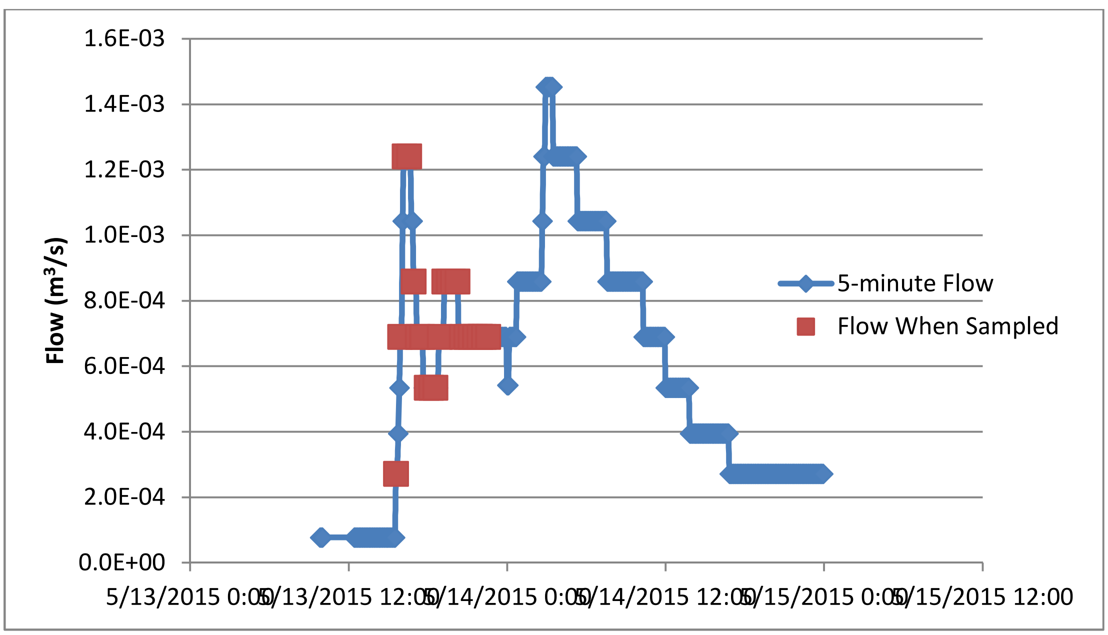

Storm 5 – 5/15/2015

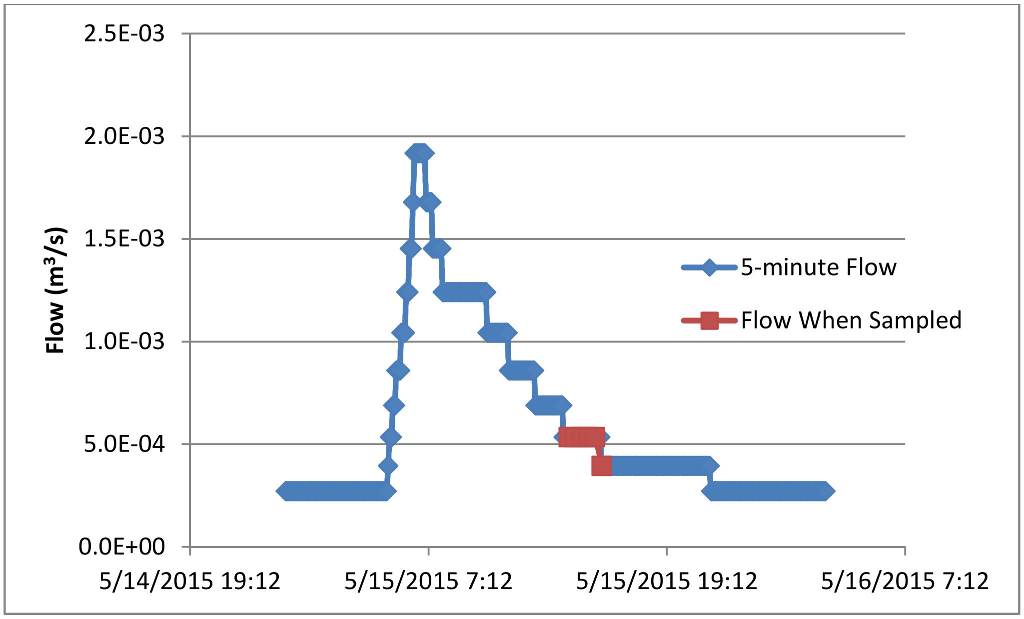

Storm 6 – 5/19/2015

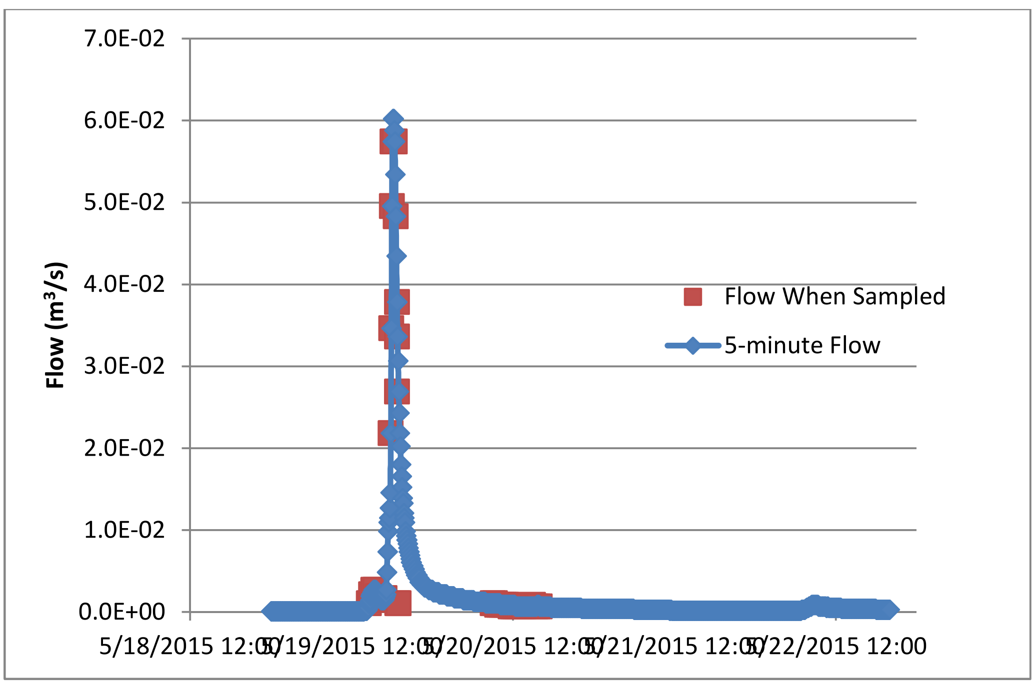

Storm 7 – 5/26/2015

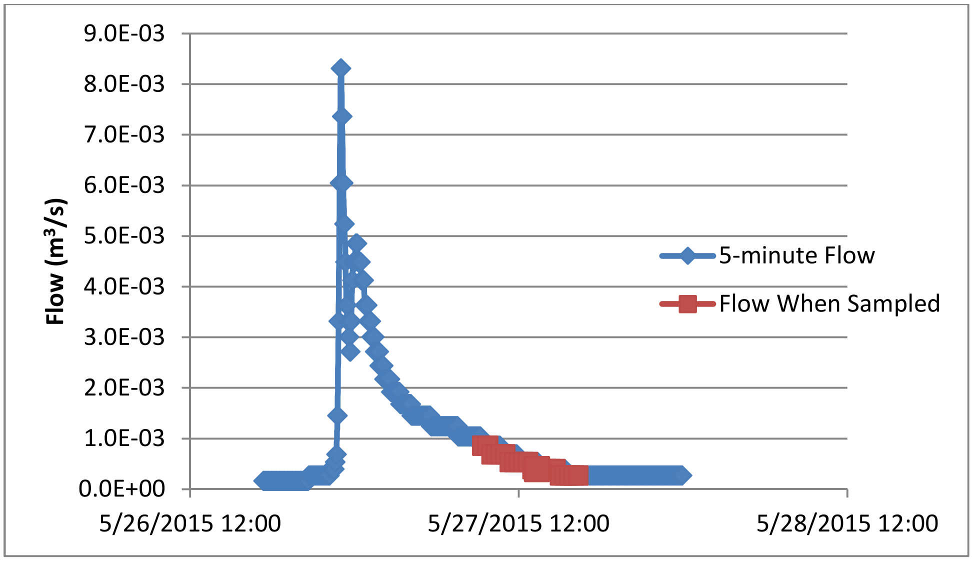

Storm 8 – 5/28/2015

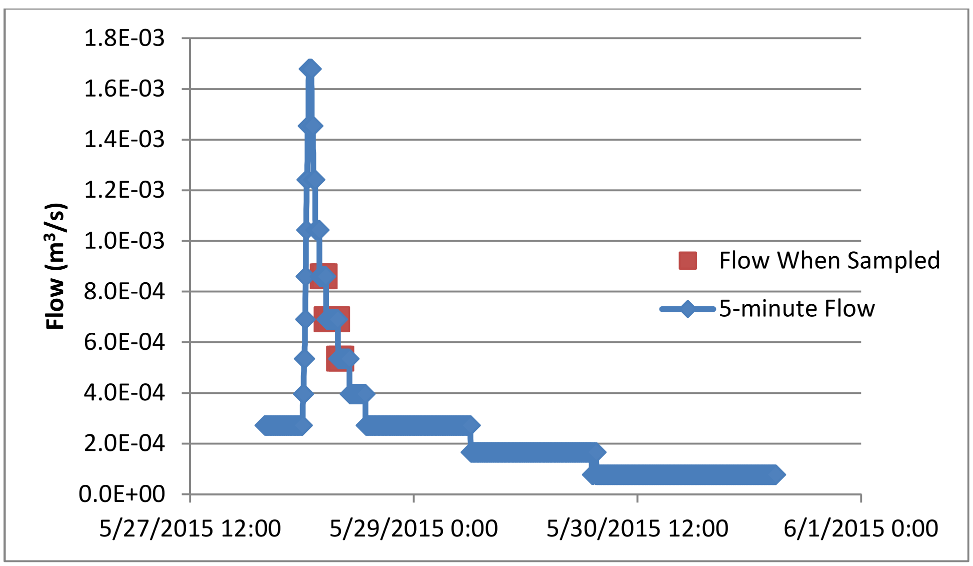

Storm 9 – 7/09/2015

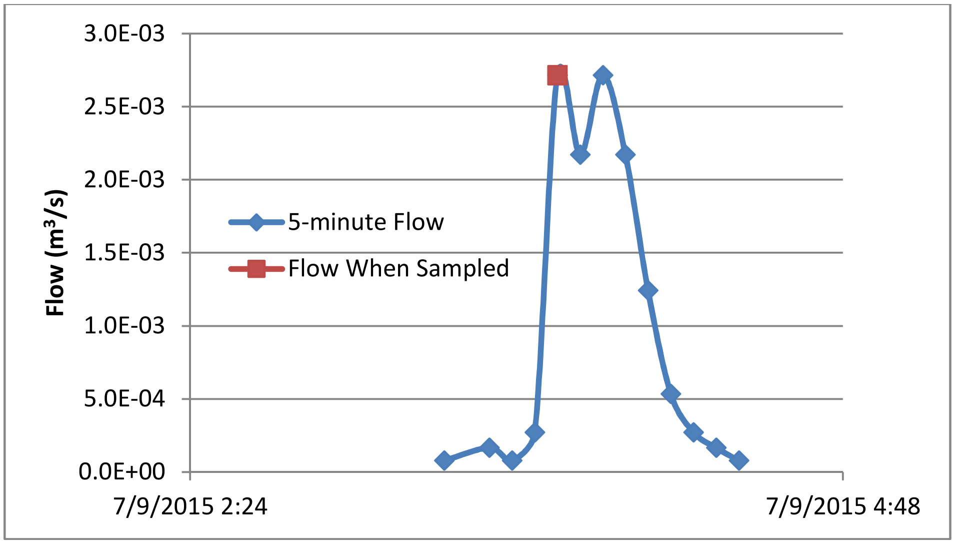

Storm 10 – 8/22/2015

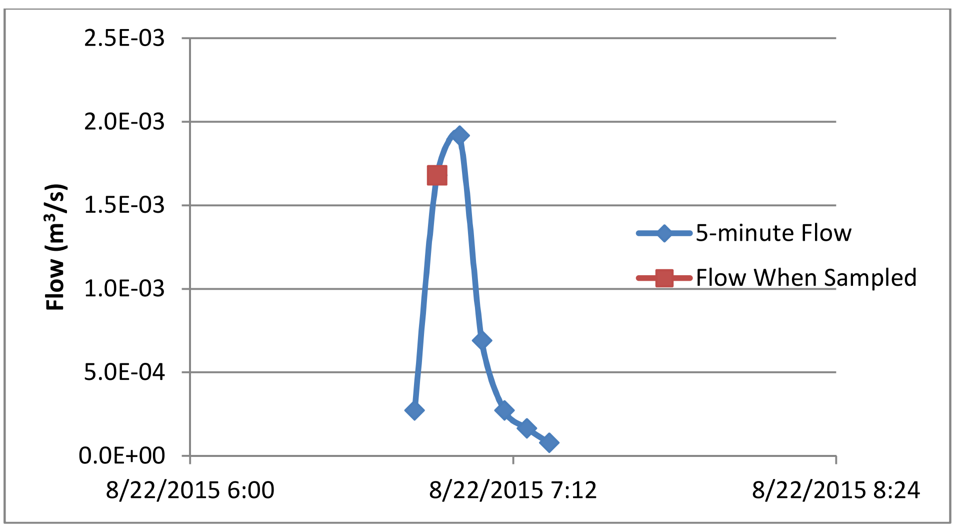

Storm 11 – 11/05/2015

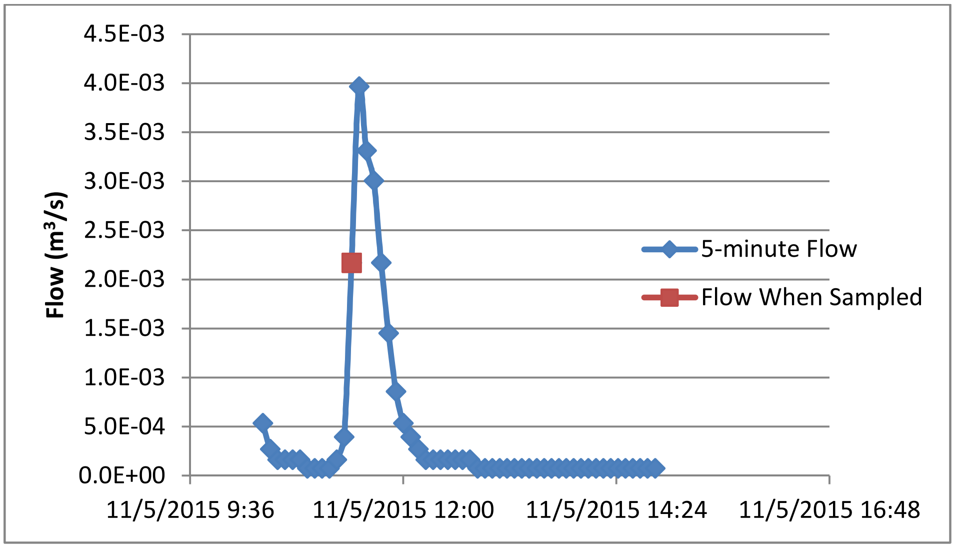

Storm 12 – 12/13/2015

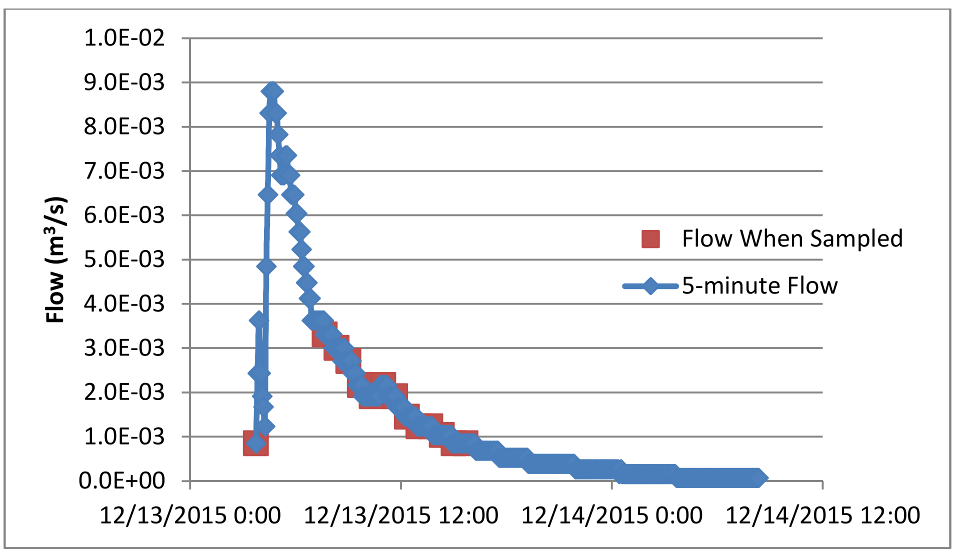

Storm 13 -12/26/2015

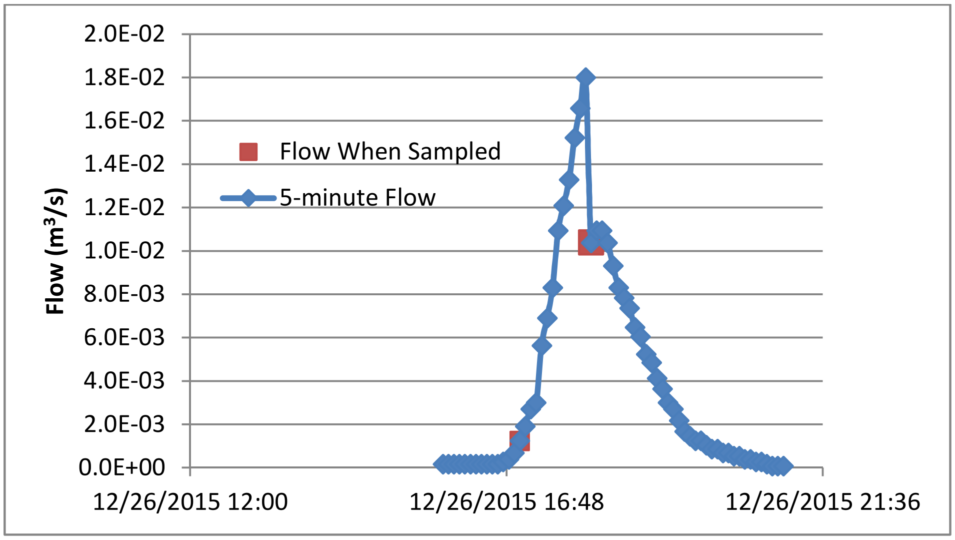

Storm 14 – 12/27/2015

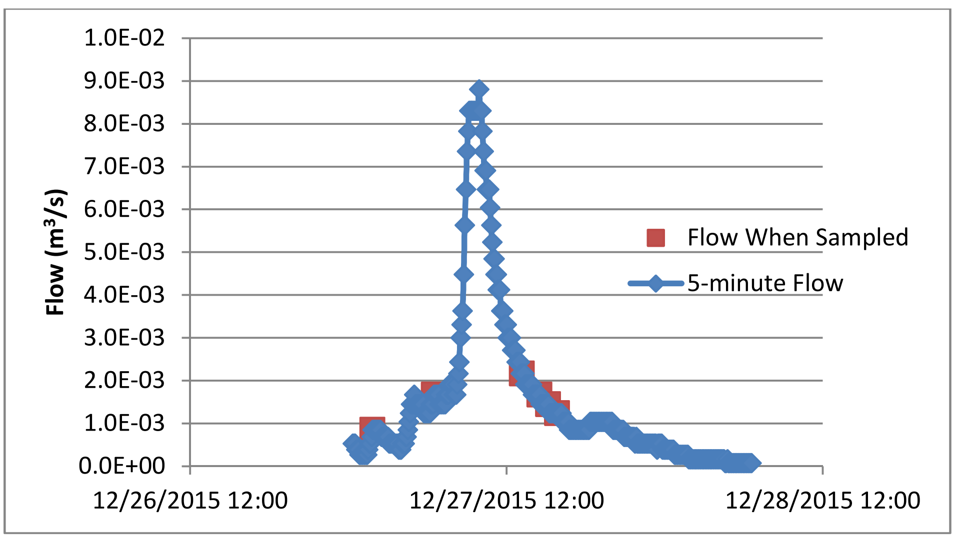

REGRESSION STATISTICS
(calculated in MiniTab 17 software)

Watershed E1

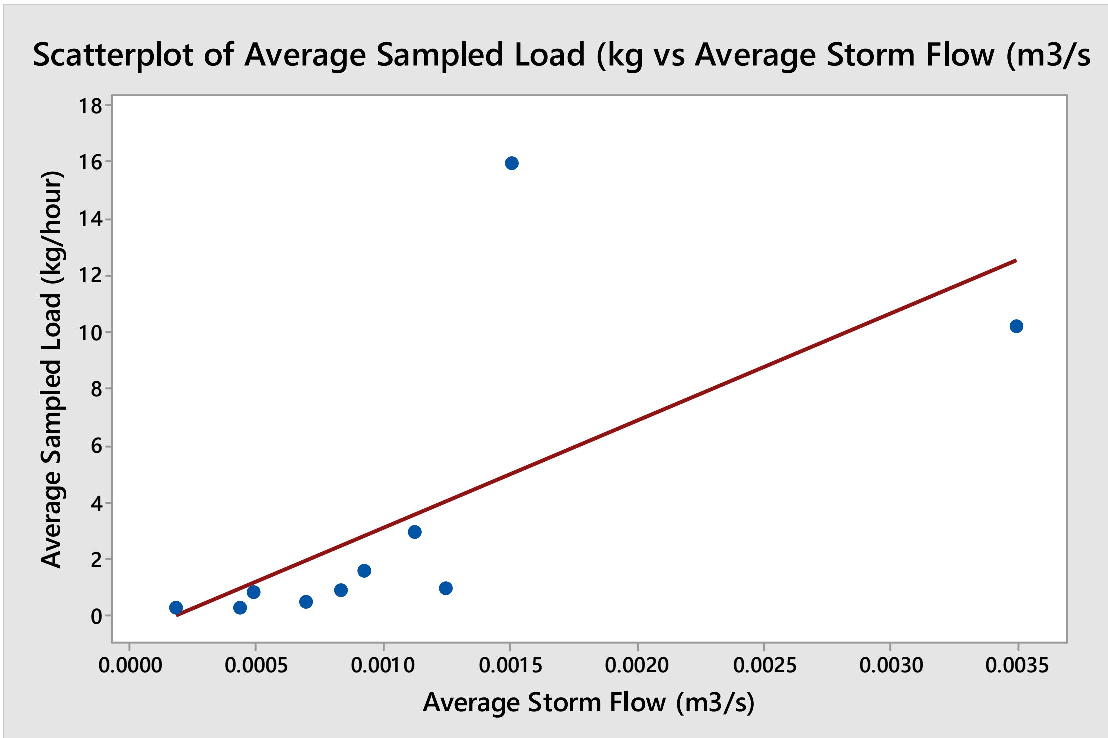

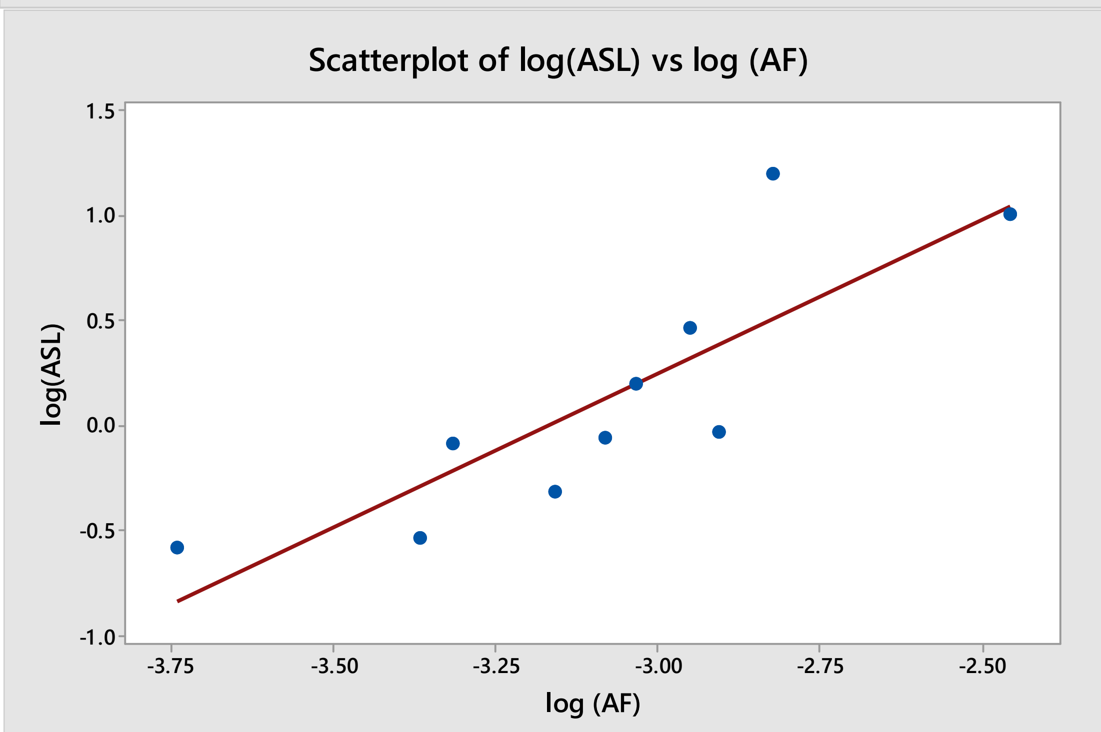

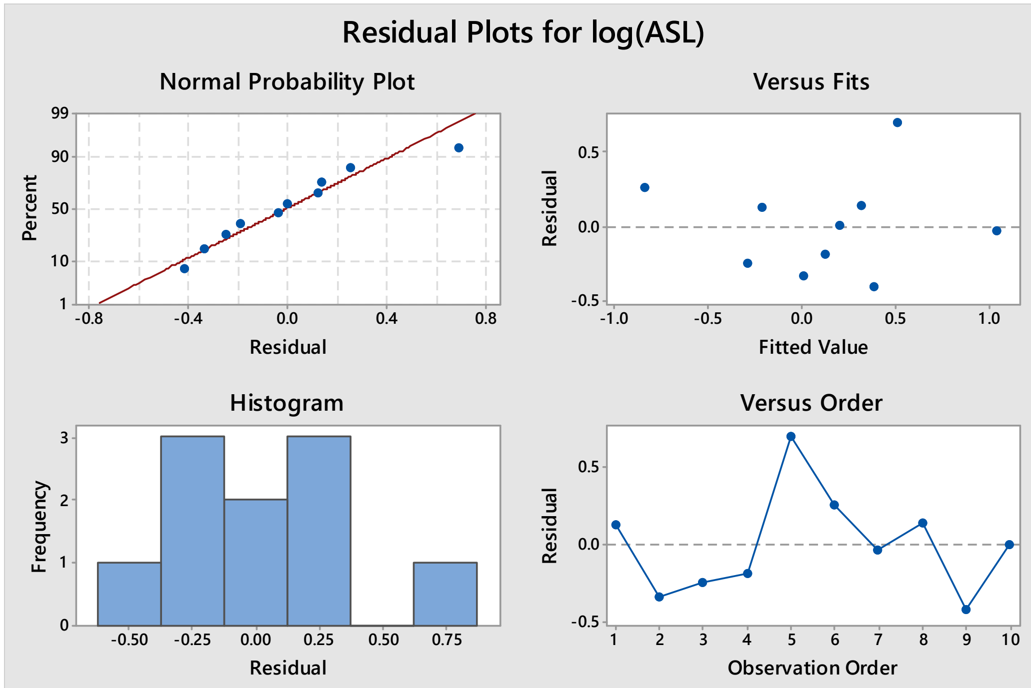

Regression Analysis: log(ASL) versus log (AF)

Analysis of Variance

Source	DF	Adj SS	Adj MS	F-Value	P-Value
Regression	1	2.3276	2.3276	19.22	0.002
log (AF)	1	2.3276	2.3276	19.22	0.002
Error	8	0.9689	0.1211		
Total	9	3.2964			

Model Summary

S	R-sq	R-sq(adj)	R-sq(pred)
0.348004	70.61%	66.94%	54.27%

Coefficients

Term	Coef	SE Coef	T-Value	P-Value	VIF
Constant	4.64	1.04	4.48	0.002	
log (AF)	1.463	0.334	4.38	0.002	1.00

Regression Equation

log(ASL) = 4.64 + 1.463 log (AF)

Fits and Diagnostics for Unusual Observations

Obs	log(ASL)	Fit	Resid	Std Resid	
5	1.204	0.510	0.695	2.18	R= Large residual

Durbin-Watson Statistic = 1.8558

Watershed E2

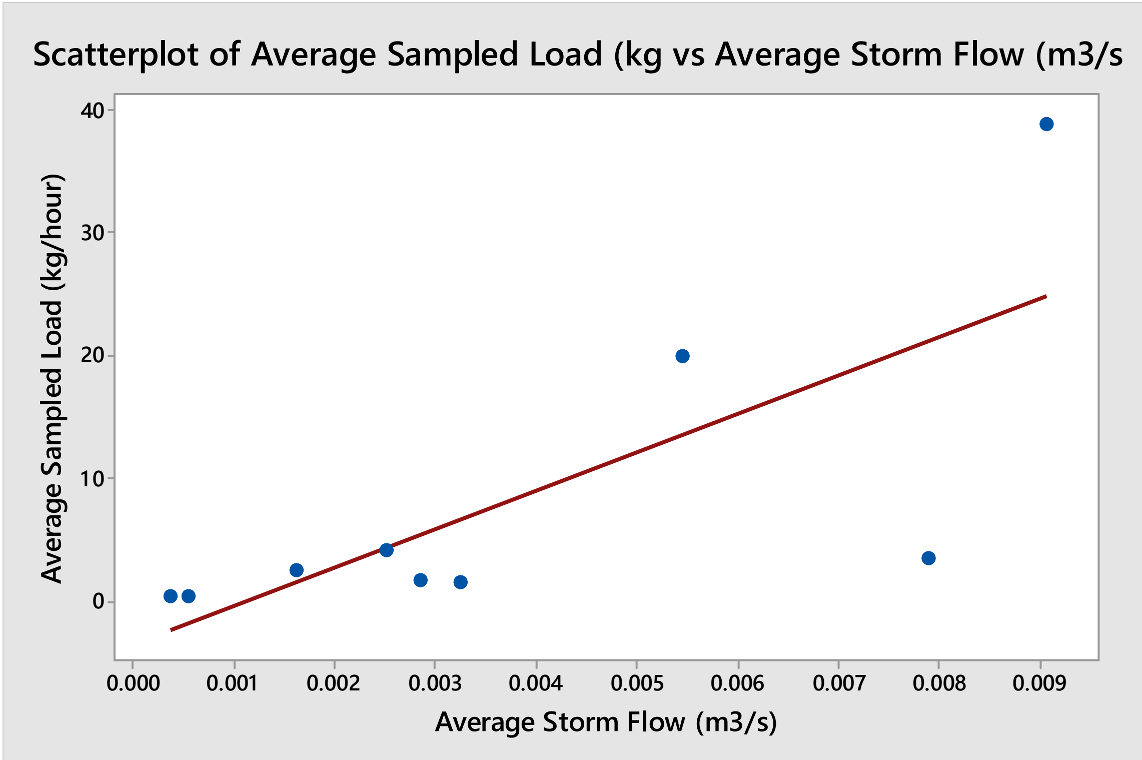

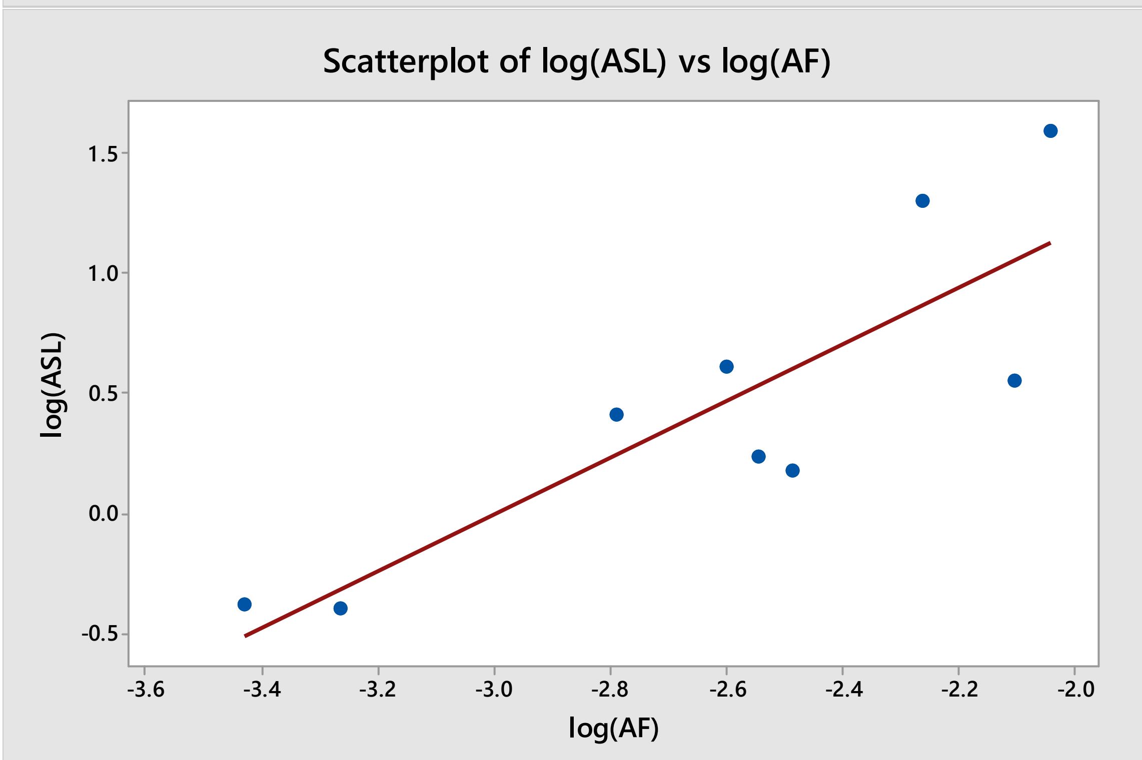

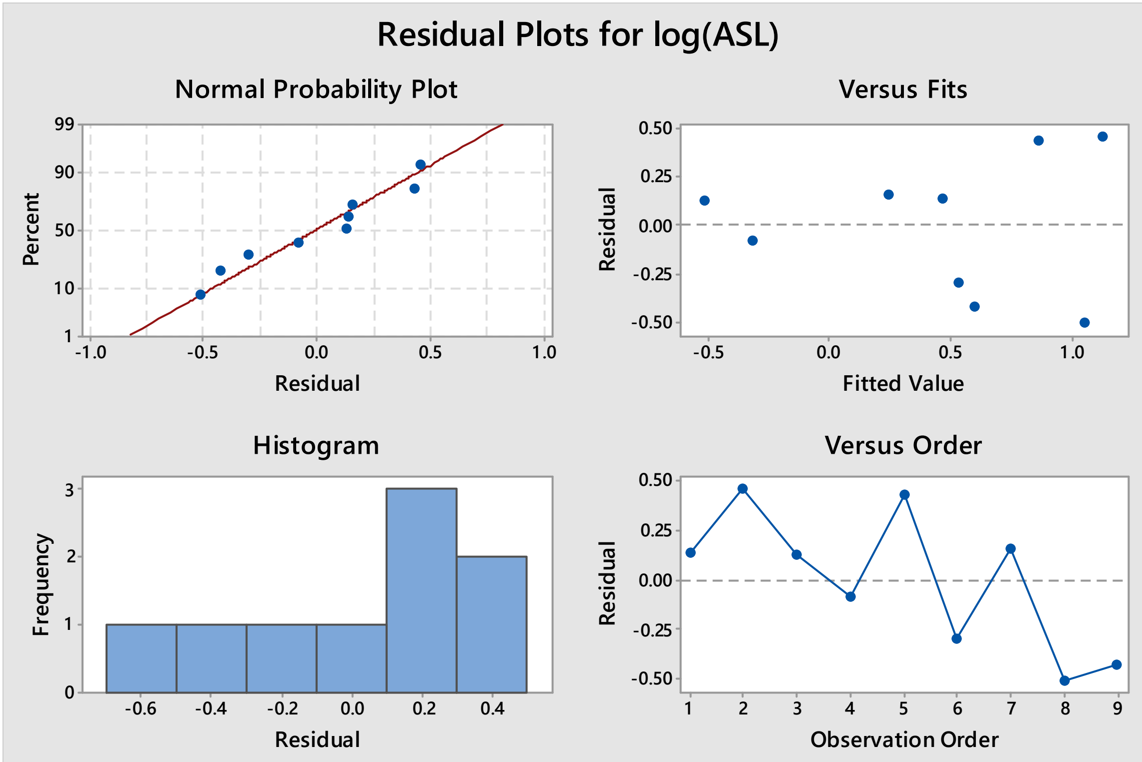

Regression Analysis: log(ASL) versus log(AF)

Analysis of Variance

Source	DF	Adj SS	Adj MS	F-Value	P-Value
Regression	1	2.5904	2.5904	18.17	0.004
log(AF)	1	2.5904	2.5904	18.17	0.004
Error	7	0.9977	0.1425		
Total	8	3.5882			

Model Summary

S	R-sq	R-sq(adj)	R-sq(pred)
0.377538	72.19%	68.22%	54.27%

Coefficients

Term	Coef	SE Coef	T-Value	P-Value	VIF
Constant	3.541	0.735	4.82	0.002	
log(AF)	1.181	0.277	4.26	0.004	1.00

Regression Equation

log(ASL) = 3.541 + 1.181 log(AF)

Durbin-Watson Statistic = 1.72908

Watershed P1

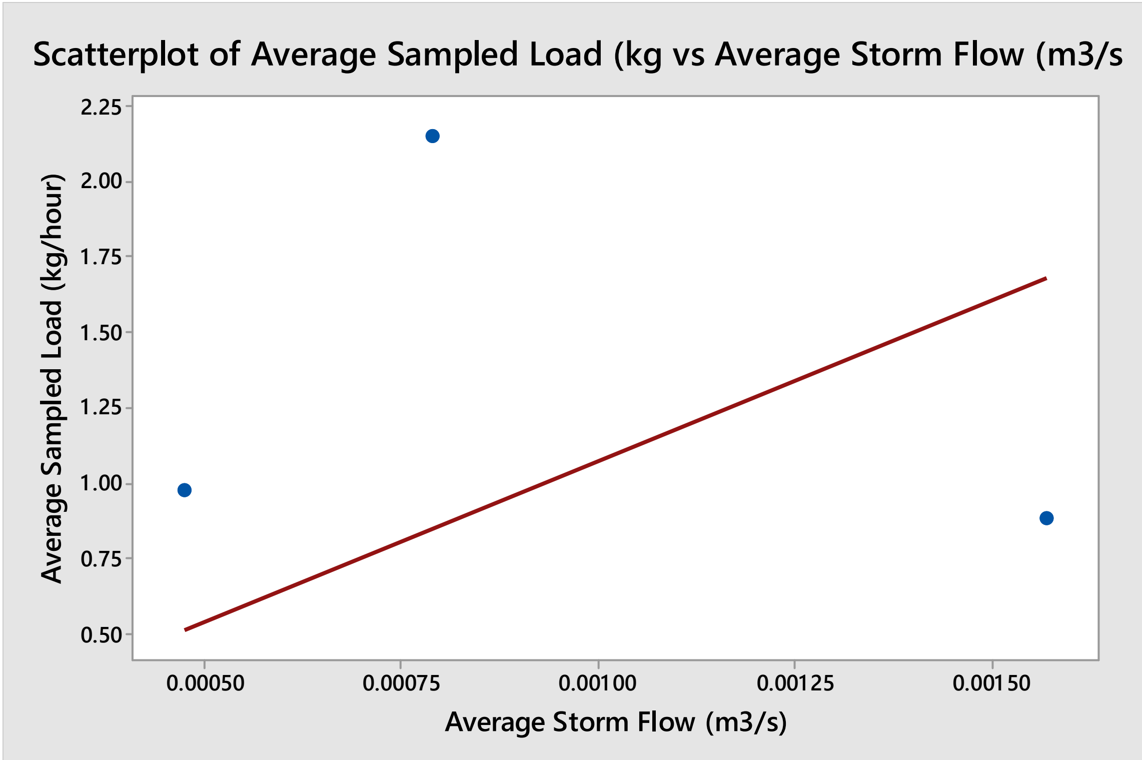

Watershed P2

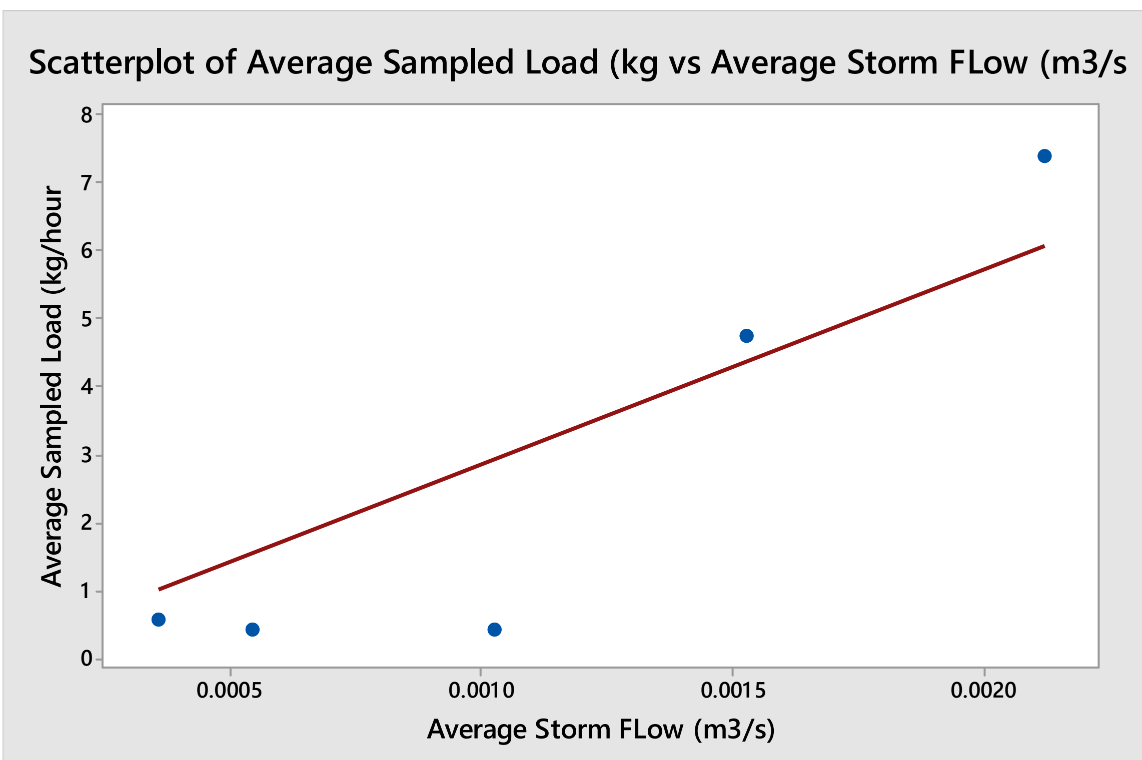

JET EROSION TEST
RAW DATA

JET characteristics for each test

Watershed	Location #	Jet #	Pressure Head (in)	Pressure Head (cm)	Test Duration (min)
E1	2	1	26.5	67.3	35.25
	6(1)	1	26	66.0	16.25
	6(2)	1	35	88.9	49.5
	13	1	25	63.5	69
	15	1	26.5	67.3	11.75
	17	1	26	66.0	28
	19	1	26	66.0	30.25
E2	4	1	26	66.0	59.5
	9	1	26	66.0	40.25
	14	1	31	78.7	47.5
	16	1	31	78.7	52
	17	1	30	76.2	52.25
	20	1	30	76.2	37.75
	21	1	30	76.2	40.5
P1	2	1	26.5	67.3	40.5
	5	1	26	66.0	39.75
	6	1	29.5	74.9	43
	9	1	28	71.1	46
	11	1	27	68.6	39.5
	12(1)	1	25.5	64.8	6
	12(2)	1	27-33	68.6-83.8	21.75
	14	1	26	66.0	65
	17(1)	1	26.5	67.3	16
	17(2)	1	34	86.4	56
	18	1	26.5	67.3	40.75
	23	1	25	63.5	51.25
P2	2	1	30	76.2	46.5
	4	1	30	76.2	58
	7	1	30	76.2	45.5
	9	1	30	76.2	69.5
	12	1	28	71.1	50.5
	14	1	30	76.2	44.5
	15	1	30	76.2	41
	19	1	28	71.1	37

Scour Depth versus Time Plots

<u>Watershed E1:</u>

JET Location # 2

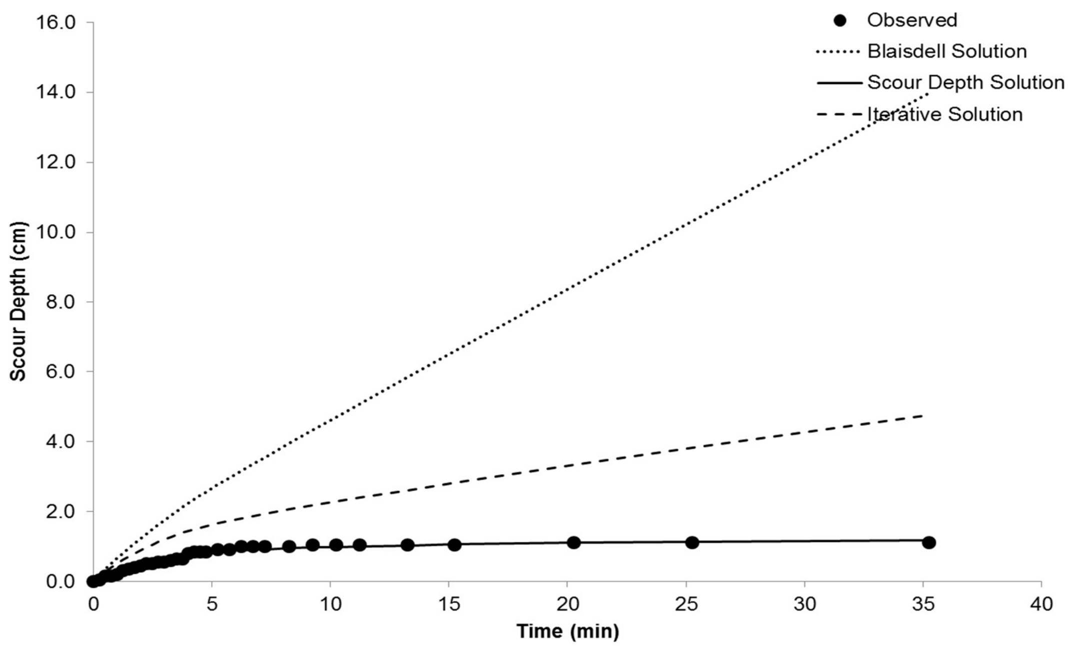

JET Location # 6-1

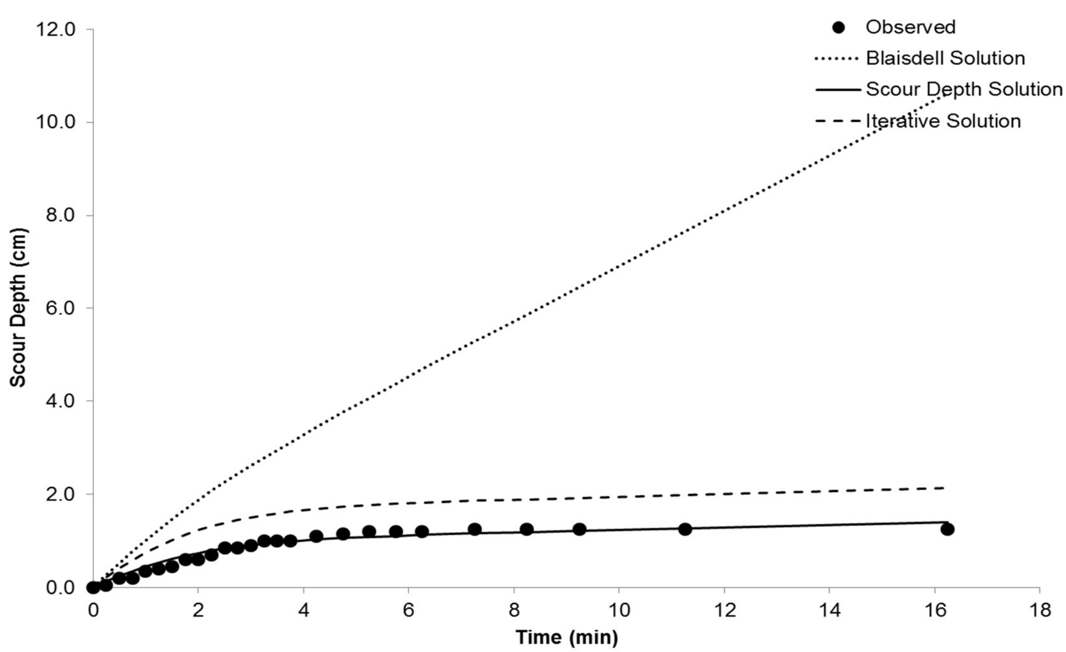

JET Location # 6-2

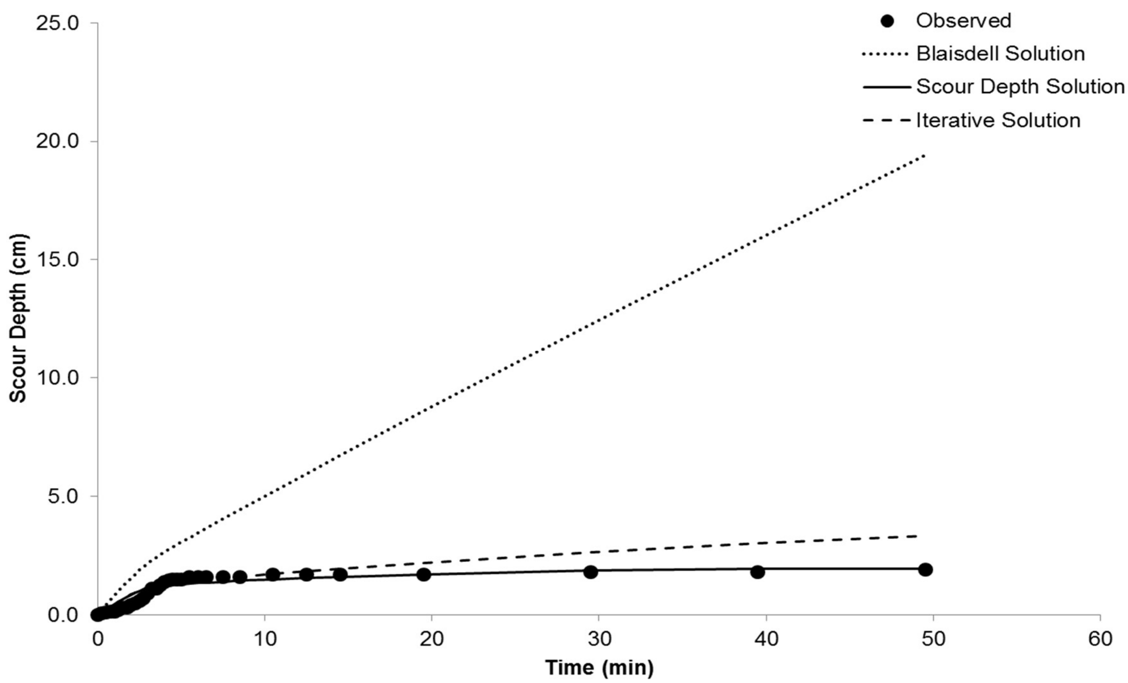

JET Location # 13

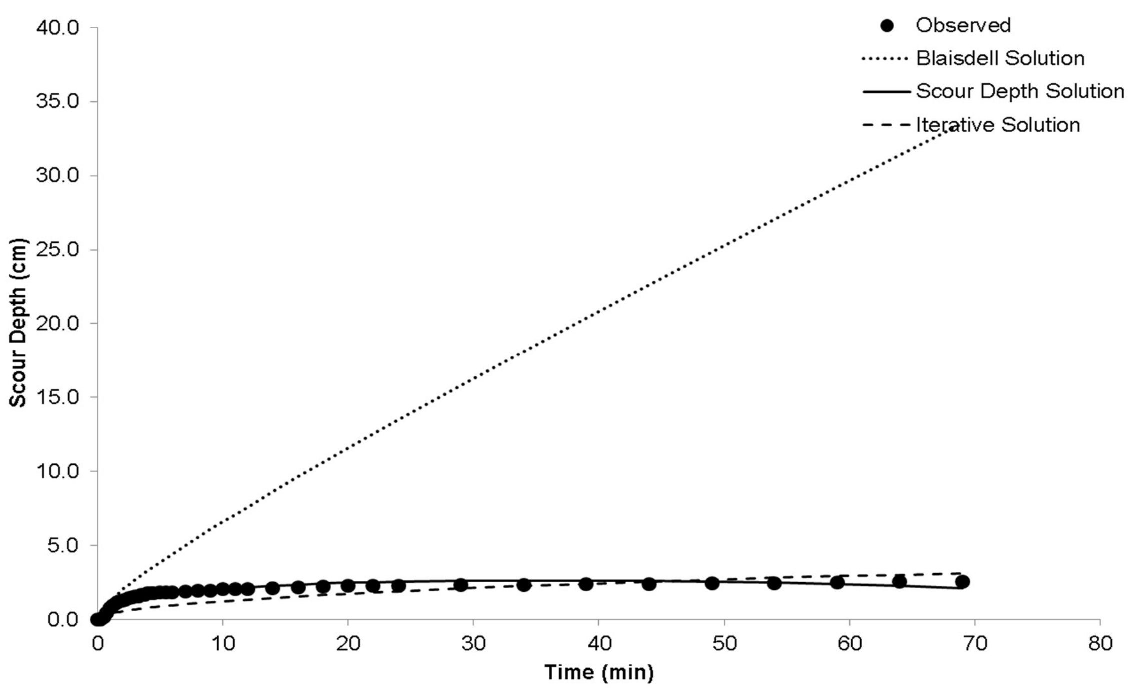

JET Location # 15

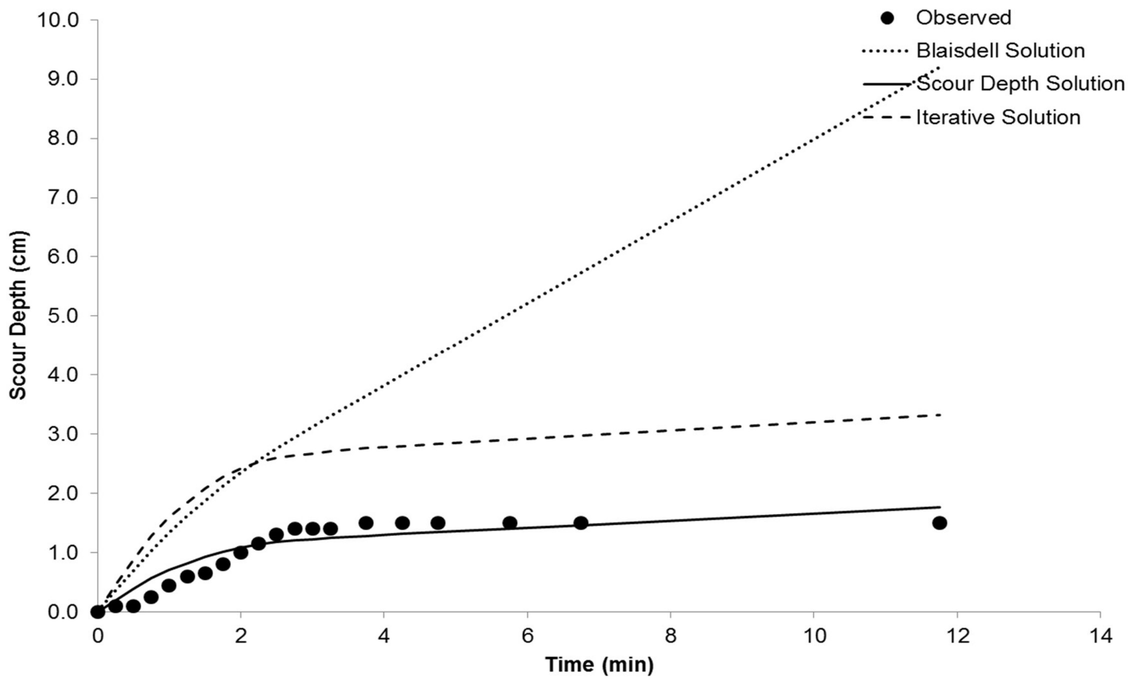

JET Location # 17

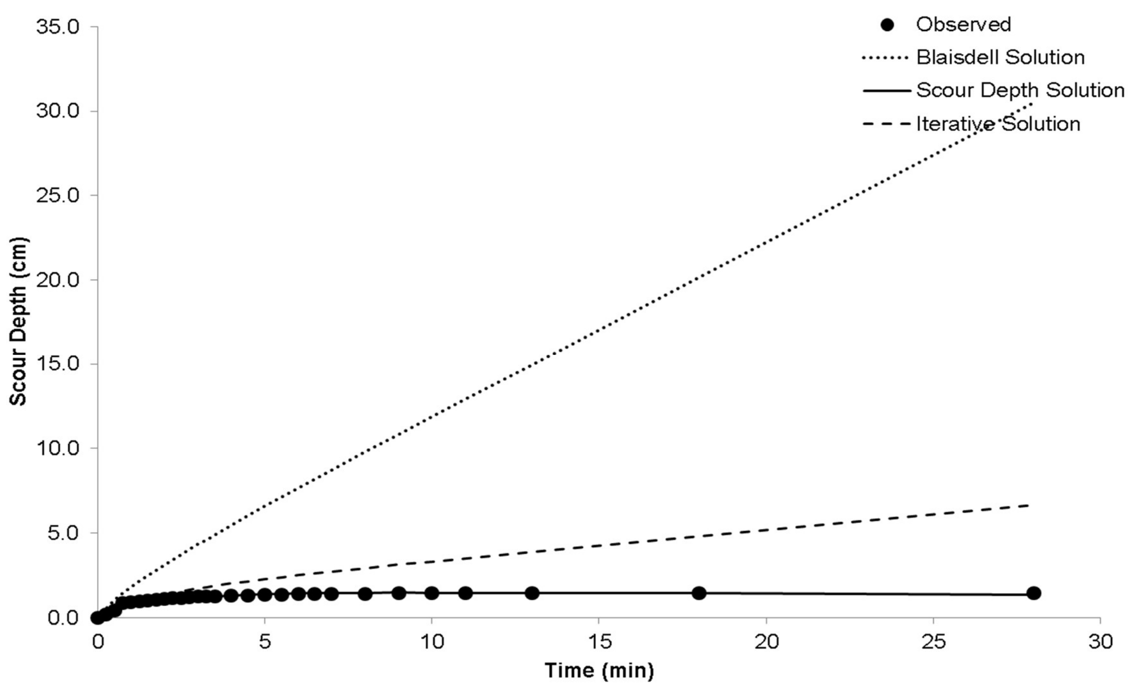

JET Location # 19

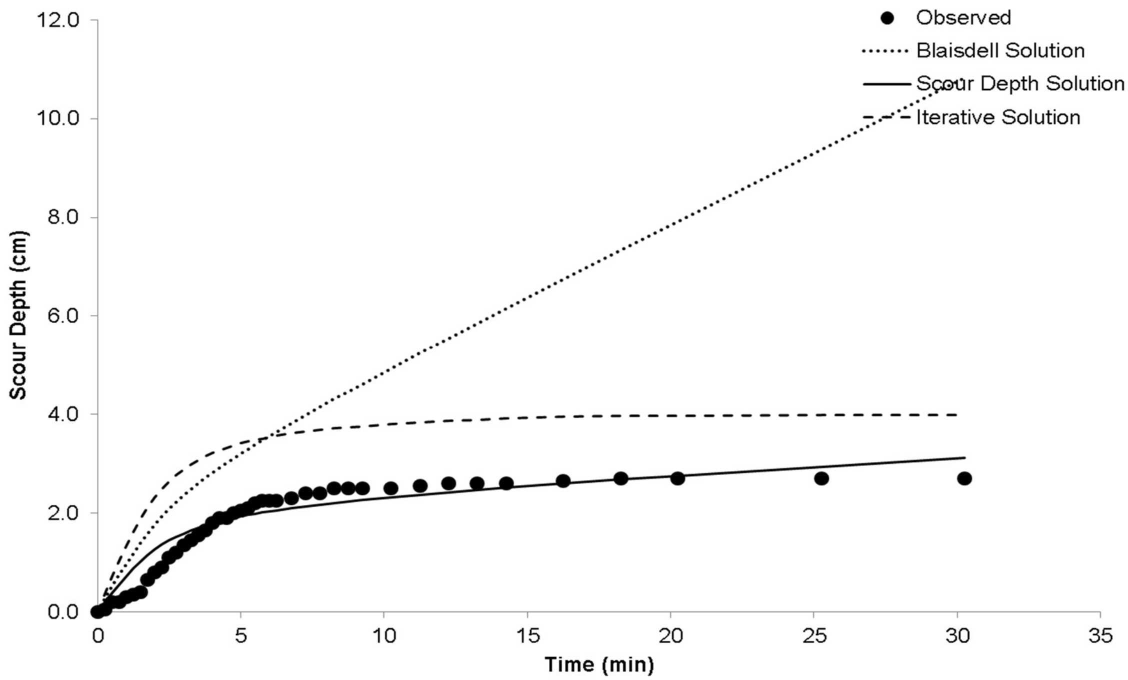

Watershed E2:

JET Location # 4

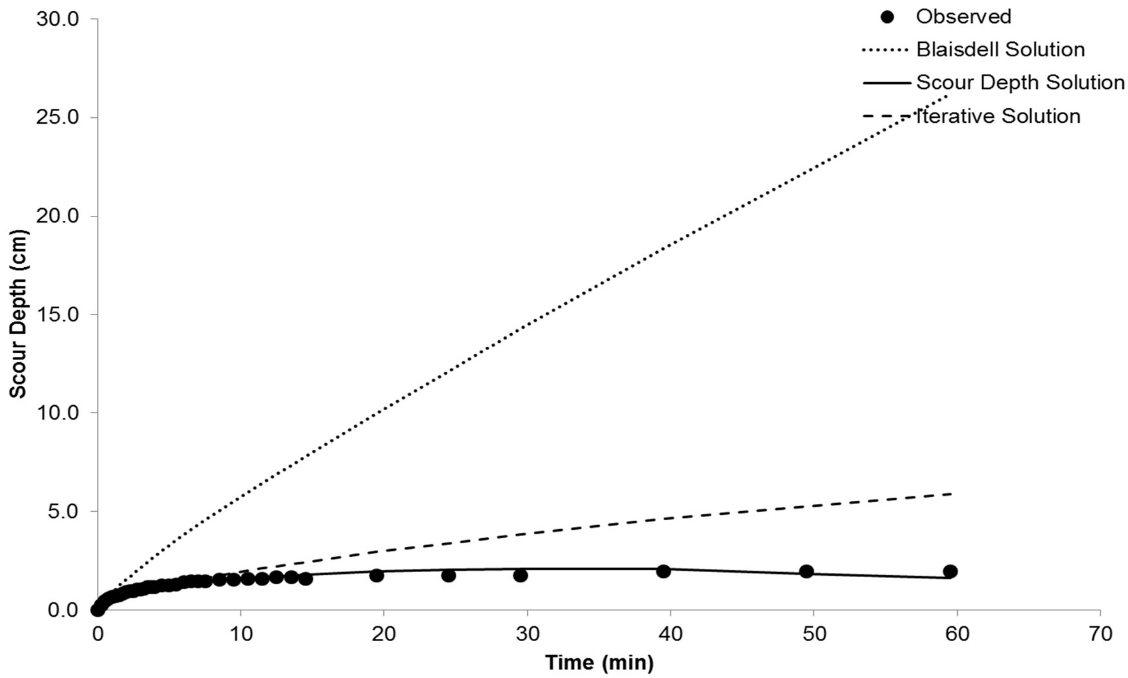

JET Location # 9

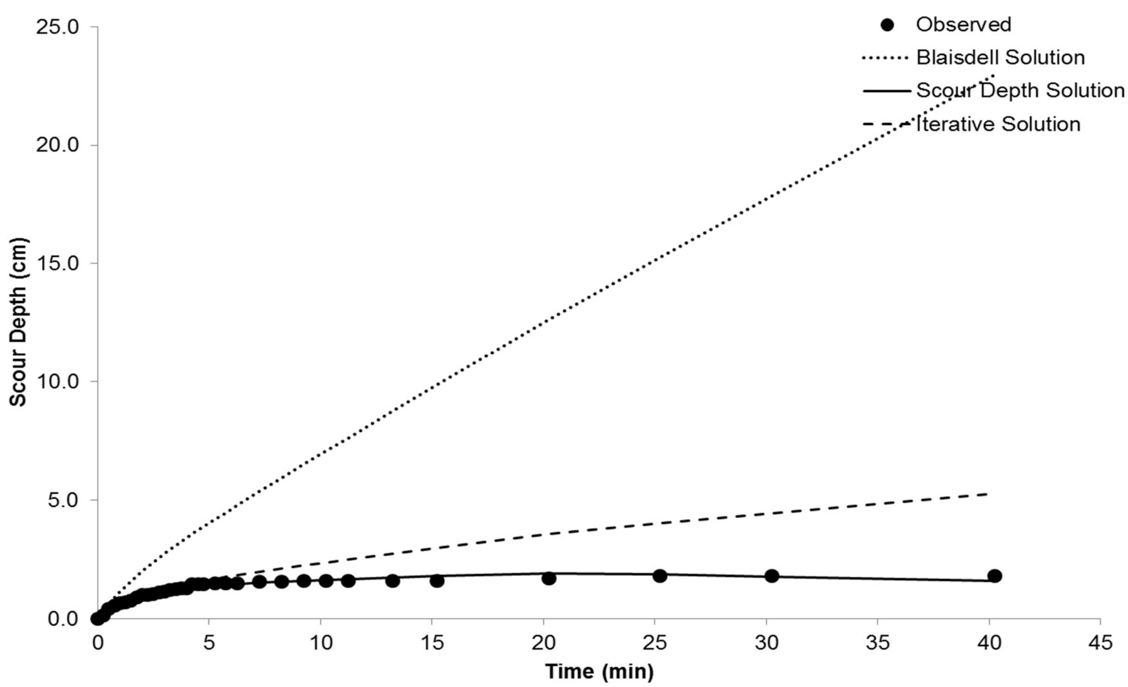

JET Location # 14

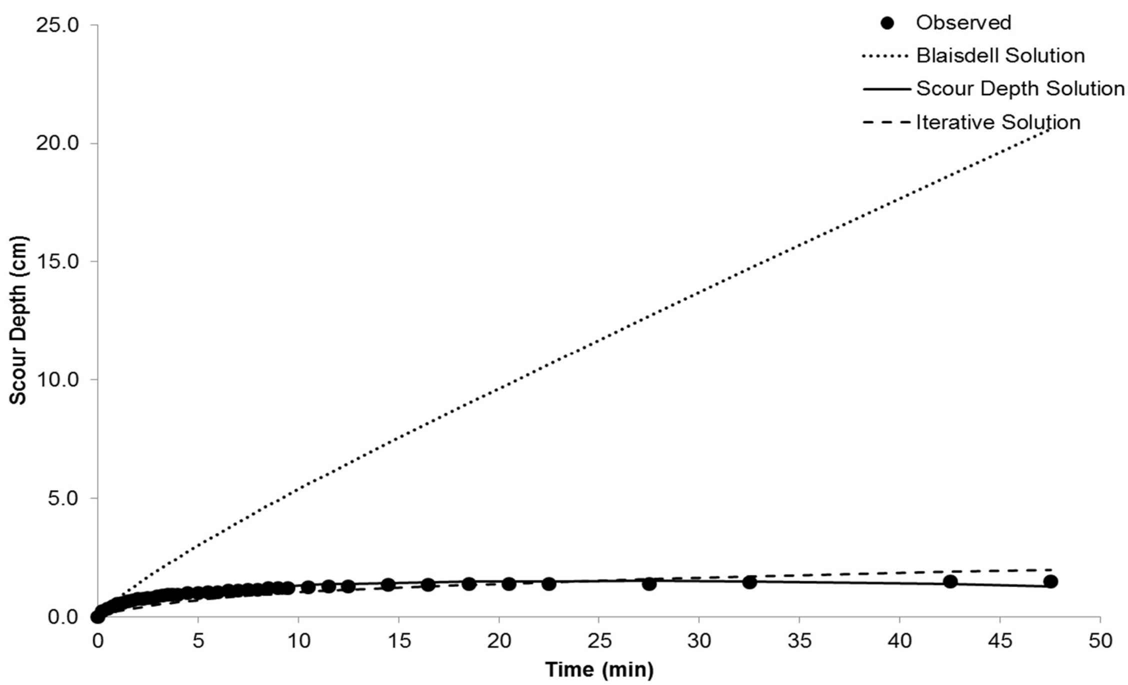

JET Location # 16

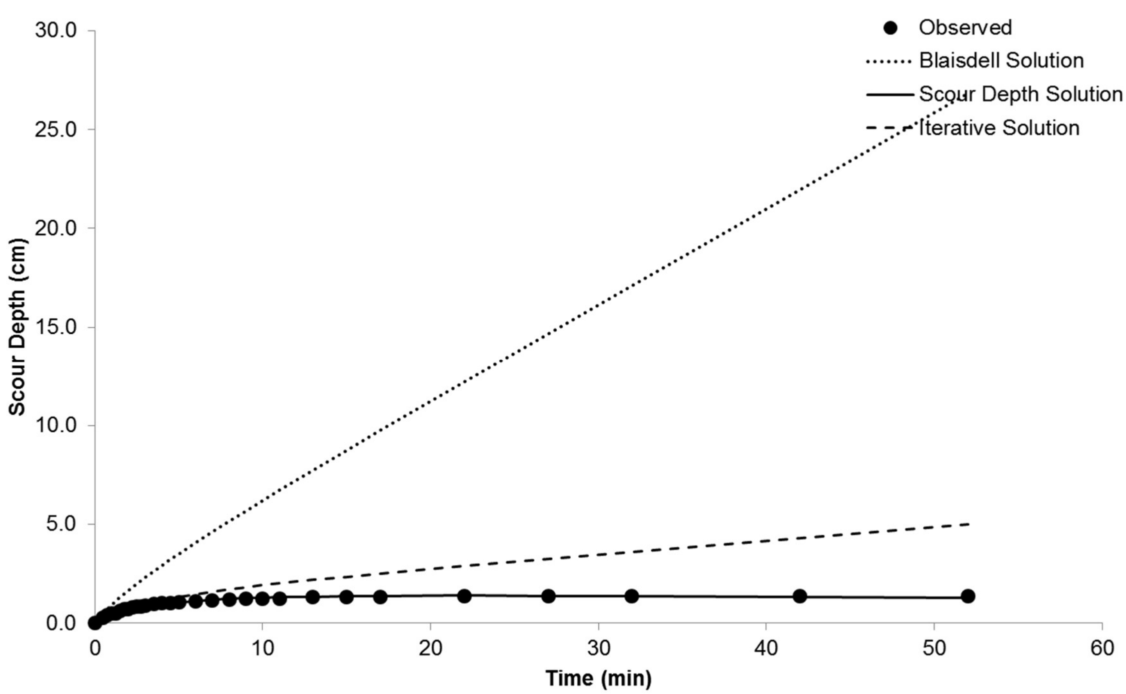

JET Location # 17

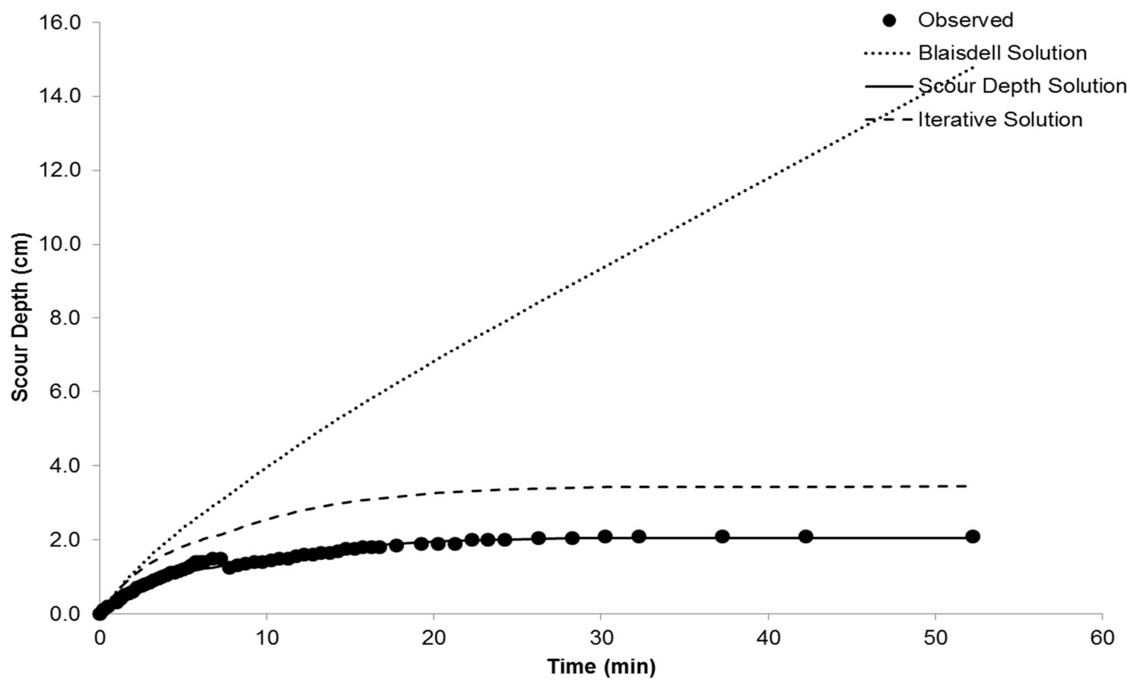

JET Location # 20

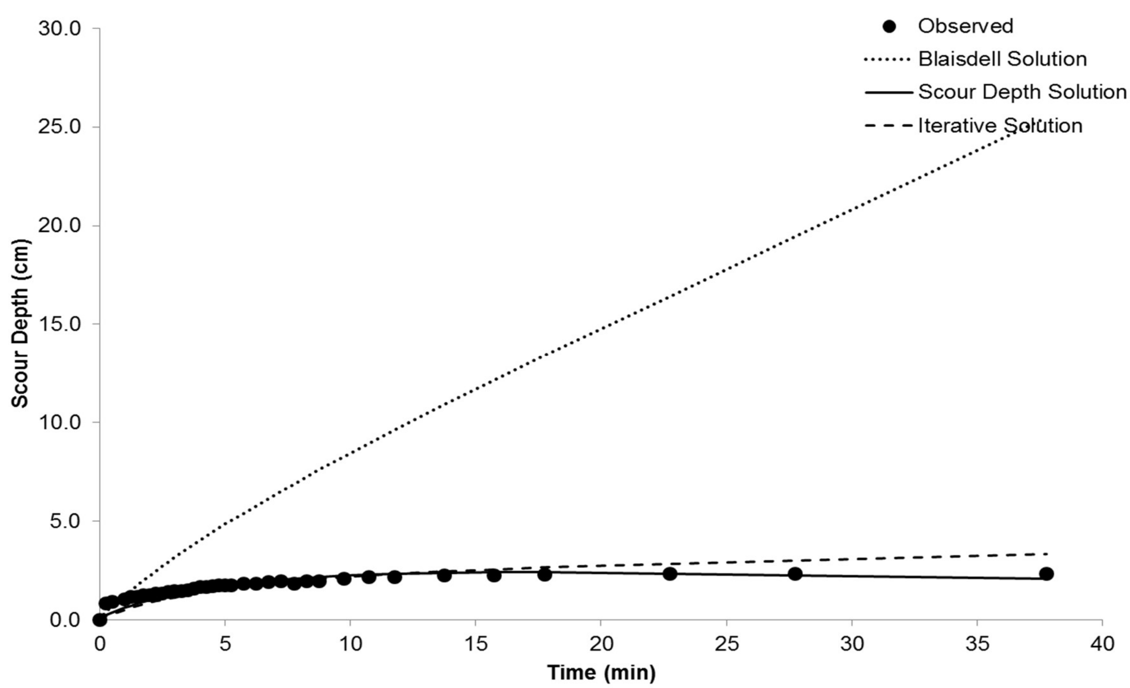

JET Location # 21

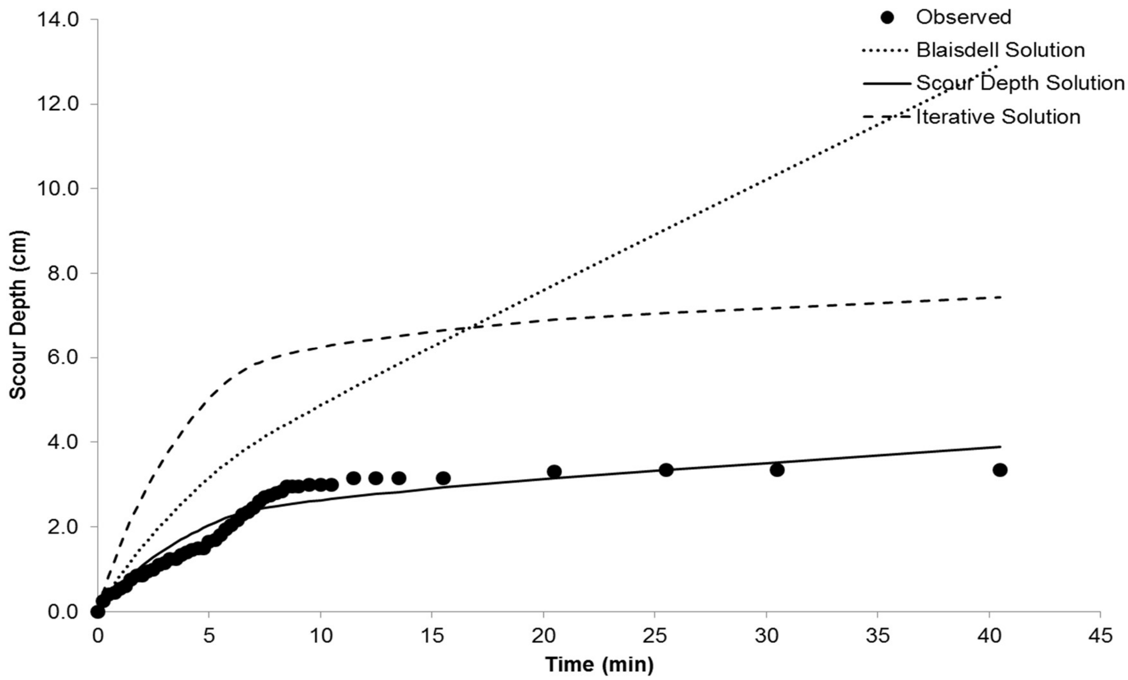

Watershed P1:

JET Location # 2

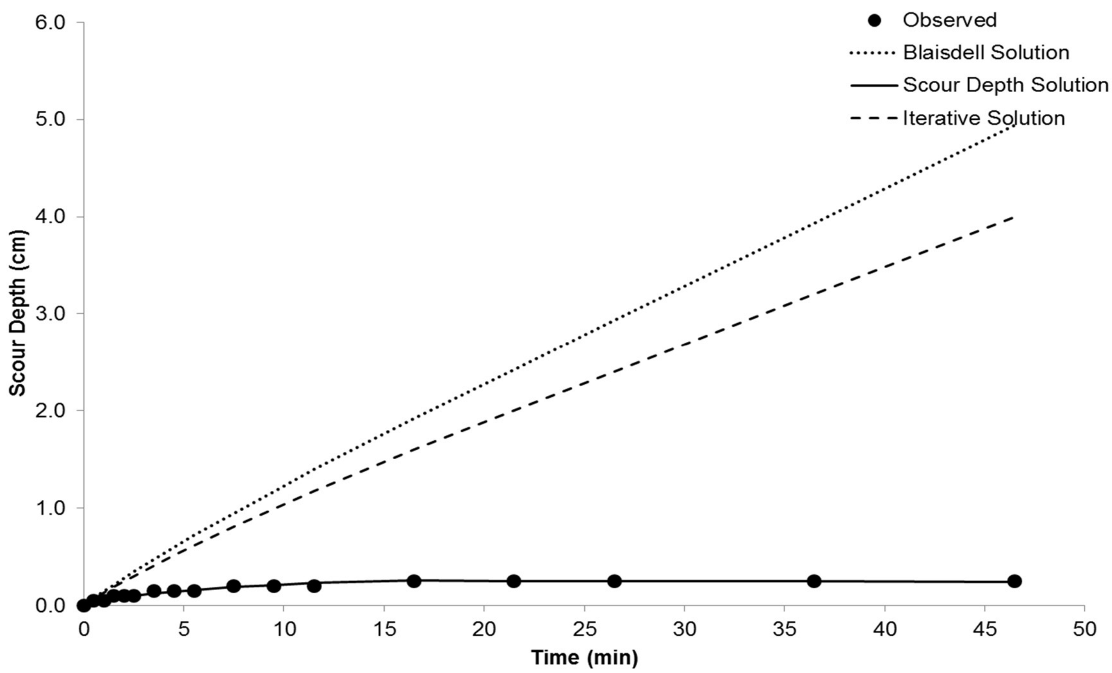

JET Location # 4

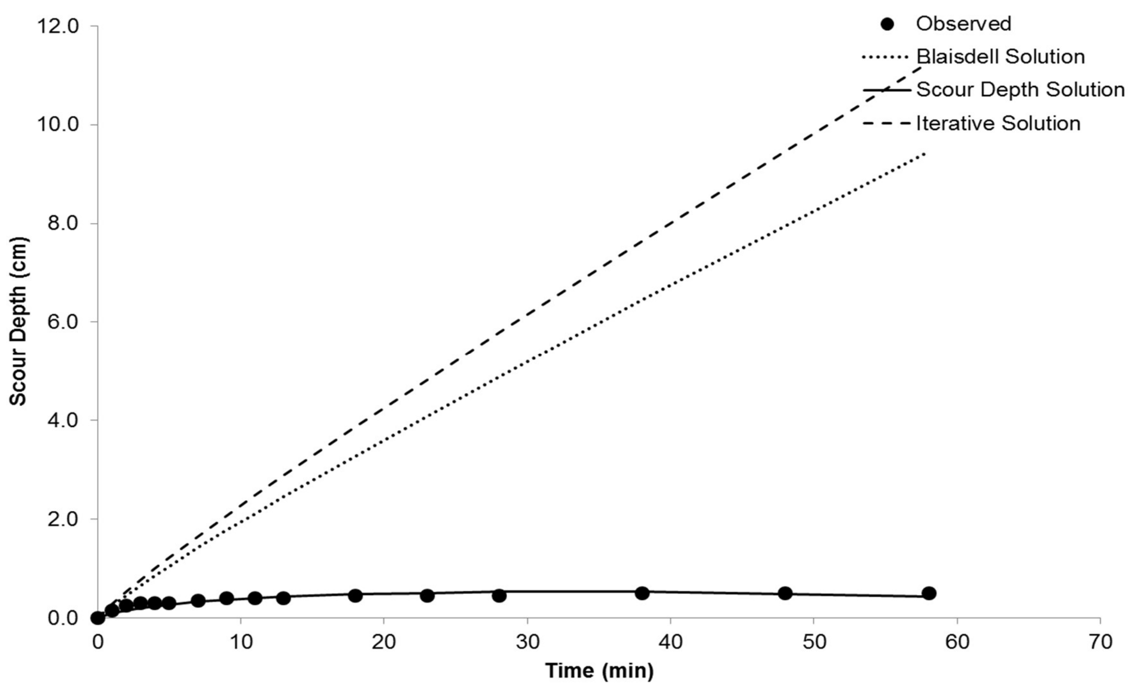

JET Location # 7

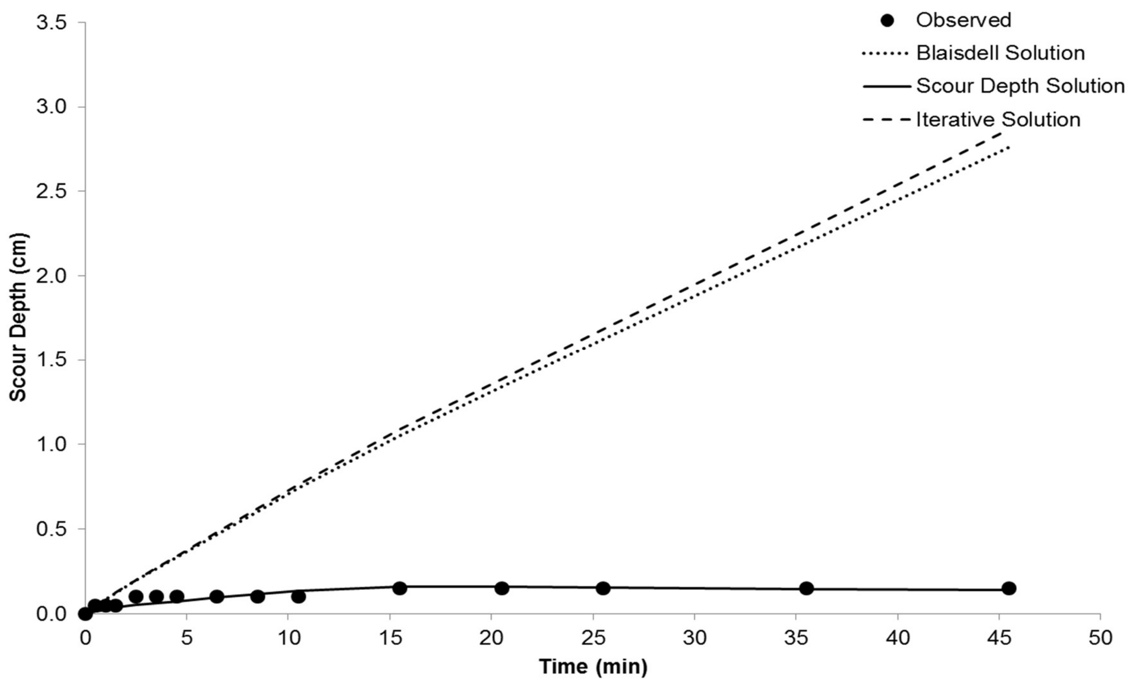

JET Location # 9

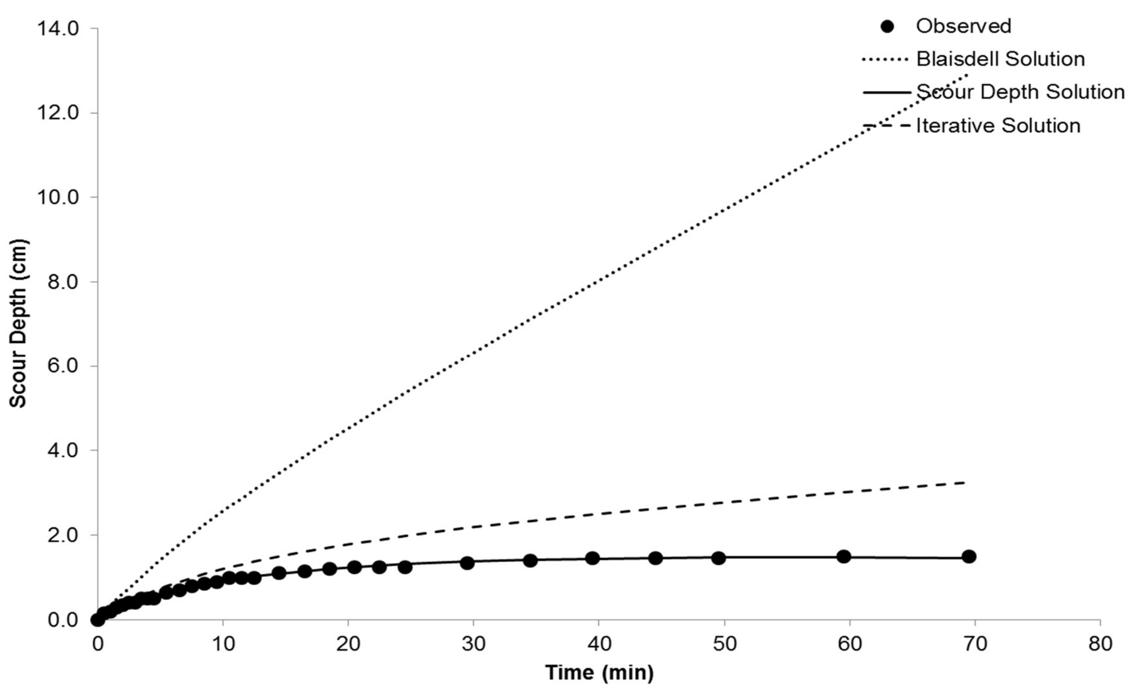

JET Location # 12

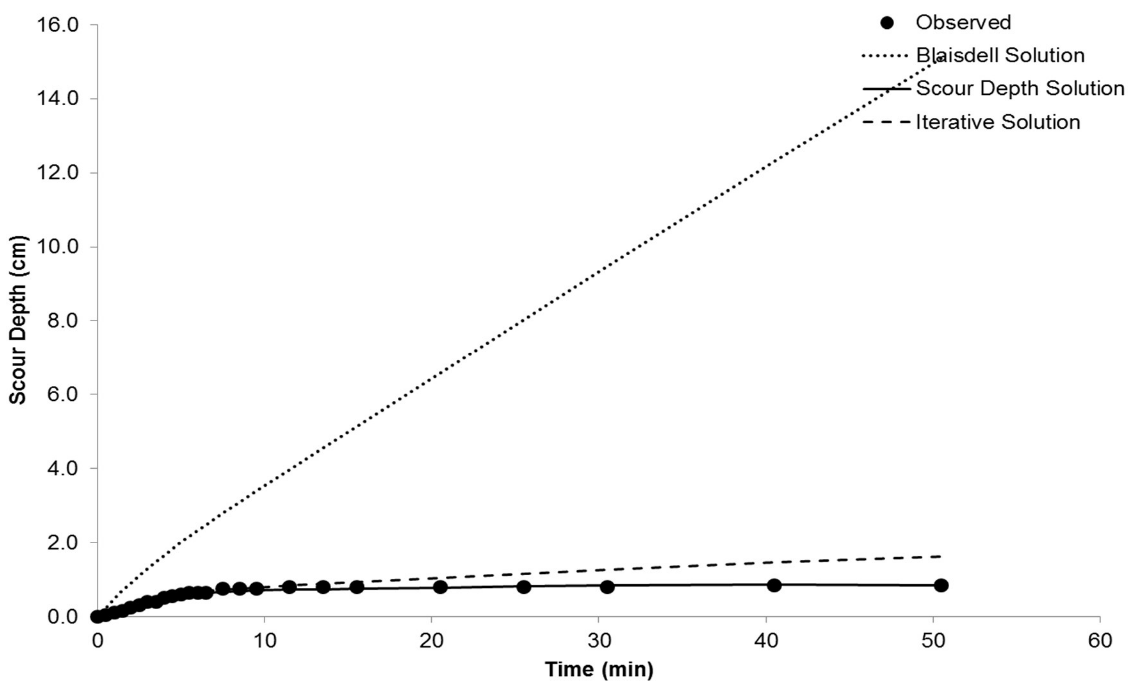

JET Location # 14

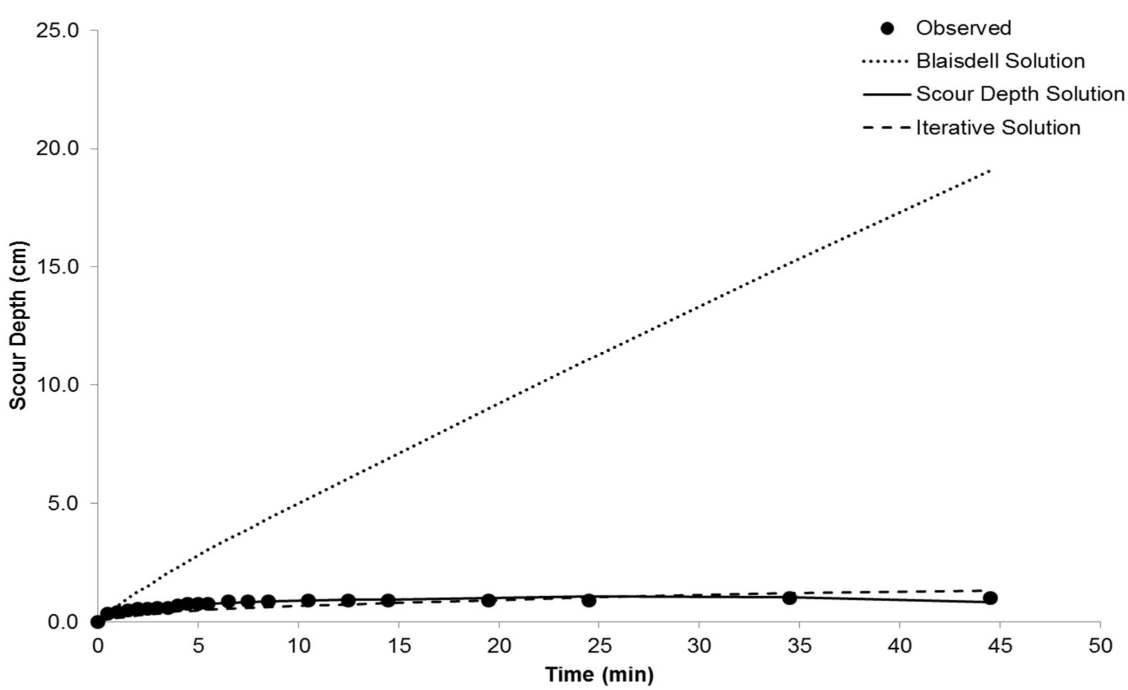

JET Location # 15

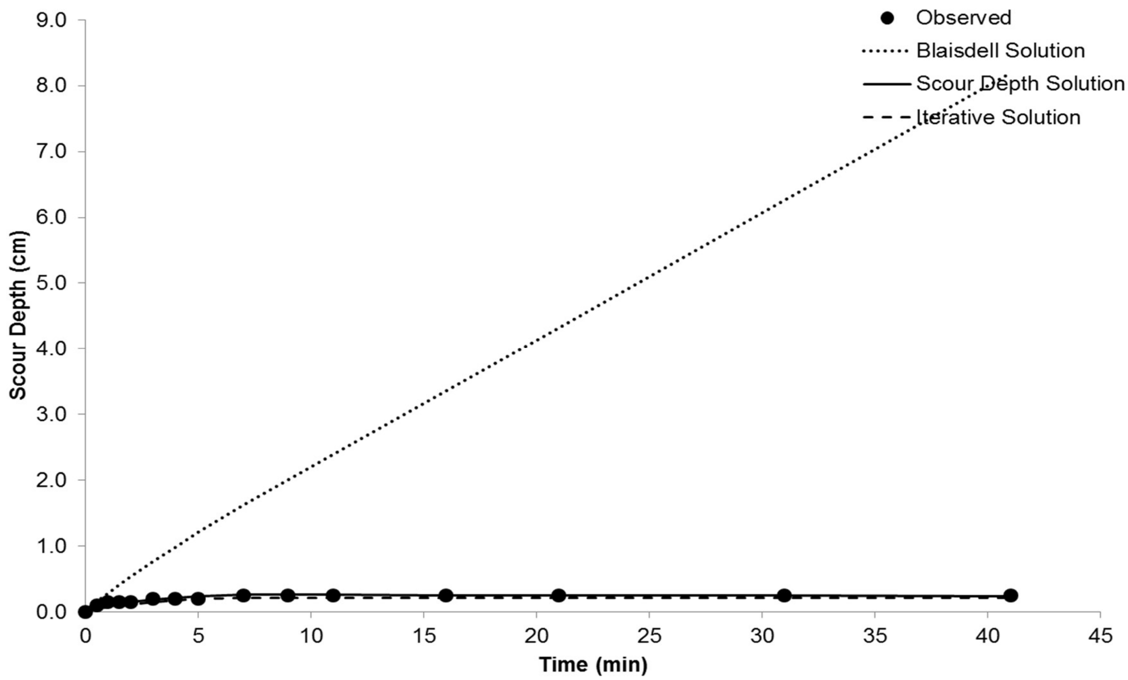

JET Location # 19

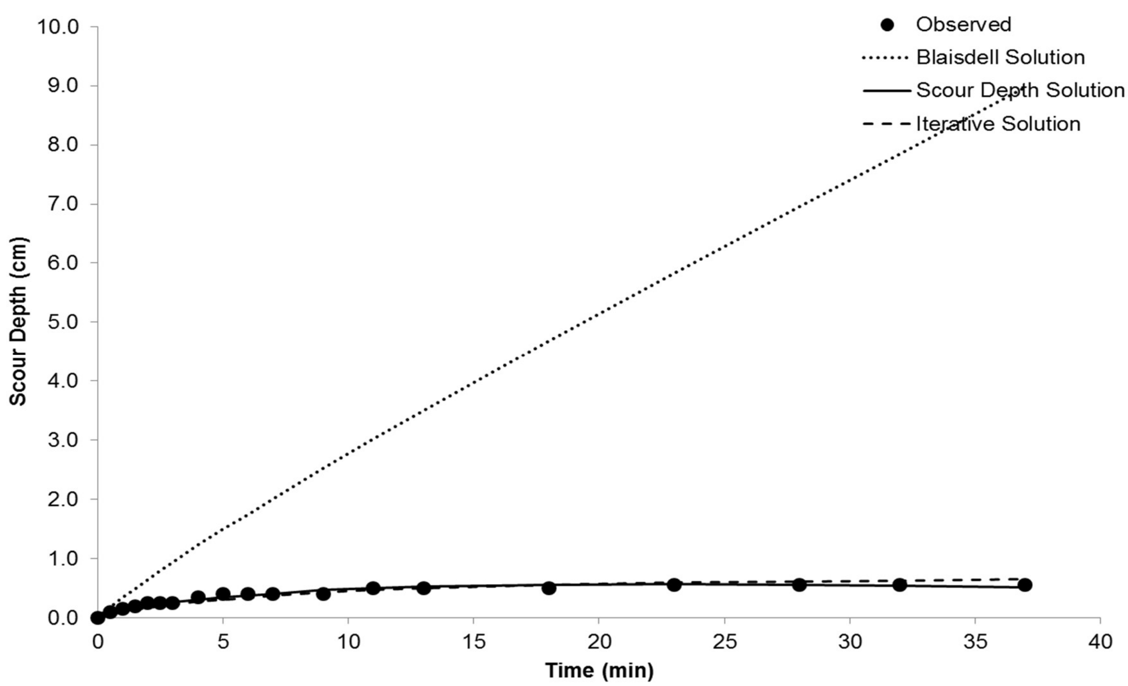

Watershed P2:

JET Location # 2

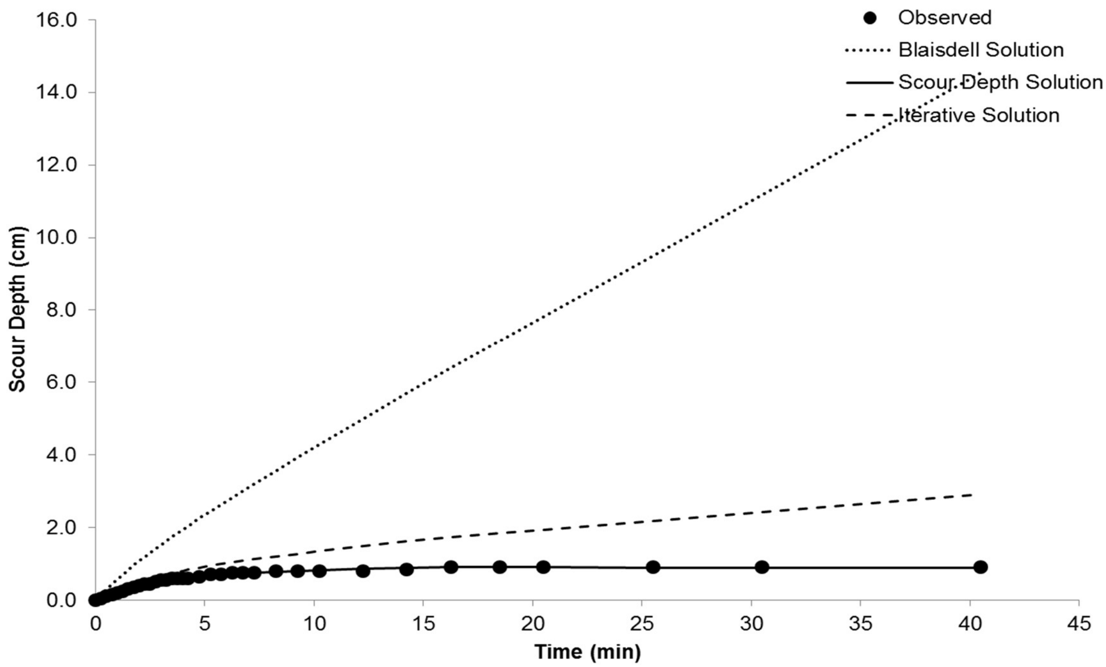

JET Location # 5

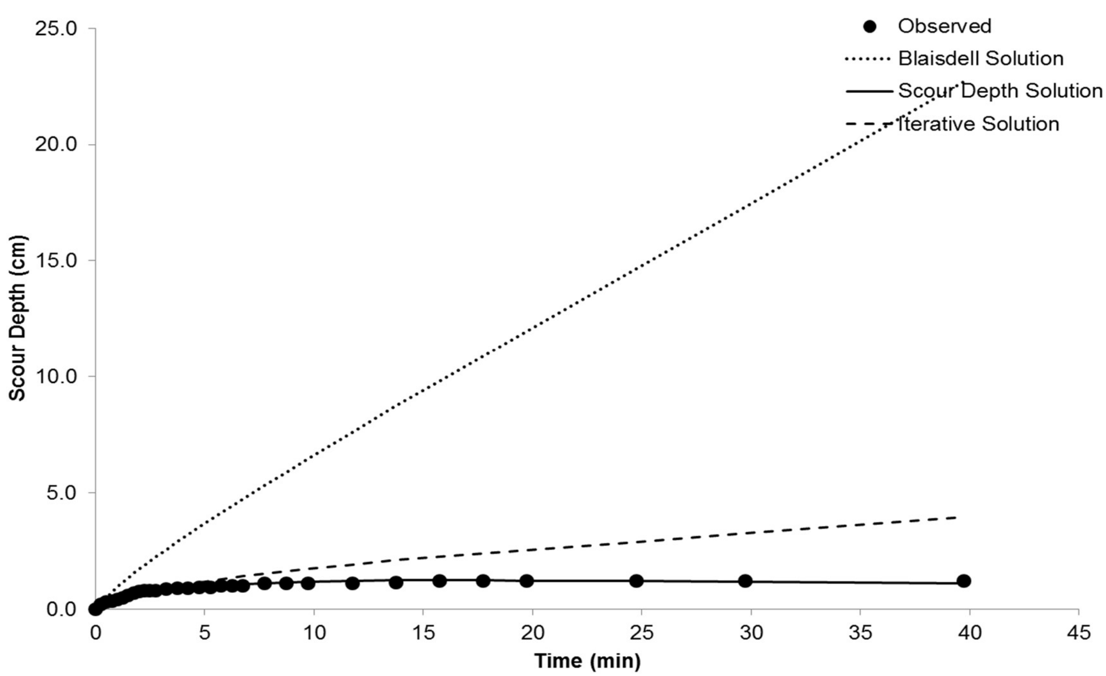

JET Location # 6

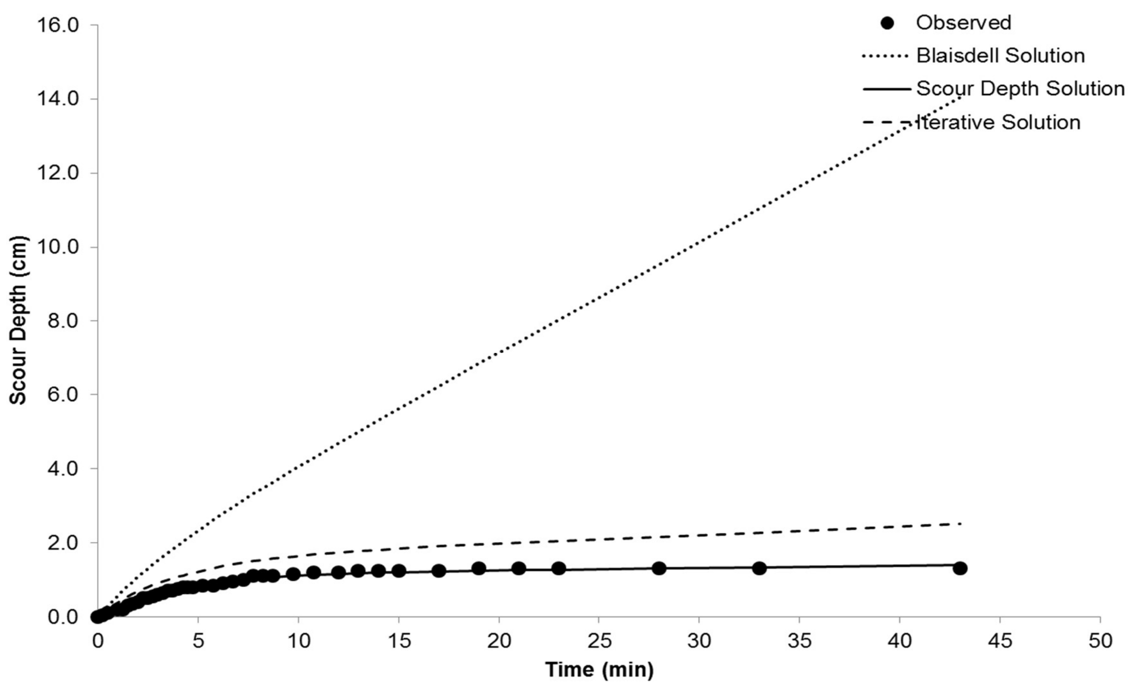

JET Location # 9

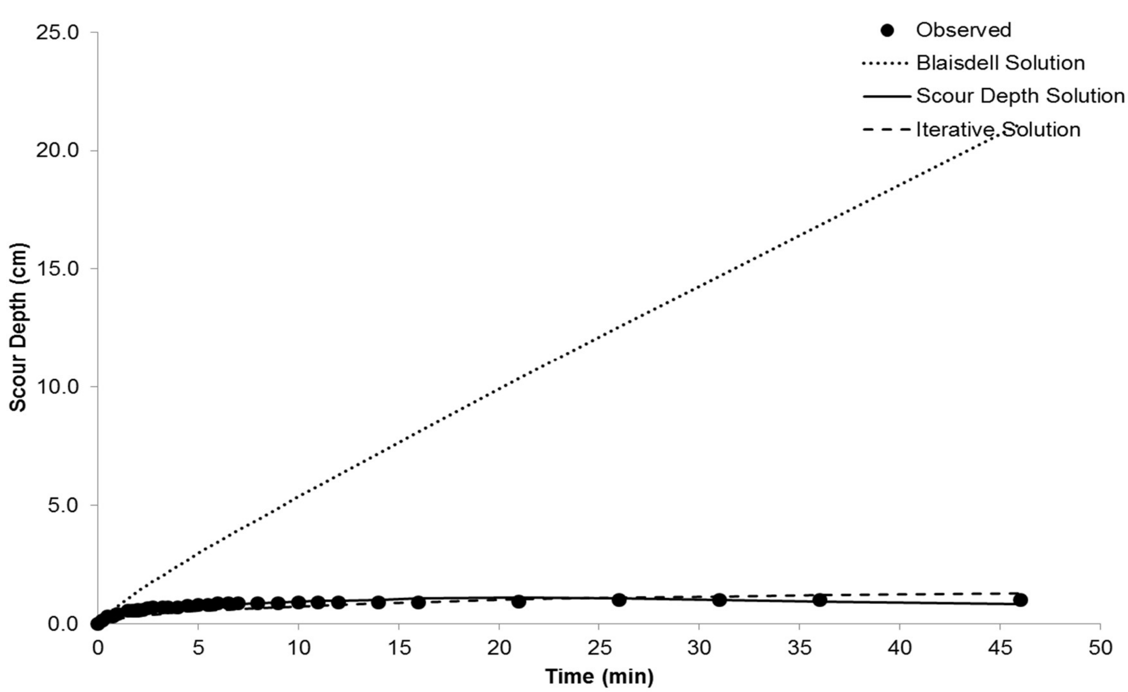

JET Location # 11

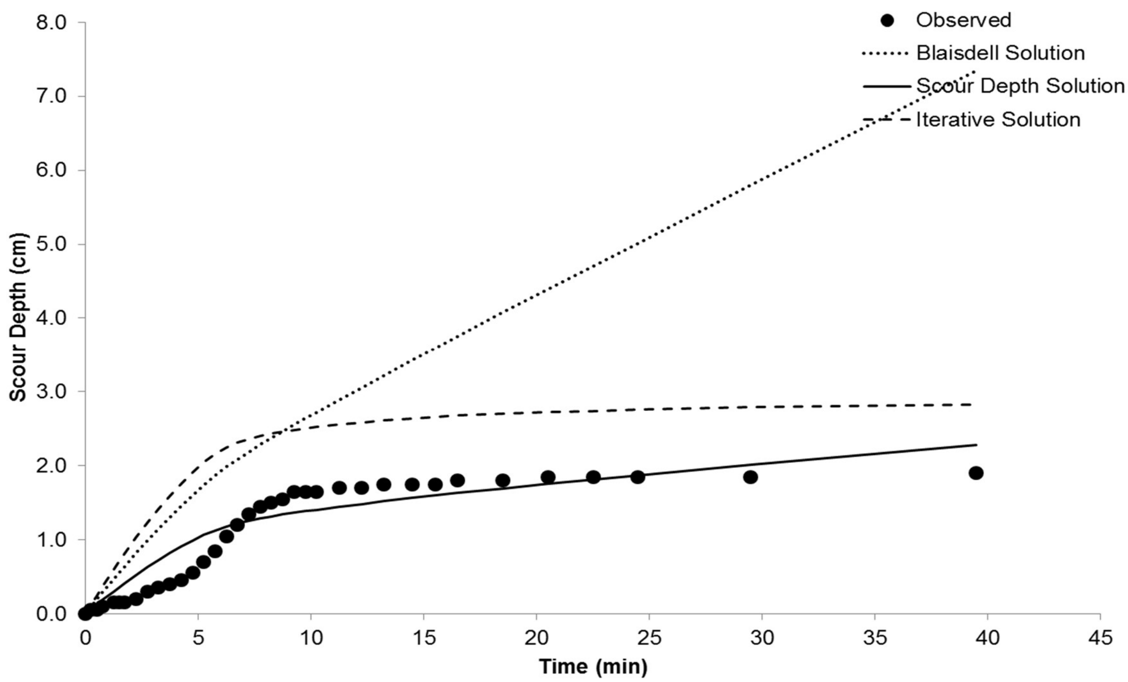

JET Location # 12-1

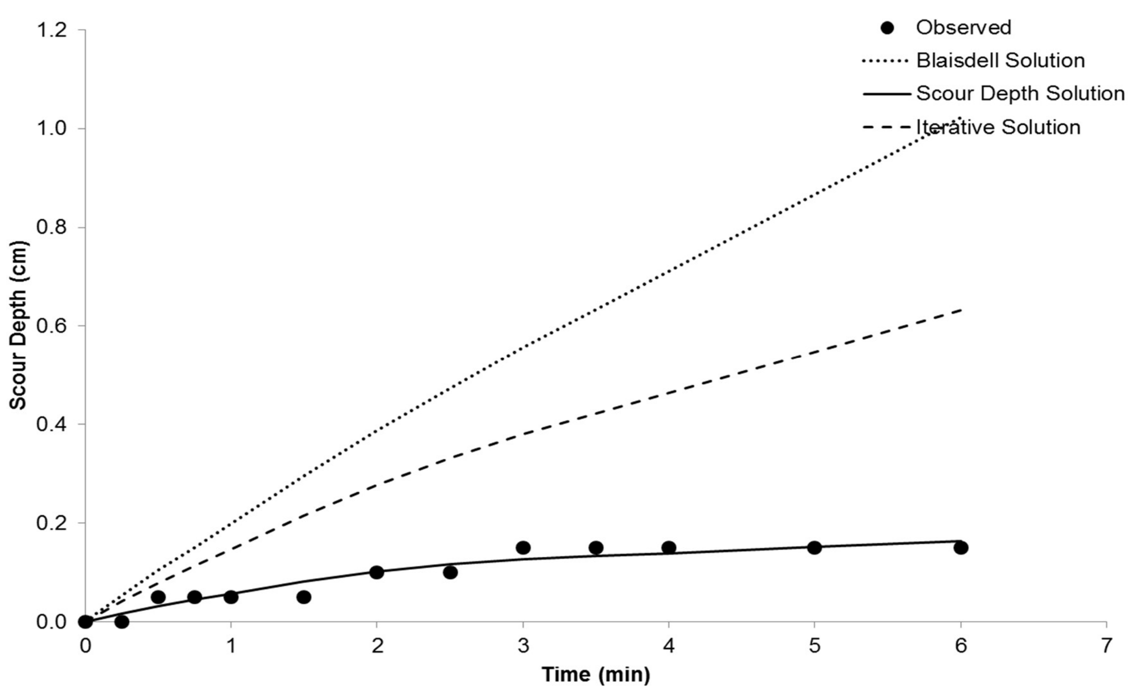

JET Location # 12-2

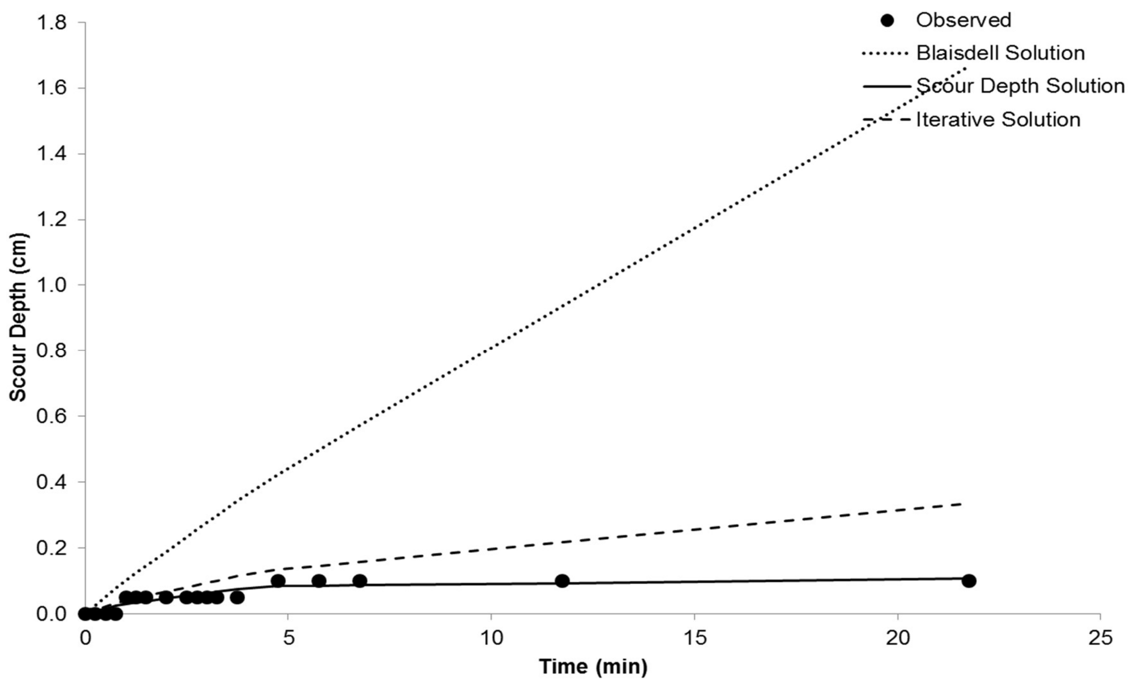

JET Location # 14

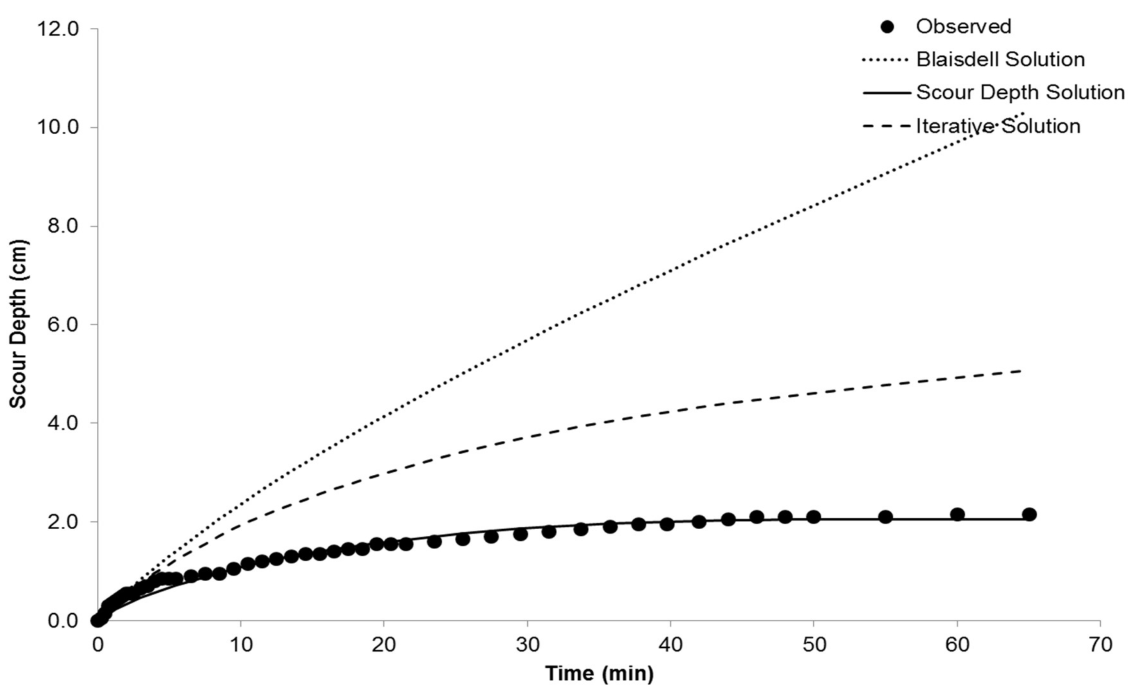

JET Location # 17-1

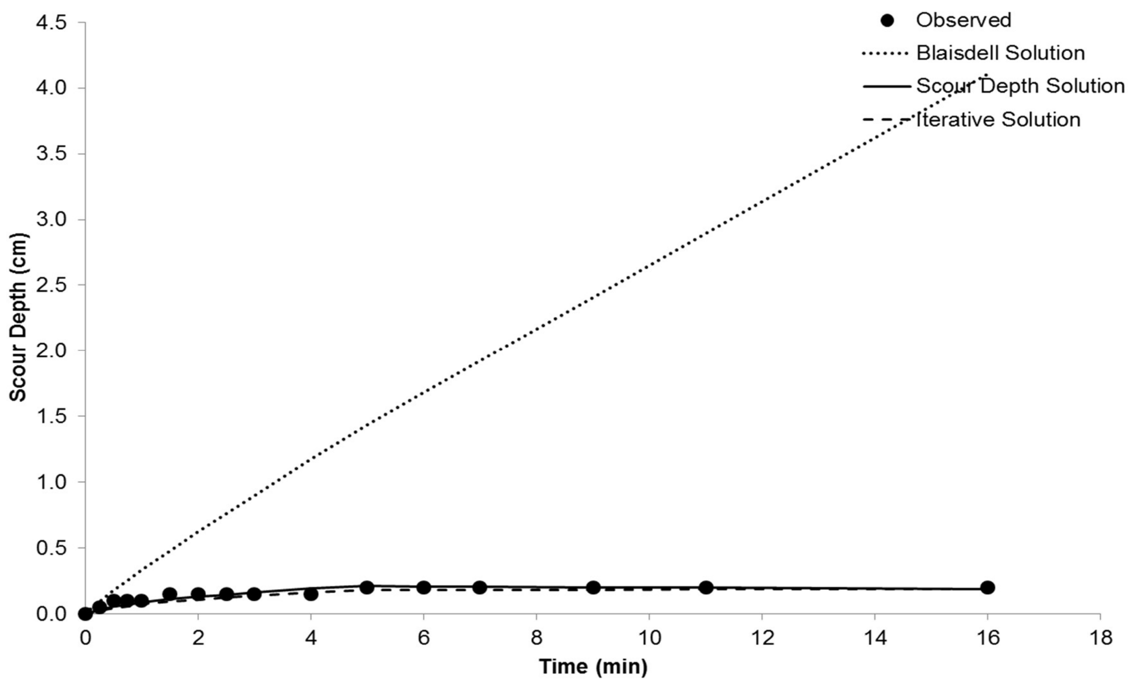

JET Location # 17-2

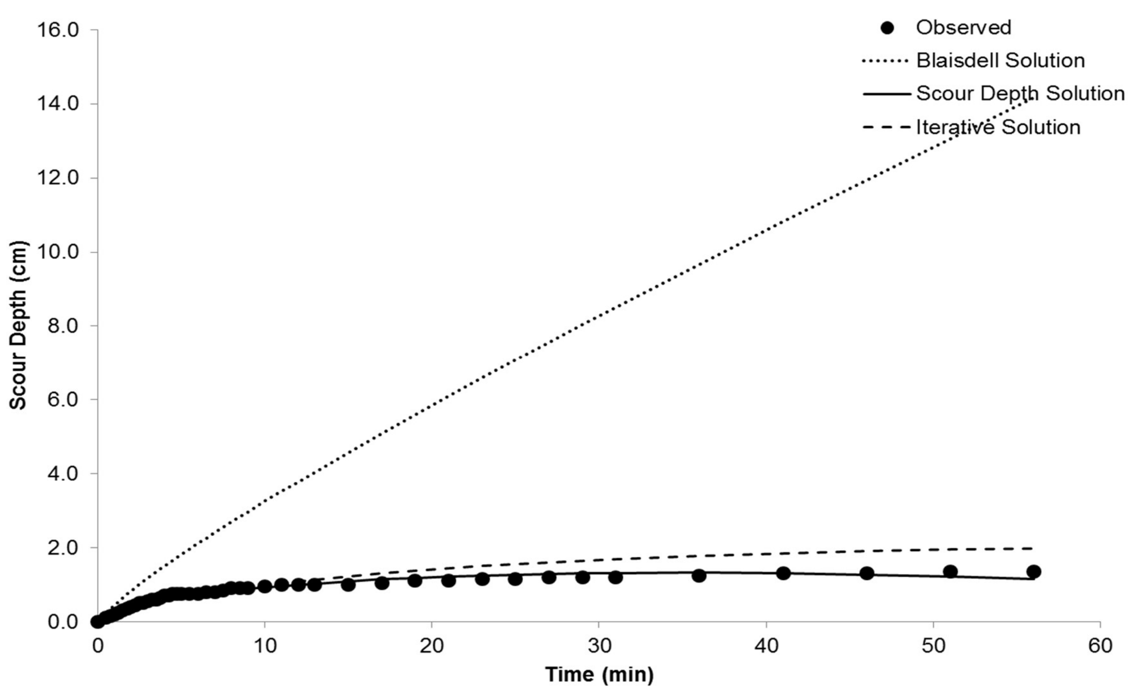

JET Location # 18

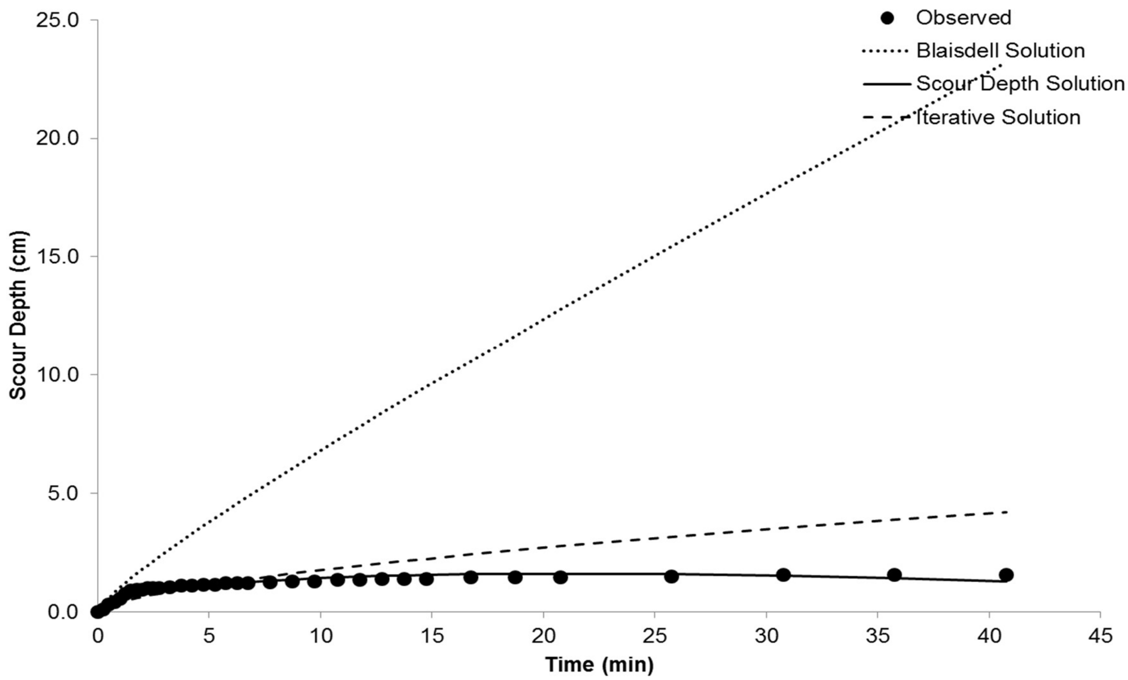

JET Location # 23

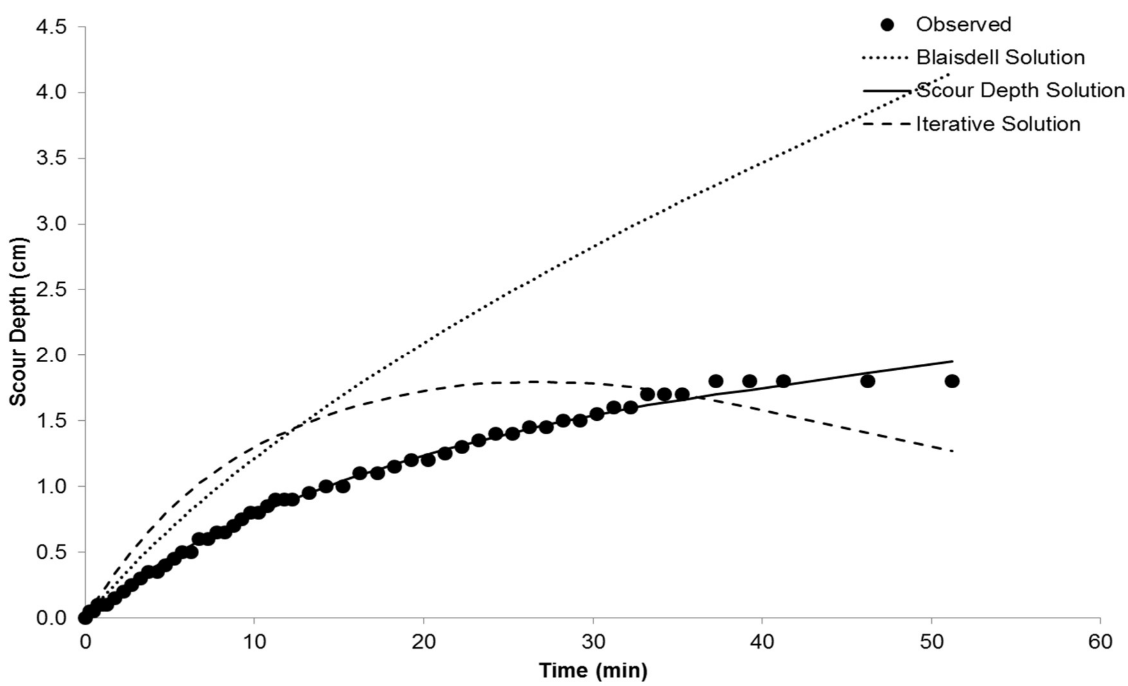

JET RESULTS

		Blaisdell		Scour Depth		Iterative	
		k_d cm^3/(N*s)	τ_c Pa	k_d cm^3/(N*s)	τ_c Pa	k_d cm^3/(N*s)	τ_c Pa
Watershed	Location						
E1	2	2.42	1.21	13.85	5.58	19.41	4.82
	6(1)	6.59	0.71	30.15	3.85	51.39	3.9
	6(2)	2.57	0.43	12.16	5.27	11.34	4.82
	13	3.14	0.36	26.78	3.2	12.11	2.76
	15	8.07	0.29	25.84	4.37	60.92	4.57
	17	6.29	1.17	53.4	4.42	51.01	3.79
	19	5.68	0.04	13.68	3.14	26.57	3.57
	average	**4.97**	**0.60**	**25.12**	**4.26**	**33.25**	**4.03**
E2	4	3.09	0.75	21.99	3.88	15.64	3.03
	9	3.18	0.65	20.26	5.01	16.95	4.05
	14	2.31	1.43	16.98	5.42	10.07	5
	16	2.11	1.4	19.51	5.6	17.94	4.92
	17	2.6	0.39	10.88	4.13	18.09	4.12
	20	6.02	0.76	35.22	3.69	26.77	3.4
	21	7.15	0.05	15.64	2.43	41.15	2.71
	average	**3.78**	**0.78**	**20.07**	**4.31**	**21.45**	**3.72**
P1	2	0.59	6.84	6.6	9.39	7.12	7.51
	4	0.58	5.32	6.59	9.26	7.1	4.89
	7	0.68	8.08	7.3	9.4	7.14	8
	9	1.45	0.88	8.18	4.24	8.47	3.74
	12	1.42	1.82	12.03	5.73	10.65	5.46
	14	2.68	1.89	6.41	18.31	6.08	9.71
	15	1.1	7.51	17.17	9.39	14.01	9.38
	19	2.17	2.62	22.26	4.33	17.65	4.27
	average	**1.33**	**4.37**	**10.82**	**8.76**	**9.78**	**6.62**
P2	2	1.92	1.88	14.46	5.77	14.85	5.21
	5	3.52	1.45	31.32	4.35	26.59	3.87
	6	2.3	0.97	12.45	4.91	16.79	4.76
	9	1.98	2.43	19.51	6.2	11.63	5.94
	11	2.83	0.27	6.47	3.58	14.2	4.23
	12(1)	1.8	7.75	9	10.39	12.89	9.54
	12(2)	1.4	7.69	10.7	8.81	10.72	8.64
	14	1.92	0.48	7.52	3.31	11.16	2.84
	17(1)	2.86	5.99	31.17	7.3	24.82	7.28
	17(2)	1.14	1.31	7.63	6.38	6.78	5.96
	18	3.35	1.08	27.98	4.28	18.23	3.52
	23	1.54	0.53	2.94	2.96	7.65	4.58
	average	**2.21**	**2.65**	**15.10**	**5.69**	**14.69**	**5.53**

HYDROMETER METHOD SOIL TEXTURE

AT JET LOCATIONS

Watershed	Location	Layer (cm)	Sand	Avg Sand	Silt	Avg Silt	Clay	Avg Clay	VFS (25% sand)	Texture
E1	2	0-10	61.4	58.3	19.2	20.3	19.4	21.3	14.6	sandy clay loam
		10-20	55.2		21.5		23.3			
	6(1)	0-10	75.0	72.3	9.8	11.3	15.2	16.4	18.1	sandy loam
		10-20	69.6		12.8		17.7			
	6(2)	0-10	75.0	72.3	9.8	11.3	15.2	16.4	18.1	sandy loam
		10-20	69.6		12.8		17.7			
	13	0-10	66.5	67.5	20.0	19.0	13.5	13.5	16.9	sandy loam
		10-20	68.5		18.0		13.5			
	15	0-10	61.2	52.1	20.3	22.1	18.5	25.8	13.0	sandy clay loam
		10-20	43.0		23.8		33.2			
	17	0-10	75.4	68.4	9.3	14.1	15.2	17.5	17.1	sandy loam
		10-20	61.3		18.9		19.7			
	19	0-10	52.0	45.1	23.8	22.7	24.3	32.3	11.3	sandy clay loam
		10-20	38.2		21.5		40.3			
	Average	0-10	65.3	60.65	17.1	18.3	17.7	21.2	16.3	sandy loam
		10-20	56.0		19.4		24.6		14.0	sandy clay loam
E2	4	0-10	60.6	56.1	24.4	25.7	14.9	18.1	14.0	sandy loam
		10-20	51.7		27.0		21.3			
	9	0-10	52.6	50.6	27.8	28.2	19.6	21.2	12.7	loam
		10-20	48.7		28.6		22.7			
	14	0-10	57.8	57.8	22.6	21.7	19.5	20.4	14.5	sandy clay loam
		10-20	57.8		20.8		21.3			
	16	0-10	60.5	58.1	29.7	29.8	9.8	12.2	14.5	sandy loam
		10-20	55.6		29.8		14.5			
	17	0-10	63.5	61.4	20.2	19.8	16.2	18.7	15.4	sandy loam
		10-20	59.3		19.5		21.2			
	20	0-10	52.5	47.0	27.0	25.2	20.5	27.8	11.7	sandy clay loam
		10-20	41.5		23.4		35.2			
	21	0-10	63.6	63.6	21.9	18.0	14.5	18.4	15.9	sandy loam
		10-20	63.5		14.2		22.4			
	Average	0-10	58.7	56.35	24.8	24.1	16.4	19.6	14.7	sandy loam
		10-20	54.0		23.3		22.7		13.5	sandy clay loam

Watershed	Location	Layer (cm)	Sand	Avg Sand	Silt	Avg Silt	Clay	Avg Clay	VFS (25% sand)	Texture
P1	2	0-10	51.8	53.5	27.8	25.1	20.3	21.3	13.4	sandy clay loam
		10-20	55.2		22.3		22.3			
	4	0-10	53.2	54.7	31.9	28.2	15.0	17.1	13.7	sandy loam
		10-20	56.3		24.5		19.2			
	7	0-10	54.1	52.1	32.8	29.3	13.2	18.7	13.0	sandy loam
		10-20	50.2		25.7		24.2			
	9	0-10	61.0	55.4	23.6	22.8	15.4	21.8	13.9	sandy clay loam
		10-20	49.8		21.9		28.2			
	12	0-10	58.2	54.2	20.9	23.7	20.9	22.1	13.5	sandy clay loam
		10-20	50.2		26.6		23.2			
	14	0-10	54.7	57.3	28.2	24.1	17.1	18.6	14.3	sandy loam
		10-20	59.9		20.1		20.0			
	15	0-10	77.2	78.4	16.2	15.6	6.7	6.1	19.6	loamy fine sand
		10-20	79.6		15.0		5.5			
	19	0-10	34.5	39.9	41.5	36.8	24.0	23.3	10.0	loam
		10-20	45.4		32.1		22.5			
	Average	0-10	55.6	55.7	27.8	25.7	16.6	18.7	13.9	sandy loam
		10-20	55.8		23.5		20.7		14.0	sandy clay loam
P2	2	0-10	66.5	55.1	14.8	15.5	18.7	29.3	13.8	sandy clay loam
		10-20	43.8		16.3		39.9			
	5	0-10	54.0	60.8	33.1	26.3	12.9	12.9	15.2	sandy loam
		10-20	67.7		19.4		12.8			
	6	0-10	72.6	73.8	18.8	18.2	8.6	8.0	18.5	sandy loam
		10-20	75.1		17.6		7.4			
	9	0-10	50.9	53.2	25.3	18.7	23.7	28.0	13.3	sandy clay loam
		10-20	55.4		12.2		32.4			
	11	0-10	47.7	51.0	34.2	29.8	18.1	19.2	12.8	loam
		10-20	54.3		25.4		20.3			
	12(1)	0-10	58.3	58.8	20.3	19.4	21.4	21.8	14.7	sandy clay loam
		10-20	59.2		18.5		22.2			
	12(2)	0-10	58.3	58.8	20.3	19.4	21.4	21.8	14.7	sandy clay loam
		10-20	59.2		18.5		22.2			
	14	0-10	64.7	65.4	22.3	19.4	13.0	15.2	16.4	sandy loam
		10-20	66.2		16.5		17.3			
	17(1)	0-10	67.7	62.5	17.7	17.6	14.6	20.0	15.6	sandy loam
		10-20	57.3		17.5		25.3			
	17(2)	0-10	67.7	62.5	17.7	17.6	14.6	20.0	15.6	sandy loam
		10-20	57.3		17.5		25.3			
	18	0-10	50.9	47.9	31.9	31.6	17.2	20.5	12.0	loam
		10-20	45.0		31.3		23.8			
	23	0-10	57.7	54.7	24.5	25.5	17.8	19.8	13.7	sandy loam
		10-20	51.6		26.5		21.9			
	Average	0-10	59.1	58.4	24.3	22.2	16.6	19.5	14.8	loam
		10-20	57.6		20.1		22.3		14.4	sandy clay loam

VITA

Whitney Alyson Lisenbee, EIT

Candidate for the Degree of

Master of Science

Thesis: COMPARISON OF WATER QUALITY AND QUANTITY IN EASTERN REDCEDAR FOREST AND NATIVE GRASSLAND WATERSHEDS: A MONITORING AND MODELING STUDY

Major Field: BIOSYSTEMS AND AGRICULTURAL ENGINEERING

Biographical:

Education:

Completed the requirements for the Master of Science in Biosystems and Agricultural Engineering at Oklahoma State University, Stillwater, Oklahoma in July, 2016.

Completed the requirements for the Bachelor of Science in Biosystems and Agricultural Engineering at Oklahoma State University, Stillwater, Oklahoma in May, 2014.

Experience:

Graduate Research Assistant | Stillwater, Oklahoma — Aug '14-Present
Oklahoma State University: Department of Biosystems and Agricultural Engineering

Fluid Mechanics Teaching Assistant | Stillwater, Oklahoma — Jan-May '15
Oklahoma State University: College of Engineering

Pilot Plant Intern | Tulsa, Oklahoma — May '14-Aug '14
AB Jewell Water Treatment Plant: City of Tulsa

Environmental Intern | Oklahoma City, Oklahoma — May '12-Aug '12
Chesapeake Energy Corporation

Professional Memberships:

American Society of Agricultural and Biological Engineers (ASABE)

American Society of Civil Engineers (ASCE)-Environmental and Water Resources Institute (EWRI)